

AL/CF-TR-1993-0167



AN INVESTIGATION WITH HUMAN SUBJECTS INTO  
THE POTENTIAL FOR DYNAMIC PRELOADING  
OF THE SPINAL COLUMN TO IMPROVE  
ESCAPE SYSTEM PERFORMANCE

Joseph P. Strzelecki

CREW SYSTEMS DIRECTORATE  
BIODYNAMICS AND BIOCOMMUNICATIONS DIVISION  
WRIGHT-PATTERSON AFB OH 45433-7901

AUGUST 1993

INTERIM REPORT FOR THE PERIOD MAY 1992 TO SEPTEMBER 1992

Approved for public release; distribution is unlimited.

AIR FORCE MATERIEL COMMAND  
WRIGHT-PATTERSON AIR FORCE BASE, OHIO 45433-6573

ARMSTRONG

LABORATORY

19950103 005

## NOTICE

When US Government drawings, specifications, or other data are used for any purpose other than a definitely related Government procurement operation, the Government thereby incurs no responsibility nor any obligation whatsoever, and the fact that the Government may have formulated, furnished, or in any way supplied the said drawings, specifications, or other data, is not to be regarded by implication or otherwise, as in any manner, licensing the holder or any other person or corporation, or conveying any rights or permission to manufacture, use or sell any patented invention that may in any way be related thereto.

Please do not request copies of this report from the Armstrong Laboratory. Additional copies may be purchased from:

National Technical Information Service  
5285 Port Royal Road  
Springfield VA 22161

Federal Government agencies and their contractors registered with Defense Technical Information Center should direct requests for copies of this report to:

Defense Technical Information Center  
Cameron Station  
Alexandria VA 22314

## TECHNICAL REVIEW AND APPROVAL

AL/CF-TR-1993- 0167

The voluntary informed consent of the subjects used in this research was obtained as required by Air Force Regulation 169-3.

This report has been reviewed by the Office of Public Affairs (PA) and is releasable to the National Technical Information Service (NTIS). At NTIS, it will be available to the general public, including foreign nationals.

This technical report has been reviewed and is approved for publication.

FOR THE COMMANDER



THOMAS J. MOORE, Chief  
Biodynamics and Biocommunications Division  
Crew Systems Directorate  
Armstrong Laboratory

<b>REPORT DOCUMENTATION PAGE</b>			Form Approved OMB No. 0704-0188	
Public reporting burden for this collection of information is estimated to average 1 hour per response, including the time for reviewing instructions, searching existing data sources, gathering and maintaining the data needed, and completing and reviewing the collection of information. Send comments regarding this burden estimate or any other aspect of this collection of information, including suggestions for reducing this burden, to Washington Headquarters Services, Directorate for Information Operations and Reports, 1215 Jefferson Davis Highway, Suite 1204, Arlington, VA 22202-4302, and to the Office of Management and Budget, Paperwork Reduction Project (0704-0188), Washington, DC 20503.				
1. AGENCY USE ONLY (Leave blank)		2. REPORT DATE August 1992		3. REPORT TYPE AND DATES COVERED Final Report May 1992 to September 1992
4. TITLE AND SUBTITLE An Investigation With Human Subjects into the Potential for Dynamic Preloading of the Spinal Column To Improve Escape System Performance			5. FUNDING NUMBERS PE - 62202F PR - 7231 TA - 723124 WU - 72312401	
6. AUTHOR(S)  Joseph P. Strzelecki				
7. PERFORMING ORGANIZATION NAME(S) AND ADDRESS(ES) Armstrong Laboratory, Crew Systems Directorate Biodynamics and Biocommunications Division Human Systems Center Air Force Materiel Command Wright-Patterson AFB OH 45433-7901			8. PERFORMING ORGANIZATION REPORT NUMBER  AL/CF-TR-1993- 0167	
9. SPONSORING / MONITORING AGENCY NAME(S) AND ADDRESS(ES)			10. SPONSORING / MONITORING AGENCY REPORT NUMBER	
11. SUPPLEMENTARY NOTES				
12a. DISTRIBUTION / AVAILABILITY STATEMENT  Approved for public release; distribution is unlimited.			12b. DISTRIBUTION CODE	
13. ABSTRACT (Maximum 200 words)  Tests were conducted at AL/CFBE using human volunteers on the Vertical Deceleration Tower. The tower was modified to provide an impulsive deceleration to the seat prior to the carriage pin striking the water in the cylinder. Measurements were made of seat pan forces, head acceleration, and chest acceleration. Each volunteer was subjected to three test conditions: Cell A was a 6 G pulse, with no preload; Cell B was an 8 G pulse with a 10 G preload; and Cell C was an 8 G pulse with no preload. The calculated Dynamic Response Index and measured physical responses of the volunteers confirmed that dynamic preload was effective, reducing the injury potential of Cell B nearly to that of Cell A.				
14. SUBJECT TERMS Dynamic Preload Escape Systems Injury Potential Dynamic Response Index			15. NUMBER OF PAGES 136	
			16. PRICE CODE	
17. SECURITY CLASSIFICATION OF REPORT UNCLASSIFIED		18. SECURITY CLASSIFICATION OF THIS PAGE UNCLASSIFIED		19. SECURITY CLASSIFICATION OF ABSTRACT UNCLASSIFIED
				20. LIMITATION OF ABSTRACT  UNLIMITED

THIS PAGE INTENTIONALLY LEFT BLANK

## PREFACE

The tests described in this report were accomplished by the Escape and Impact Protection Branch, Biodynamics and Biocommunications Division, Crew Systems Directorate of the Armstrong Laboratory. The tests were conducted under Workunit 72313101.

The impact facilities, data acquisition equipment, and data processing system were operated by the Scientific Division of DynCorp under Air Force contract F33615-86-C-0531. Mr Marshall Miller was the Engineering Supervisor for DynCorp. Mr Steve Mosher of DynCorp did the computer programming required for the data analysis.

Accession For	
NTIS CRA&I	<input checked="checked" type="checkbox"/>
DTIC TAB	<input type="checkbox"/>
Unannounced	<input type="checkbox"/>
Justification _____	
By _____	
Distribution / _____	
Availability Codes	
Dist	Avail and/or Special
A-1	

## TABLE OF CONTENTS

INTRODUCTION . . . . .	1
Background . . . . .	1
Objectives . . . . .	2
TEST METHODS . . . . .	3
Facilities and Procedures . . . . .	3
Electronic Data Acquisition System . . . . .	4
Video System . . . . .	4
Data Processing . . . . .	4
RESULTS . . . . .	6
The Effect of Dynamic Preload on Human Response to Impact . . . . .	6
DISCUSSION . . . . .	14
Physical Measurement of Injury Potential Indicators	14
Results of Tests with the ADAM Manikin . . . . .	17
Component Failures . . . . .	17
SUMMARY AND CONCLUSION . . . . .	18
REFERENCES . . . . .	19
Appendix A. . . . .	20
Appendix B. . . . .	71

# LIST OF FIGURES

<u>FIGURE</u>		<u>PAGE</u>
1	Seat Z Axis Acceleration for Cell A . . . . .	8
2	Seat Z Axis Acceleration for Cell C . . . . .	10
3	Seat Z Axis Acceleration for Cell B . . . . .	11
4	Correlation Between Lumbar Load and Peak . . . . . Chest Acceleration	16

# LIST OF TABLES

<u>TABLE</u>		<u>PAGE</u>
1	Test Numbers of Tests Conducted in Support of This Study . . . . .	6
2	Peak Seat Z Accelerations and Calculated DRIs . .	7
3	Summary of Velocity Change and Displacement for Characteristic Tests . . . . .	9
4	Seat Pan Z-Axis Loading Divided by Subject Weight . . . . .	12
5	Nondimensionalized Chest Z Axis Accelerations . .	13
6	Nondimensionalized Head Z Axis Accelerations . .	13
7	Estimated Relative Difference in Lumbar Loading Between Cells . . . . .	15
8	Comparison of Human and ADAM Responses . . . . .	17

THIS PAGE INTENTIONALLY LEFT BLANK



## INTRODUCTION

### Background

The maximum safety factor in the operation of a manned escape system is achieved when the system is ejected from the cockpit as rapidly as possible in order to clear the empennage of the aircraft. However, physiological limitations associated with spinal loads on the occupant dictate an upper bound on the acceleration levels of the escape system. The optimum acceleration-time history of the escape system is that time history which leads to maximum escape velocity and escape distance achievable within the acceleration limits allowable on the occupant (Payne and Shaffer, 1974).

In March of 1990 the Escape and Impact Protection Branch of Armstrong Laboratory (AL/CFBE) conducted a series of tests using the large ADAM manikin on the Vertical Deceleration Tower (VDT) to collect preliminary data for a follow-on test program with human subjects (Strzelecki, 1990). Dynamic preload was induced by blades attached to the carriage shearing aluminum blocks attached to the rails. These tests examined the effect of time separation between the preload and main plunger decelerations.

The tests showed that chest acceleration, Dynamic Response Index (DRI), seat pan load, and head acceleration all varied with pulse separation.

A computer simulation was then run which varied the amplitudes and separations of the acceleration peaks in simulated time histories to determine what parameters would provide a maximum displacement change versus a case with a 6 G peak acceleration where no preload was present, in the same amount of time, and with no greater DRI.

The results of the simulations showed that the optimum parameters for testing which met these criteria were:

Preload pulse amplitude = 10 G  
Main plunger Deceleration amplitude = 8 G  
Preload/Main plunger pulse separation = 0.070 seconds

These parameters were expected to produce the same DRI (and thus the same injury potential) as a 6 G drop with no preload on the VDT. The benefit of the preload would be a 50% increase in theoretical escape displacement versus the 6 G case in the same time.

A further series of tests was conducted later to determine what shear block size and carriage drop height were required to

produce the optimum acceleration profile determined from the computer model.

The test program documented here is based on the results of this previous work, which is documented in AAMRL-TR-90-075, "The Effect of Pulse Separation on Subject Response Using a Dynamic Preload Device".

### Objectives

This test program had three main issues to address:

(1) Will the use of dynamic preload significantly increase the theoretical escape displacement possible versus an acceleration pulse with no preload for a given allowable DRI?

(2) How much variability can be expected in the dynamic response of human subjects to the test conditions?

(3) Does the Advanced Dynamic Anthropomorphic Manikin (ADAM) have a response to the test conditions similar to that of humans?

## TEST METHODS

### Facilities and Procedures

The tests were conducted using the VDT. This device consists of a carriage constrained to vertical motion between two guide rails by means of guide wheels on the carriage. Attached to the carriage is a metal plunger aligned with a floor-mounted water cylinder.

To conduct a test, the carriage is hoisted to a predetermined height and released. The carriage falls, guided by the rollers and rails, until the plunger strikes the open face of the water cylinder. Compression and displacement of the water in the cylinder decelerate the carriage. In this program plunger 102 was used. This plunger generates a deceleration pulse with an approximately half-sine waveform.

Attached to the front face of a carriage was a generic seat with a headrest. The seat geometry conformed to MIL-S-9479B (USAF) except that the included angle between the seat pan and backrest planes was 90 degrees. The included angle between the seat back plane and acceleration axis was zero degrees (i.e., vertical). The seat was instrumented to provide accelerations and seat pan loads.

The restraint harness used consisted of a pair of shoulder straps tying into a generic lap belt at the belt buckle. The ends of the harness system were attached to triaxial load cells which served as anchor points. For each test, after the test subject was strapped in, the harness system was preloaded to  $20 \pm 5$  lb as measured at each of the load cells.

The test subjects were human volunteers and the large (approximately 95th percentile) prototype ADAM manikin weighing 218 lb and instrumented to provide neck and lumbar loads. All subjects were instrumented to provide chest accelerations (by means of an accelerometer array on a velcro belt wrapped around the chest) and head accelerations (for humans by means of a bite block with an accelerometer array attached). Subjects were dressed in a flight suit, gloves, BDU boots, HGU-55/P helmet (with visor down), and goggles under the visor.

The preload deceleration pulse was provided by a device designed by Survival Engineering Corporation of Asheville, North Carolina (SEC, 1987). Attached to each side of the carriage is a blade with a vertical adjustment capability of two inches up or down. Attached to the VDT rail on each side of the carriage is a magazine containing a shear sample holder and a shear sample. For this test program the shear samples were made from 7075-T6 aluminum blocks 6.8 inches long. The block cross section was 1.50 inches by 0.75 inches. A 0.75

inch wide channel was milled out of the length of the block leaving a web thickness of 0.55 inches. Figure A-5 (Appendix A, page A-26) shows a shear sample and shear sample holder. Attached to the bottom of the shear sample holder in the figure are shims which allow an adjustment of the vertical position of the shear sample of up to 1.75 inches.

In this test series the blades were at the "high" position (maximum height on the carriage), and the sample holder shim height was 0.25 inches. Figure A-6 (Appendix A, page A-27) shows the complete test setup.

Each subject was exposed to three test conditions:

Cell A was a 6 G drop with no preload pulse  
Cell B was a 10 G preload pulse followed 70 msec later  
by an 8 G main plunger pulse  
Cell C was an 8 G drop with no preload pulse

Measurements taken during the impact tests included carriage and seat acceleration, seat and restraint anchor forces, head and chest accelerations, and manikin lumbar and neck forces.

#### Electronic Data Acquisition System

Both data acquisition and processing requirements were satisfied using the system described in Appendix A. Electronic equipment mounted on the carriage was used to amplify, filter, and encode the data from all data channels into a digital format (pulse code modulated), which was then transmitted via an umbilical cable to a word formatter. The word formatter reformatted the serial data into parallel data, which were then routed to a VAX computer for storage and analysis.

#### Video System

No high speed on board video or SELSPOT data were collected from the tests as the camera mount was removed to minimize off-axis vibration. A Kodak video system was located off-board to record the impacts. This system is described in Appendix A.

#### Data Processing

Data from each test were reduced in a standardized format. Reduced electronic data are available for review within Appendix B. Computer summaries provide relevant maxima and minima for all recorded signals. Relevant sums

and times were also computed. The sums of the measured forces are the maximum value of continuously summed measurements. Scaled plots of selected signals and computed resultants were also provided.

## RESULTS

### The Effect of Dynamic Preload on Human Response to Impact

Eleven human subjects completed tests at all three cells. Three subjects were tested twice at Cell B when the initial test produced a low preload. Testing was terminated when the shear blades failed.

Table 1 summarizes the tests conducted in this study.

TABLE 1. TEST NUMBERS OF TESTS CONDUCTED  
IN SUPPORT OF THIS STUDY

<u>SUBJECT</u>	<u>CELL A</u>	<u>CELL B</u>	<u>CELL C</u>
C10	2709	2721	2717
B1	2698	2740	2691
L9	2692	2728	2699
O3	2695	2731	2708
F6	2686	2727	2707
A4	2684	2719	2703
S13	2682	2735	2694
H12	2701	2733	2722
G9	2704	2720/2739	2714
A5	2687	2732/2743	2710
C9	2683	2729/2742	2702
ADAM-L	2679	2678	2680

The parameters for the Cell B acceleration pulse were calculated based on idealized geometric components - the preload pulse was modelled as an isosceles triangle and the main plunger pulse as a half-sine wave. The actual pulse shape varied from this ideal somewhat so that the DRI calculated from the Cell B acceleration pulse is not the same as that of the Cell A pulse. Furthermore, due to natural variability in the shear samples and other causes, the peak acceleration achieved in the preload pulse of Cell B varied somewhat, causing variations between Cell B tests in the DRI calculated.

Table 2 summarizes the peak accelerations and calculated DRI's for each test. Because the seat Z accelerations contain a high frequency component to which the DRI is insensitive and which causes difficulty in specifying a "peak" acceleration for comparison purposes, the peak accelerations listed in the table are from data filtered at 30 hz.

For the human subjects as a group, the mean peak seat z acceleration for Cell A is 6.04 G with a standard deviation of 0.03. The corresponding mean DRI is 7.39 with a standard

deviation of 0.03. Test 2683 is taken as representative of all Cell A tests, and is shown filtered in Figure 1. Integrating the unfiltered pulse over the interval shown gives a velocity change of 248.5 in/sec and displacement of 21.5 inches.

TABLE 2. PEAK SEAT Z ACCELERATIONS AND CALCULATED DRIS

SUBJECT	CELL A		CELL B			CELL C	
	PEAK G	DRI	PRELOAD PEAK G	PLUNGER PEAK G	DRI	PEAK G	DRI
C10	6.07	7.42	9.48	8.38	8.59	8.26	10.40
B1	6.09	7.43	10.91	7.83	7.83	8.29	10.50
L9	6.05	7.40	7.08	8.25	8.39	8.18	10.35
O3	6.07	7.39	10.12	7.90	7.93	8.21	10.40
F6	6.02	7.39	9.97	8.39	8.55	8.14	10.32
A4	5.99	7.35	10.25	8.37	7.98	8.12	10.31
S13	6.00	7.33	10.28	8.27	7.85	8.17	10.33
H12	6.09	7.40	7.78	8.46	8.93	8.22	10.36
G9	6.03	7.36	7.93	8.20	8.29	8.07	10.27
			9.16	8.21	7.98		
A5	6.05	7.41	7.68	8.58	8.96	8.20	10.34
			8.13	8.29	8.57		
C9	6.03	7.41	13.52	7.97	9.39	8.21	10.40
			8.21	8.38	8.62		
MEAN	6.04	7.39	10.02*	8.19*	8.10*	8.19	10.36
STD DEV	0.03	0.03	0.57*	0.23*	0.33*	0.06	0.06
ADAM-L	6.04	7.36	6.96	8.05	8.92	8.22	10.39

\*Includes only tests with  $9.0 < \text{Peak G} < 11.0$

Repeating this analysis for Cell C, the mean ( $\bar{x}$ ) peak seat Z acceleration for Cell C is 8.19 G with a standard deviation of 0.06 G. The corresponding mean DRI is 10.36 with a standard deviation of 0.06 G. Test 2699 is taken as representative of all Cell C tests and is shown filtered in

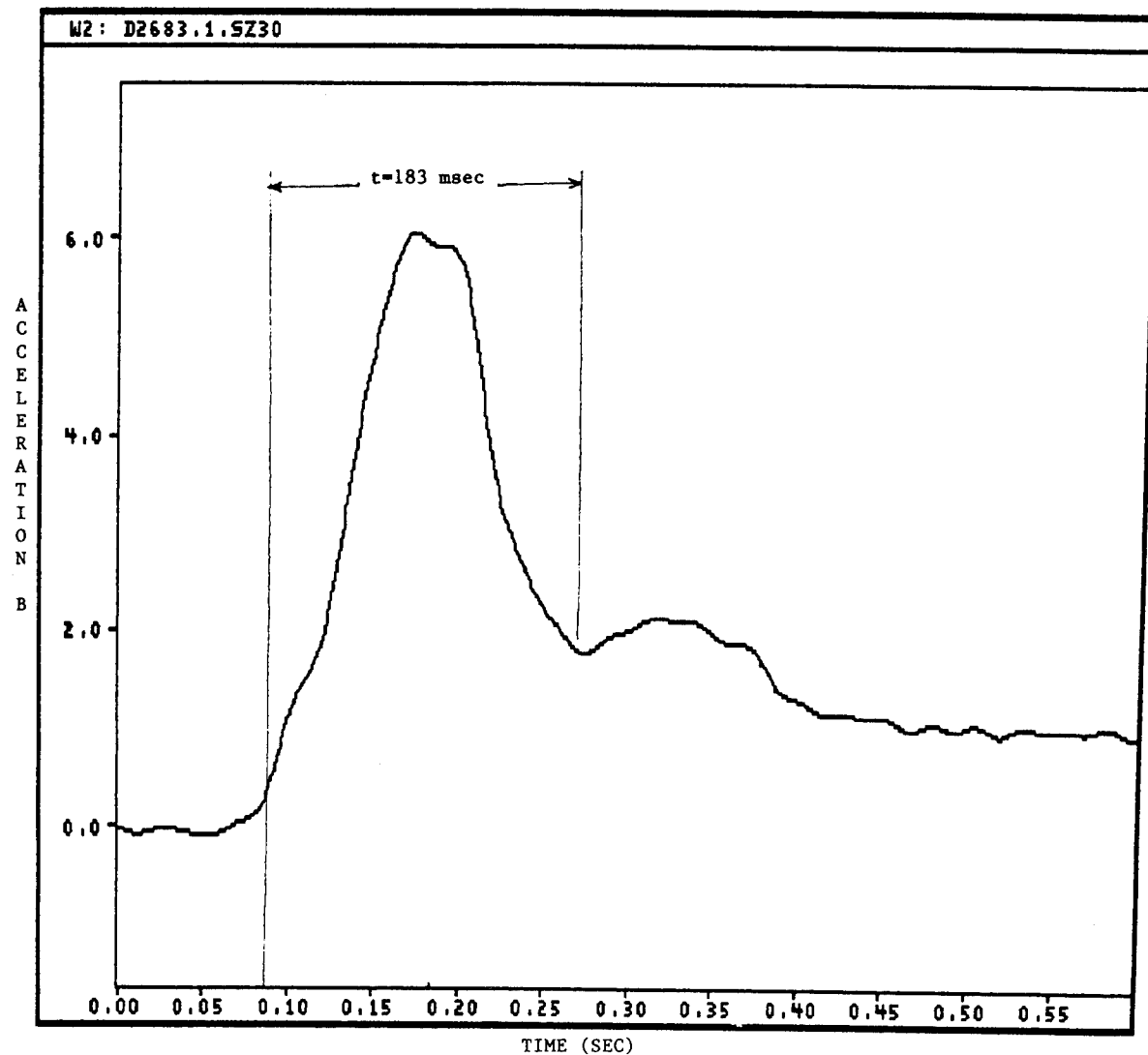


FIGURE 1. SEAT Z AXIS ACCELERATION FOR CELL A



Figure 2. Integrating the unfiltered pulse over the same time interval as that of Figure 3 gives a velocity change of 303.4 in/sec and displacement of 28.3 inches.

Table 2 shows that the Cell B preload peak G achieved varied between tests. For those tests in the range  $9.0 < \text{Peak G} < 11.0$ ,  $\bar{x}$  for the preload peak = 10.02 G with a standard deviation of 0.57 G.  $\bar{x}$  for the main plunger peak = 8.19 G with a standard deviation of 0.23 G.  $\bar{X}$  for the DRI is 8.10 with a standard deviation of 0.33. Test 2731 is representative of this subset and is shown filtered in Figure 3. Integrating the unfiltered pulse over the same time interval as that of Figure 3 gives a velocity change of 344.9 in/sec and displacement of 33.6 inches.

Table 3 summarizes these results.

TABLE 3. SUMMARY OF RESULTS FOR CHARACTERISTIC TEST

CELL	NOMINAL PEAK G	DRI	VELOCITY CHANGE IN 0.183 SEC	DISPLACEMENT IN 0.183 SEC
A	6	7.4	248.5 in/sec	21.5 in
B	8*	8.1	344.9 in/sec	33.6 in
C	8	10.4	303.4 in/sec	28.3 in

\*10 G preload

The table shows a significant potential improvement in escape system performance is possible using dynamic preload. For a given seat rocket acceleration, incorporation of dynamic preload would allow a higher thrust to be used without increasing the risk of injury (as determined by the DRI).

The DRI is a quantity calculated from a simple model of spinal compression. Data was collected in this experiment to show that measured physical responses confirm the reduced potential for spinal injury indicated by the DRI. These measured quantities are seat pan force, chest acceleration, and head acceleration.

Table 4 gives the seat pan Z axis force (minus tare) divided by subject weight for those subjects whose cell B preload was in the range from 8 G to 12 G. Note that this range includes a few more tests than the range used to produce Table 3 in which the effect of the optimum Cell B acceleration history is displayed. The mean DRI for Cell B tests with a preload peak in the range of 8 G to 12 G is 8.2.

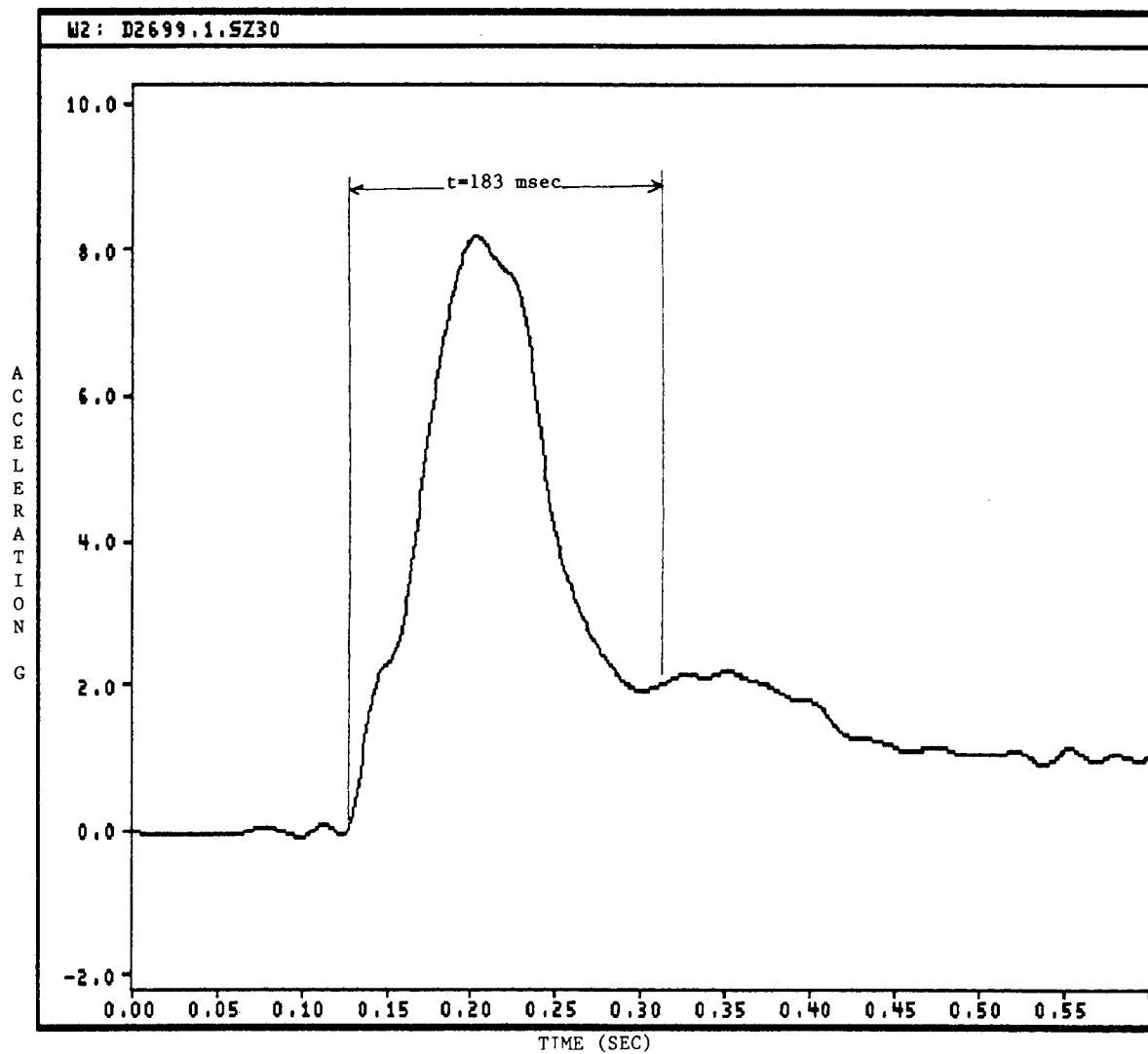


FIGURE 2. SEAT Z AXIS ACCELERATION FOR CELL C

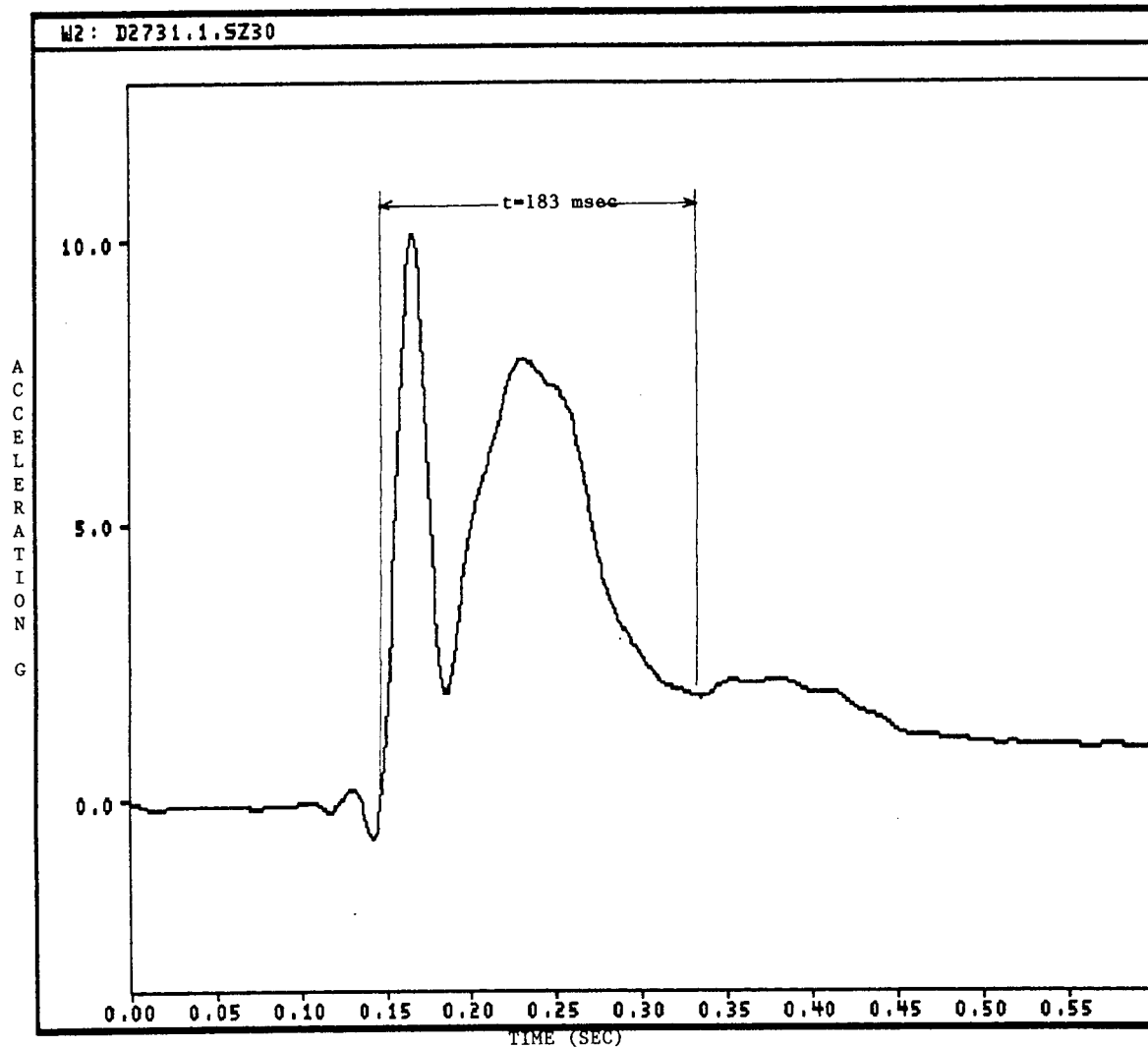


FIGURE 3. SEAT Z AXIS ACCELERATION FOR CELL B

Taking seat pan force as an indicator of spinal loading, Table 4 shows that lumbar load is reduced when preload is used versus the case where no preload is present. These results are in line with those of Table 3.

Measured peak chest Z axis acceleration is another external indicator of spinal compression which should follow the trend of the DRI. This measurement tends to have a large variation among individuals which could be caused by factors other than chest motion, such as velcro belt slippage, amount of body fat, etc. In an attempt to reduce this effect, the data in Table 5 are nondimensionalized by dividing the chest Z accelerations for each cell for each subject by the subject's Cell A measurement.

TABLE 4. SEAT PAN Z AXIS LOADING (MINUS TARE)  
DIVIDED BY SUBJECT WEIGHT

SUBJECT	WEIGHT (LB)	CELL A	CELL B	CELL C
C10	121	7.70	9.99	10.72
B1	185	7.58	9.79	10.44
G9	185	7.95	8.94	10.59
O3	142	7.91	8.98	11.10
A5	169	6.87	8.69	9.66
F6	185	7.92	9.55	10.49
A4	198	7.65	9.82	10.92
C9	202	7.00	8.79	9.62
S13	188	7.68	8.89	9.98
MEAN	175.0	7.58	9.27	10.39
STD DEV	26.9	0.39	0.51	0.53

This parameter follows the general trend seen previously. Maximum head Z axis acceleration is not a good indicator of lumbar loading, but does give an indication of the forces acting on the neck and the effect on potential neck injury. Table 6 summarizes the available data for the Cell B preload range of 8 G to 12 G, nondimensionalized as was done for Table 5.

Table 6 indicates that the dynamic preload used in this study does not have any beneficial effect on neck forces, i.e., using dynamic preload to increase allowable lumbar

loading does not increase allowable neck loading. Any increase in seat pan acceleration feeds through as increased neck loading.

TABLE 5. NONDIMENSIONALIZED CHEST Z AXIS ACCELERATIONS

SUBJECT	CELL A	CELL B	CELL C
C10	1.00	1.35	1.35
B1	1.00	1.50	1.47
G9	1.00	1.28	1.44
O3	1.00	1.26	1.51
A5	1.00	1.30	1.46
F6	1.00	1.62	1.45
A4	1.00	1.05	1.75
C9	1.00	1.51	1.49
S13	1.00	1.22	1.39
MEAN	1.00	1.34	1.48
STD DEV	0.00	0.17	0.11

TABLE 6. NONDIMENSIONALIZED HEAD Z AXIS ACCELERATIONS

SUBJECT*	CELL A	CELL B	CELL C
C10	1.00	1.35	1.29
B1	1.00	1.58	1.59
G9	1.00	1.42	1.61
A5	1.00	1.78	1.31
F6	1.00	1.21	1.21
A4	1.00	1.08	1.53
C9	1.00	1.00	1.04
S13	1.00	1.31	1.30
MEAN	1.00	1.34	1.36
STD DEV	0.00	0.26	0.20

\*Incomplete data for Subject O3

## DISCUSSION

### Physical Measurement of Injury Potential Indicators

The seat pan Z axis loading provides an indication of the forces acting on the lower spine. Examining Table 4 it can be seen that for every subject the peak seat pan load is higher for Cell C than for Cell B. The loading in Cell B is higher than that of Cell A, but this is to be expected given the main plunger G loading is 1.33 times higher. A better estimate of the relative lumbar loading induced by each cell can be obtained by subtracting out the weight of the legs as these do not bear down on the spine. The weight of the pelvic area could be subtracted out for the same reason. If one knew the distribution of body weight along the spine, one could further refine the analysis by assuming the spine acts as a linear spring and using an energy balance to calculate an effective mass.

The thighs, calves, and feet of the large ADAM prototype manikin comprise about 36% of its total body weight. Taking this value as approximately correct for the human subjects and adding an estimated four percent more of total body weight to account for the pelvic area gives a total of 40% of body weight which does not bear on the spine.

Table 7 is a rough estimate of relative lumbar loading based on Table 4 and the above discussion. In the table, subject body weight is multiplied by .40 and also by the peak main plunger Z acceleration to represent the dynamic effect of the lower body. This is subtracted from the seat pan loading in Table 4 to give an approximation of lumbar loading. Finally, for each subject all the table entries are divided by the Cell A value to remove the effect of variation in subject weight. As a mathematical formula:

$$[(\text{Seat Pan Loading}) - (0.40)(\text{Body weight})(\text{Acceleration})]/(\text{Cell A Seat Pan Load})$$

As calculated previously, the mean Cell A seat pan Z acceleration was 6.04 G, while in comparison Cell C was 8.19 G, a difference of a factor of 1.36. This matches well with the results seen in Table 7 and clearly shows the attenuation in loading produced by the dynamic preload.

The results of the chest acceleration measurements are less clear cut. Probably the greatest influence on the quality of the measurements is the imperfections in the accelerometer mounting system. This is a non-rigidly attached belt separated by varying amounts of human tissue.

Table 5 shows that the attenuation in severity of impact is discernable between Cases B and C in the mean, though the standard deviation of the data is large. There are a few cases where the peak chest acceleration in Cell B is larger than that measured in Cell C. If this was in fact true, one would expect it to affect the calculated lumbar loading.

TABLE 7. ESTIMATED RELATIVE DIFFERENCE IN LUMBAR LOADING BETWEEN CELLS

SUBJECT	CELL A	CELL B	CELL C
C10	1.00	1.26	1.41
B1	1.00	1.29	1.38
G9	1.00	1.02	1.33
O3	1.00	1.06	1.43
A5	1.00	1.16	1.43
F6	1.00	1.12	1.31
A4	1.00	1.23	1.46
C9	1.00	1.29	1.38
S13	1.00	1.06	1.27
MEAN	1.00	1.17	1.38
STD DEV	0.00	0.11	0.06

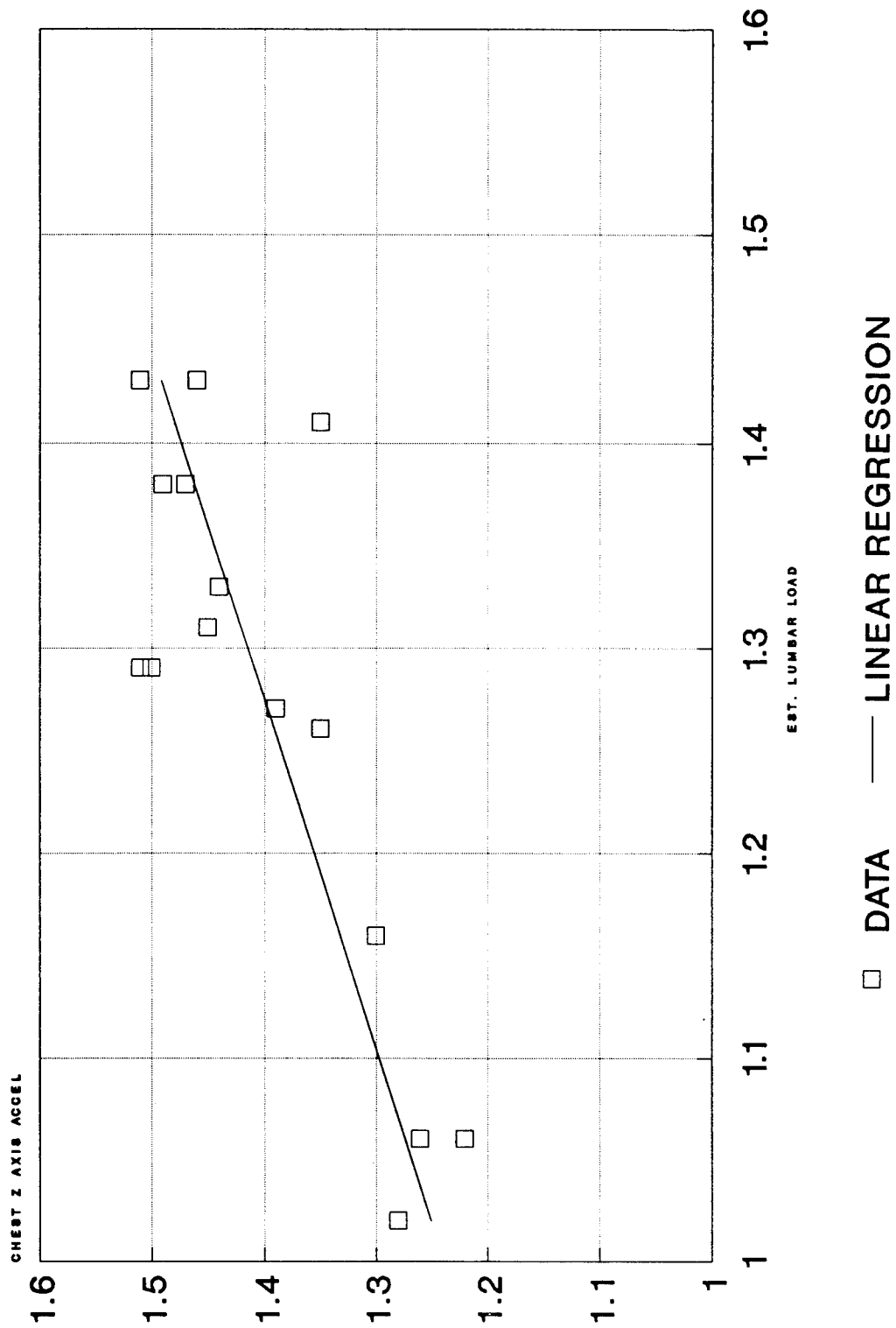
Figure 4 is a plot of maximum normalized chest acceleration from Table 5 versus calculated normalized lumbar load from Table 7 for Cells B and C with a linear regression line through the data. Three data points were excluded: readings for subjects F6 and A4 in Cell B and subject A4 in Cell C. These were judged to be grossly anomalous. The linear regression line is given by:

$$y = 0.651 + 0.588X$$

with a correlation coefficient of  $r = 0.82$

Using this equation for the mean lumbar load for Cell B from Table 7, the expected normalized mean peak chest acceleration from the linear regression equation is found to be 1.34. Repeating this procedure for Cell C yields a normalized mean peak chest acceleration of 1.46. These values agree very well with the measured data of Table 5.

FIGURE 4: CORRELATION BETWEEN EST.  
LUMBAR LOAD AND PEAK CHEST ACCEL.  
(NORMALIZED DATA)





These results confirm that measurements error is responsible for the anomalies seen in the chest acceleration data, and that the chest acceleration trend verifies the preload benefits indicated by the DRI.

#### Results of Tests With the ADAM Manikin

Only one test was completed with the ADAM at Cell B due to the early termination of the test program. The preload achieved (6.96 G) was much lower than desired yielding a correspondingly higher DRI for the test. Taking this into consideration, the measurements made with the ADAM can be compared with the mean values from the human tests as follows:

TABLE 8. COMPARISON OF HUMAN AND ADAM RESPONSES

RESPONSE	POPULATION	CELL A	CELL B	CELL C
Chest Accel	Human Mean	1.00	1.34	1.48
	ADAM	1.00	1.21	1.65
Head Accel	Human Mean	1.00	1.34	1.36
	ADAM	1.00	1.85	1.44
Lumbar Load	Human Mean	1.00	1.17	1.38
	ADAM*	1.00	1.13/1.53	1.43

\*Measured by lumbar load cell

Taking into consideration that this discussion is based on results from a single test, the table shows the chest acceleration of the ADAM is in line with expected results. The ADAM head responded strongly to the preload pulse as the data trace shows (see Appendix B). The lumbar loading is in line with the estimates made for the human population. The value of 1.53 given in the table represents the actual measured peak which includes a sharp spike at the time of the preload. This may be due to the head response. Ignoring the superimposed spike gives the more realistic value of 1.13 also presented.

#### Component Failures

In the previous test program the life-limited hardware item was the shear sample holder. In this program, because the shear sample web was increased to 0.55 inches, shear blade failures became apparent. Testing was terminated after two pairs of blades had been destroyed.

## SUMMARY AND CONCLUSION

The theory that dynamic preloading of the spine could reduce injury potential was demonstrated with human subject in the laboratory. The reduced DRI to be expected from a test with dynamic preload versus one without was corroborated by physical measurements.

A potential limit on the increase in acceleration tolerance made possible by dynamic preload is the capacity of the neck to sustain the increased loading as the dynamic preload demonstrated here had no beneficial effect on head acceleration.

## REFERENCES

1. Bartol, Aileen M. and Hazen, Vernon L. Advanced Dynamic Anthropomorphic Manikin (ADAM) Final Design Report. AAMRL-TR-90-023, March 1990.
2. Brinkley, James W. and Schimmel, Dale E. Impact Tests of T-46A Personnel Restraint Systems. AAMRL-TR-87-043, June 1987.
3. Brinkley, James W., Raddin, James H., Jr., and DeHart, Roy L. Fundamentals of Aerospace Medicine. Philadelphia, PA: Lea and Febiger, 1985.
4. Brinkley, James W. and Shaffer, John T. Dynamic Simulation Techniques for the Design of Escape Systems: Current Applications and Future Air Force Requirements, In Biodynamic Models and Their Applications. AMRL-TR-71-29-2, 1972.
5. Hearon, Bernard F., Raddin, James H., Jr., and Brinkley, James W. Evidence for the Utilization of Dynamic Preload in Impact Injury Prevention. AMRL-TR-82-6, 1982.
6. Payne, Peter R. and Shaffer, David A. An Optimum Acceleration-Time History for an Escape System. AMRL-TR-70-143, August 1971.
7. Phillips, Norman S. and Carr, Richard W. A Statistical Evaluation of the Injury Potential of a Square Wave Energy Absorber. USAAMD TR-72-9.
8. Stech, Ernest L. and Payne, Peter R. Dynamic Models of the Human Body. AMRL-TR-66-157, 1965.
9. Strzelecki, Joseph P. The Effect of Pulse Separation on Subject Response Using a Dynamic Preload Device. AAMRL-TR-90-075, July 1990.
10. Survival Engineering Corporation. Dynamic Preload System Technical Manual. Document 87-020-600, Survival Engineering Corporation, Asheville, NC, 1987.

TEST CONFIGURATION AND  
DATA ACQUISITION SYSTEM FOR  
VERIFICATION OF THE DYNAMIC PRELOAD  
PRINCIPLE USING HUMAN TEST SUBJECTS  
DURING +Gz IMPACT ACCELERATIONS  
(DP2 STUDY)  
TEST PROGRAM

Prepared under  
Contract F33615-91-C-0531

August 1992

Prepared by  
Marshall Z. Miller  
and  
Stephen E. Mosher

DynCorp  
T & E Divisions  
AAMRL Division  
Building 824, Area B  
Wright-Patterson AFB, Ohio 45433

## TABLE OF CONTENTS

	<u>PAGE</u>
INTRODUCTION.....	4
1. TEST FACILITY.....	4
2. SEAT FIXTURE.....	4
3. DYNAMIC PRELOAD DEVICE.....	5
4. TEST SUBJECTS.....	5
5. INSTRUMENTATION.....	5
5.1 ACCELEROMETERS.....	7
5.2 LOAD TRANSDUCERS.....	7
5.3 CALIBRATION.....	8
6. DATA ACQUISITION.....	9
6.1 AUTOMATIC DATA ACQUISITION AND CONTROL SYSTEM (ADACS).....	9
6.2 SELSPOT MOTION ANALYSIS SYSTEM.....	10
7. PROCESSING PROGRAMS.....	10
7.1 ADACS PROGRAM OPERATION.....	10
7.2 ADACS PROGRAM FLOWCHARTS.....	11

## LIST OF TABLES

<u>TABLE</u>	<u>PAGE</u>
A-1. INSTRUMENTATION REQUIREMENTS	
A-1a. PAGE 1 OF 4.....	A-1
A-1b. PAGE 2 OF 4.....	A-2
A-1c. PAGE 3 OF 4.....	A-3
A-1d. PAGE 4 OF 4.....	A-4
A-2. TYPICAL TRANSDUCER SPECIFICATIONS.....	A-5
A-3. TRANSDUCER PRE- AND POST-CALIBRATION	
A-3a. PAGE 1 OF 5.....	A-6
A-3b. PAGE 2 OF 5.....	A-7
A-3c. PAGE 3 OF 5.....	A-8
A-3d. PAGE 4 OF 5.....	A-9
A-3e. PAGE 5 OF 5.....	A-10

## LIST OF ILLUSTRATIONS

<u>FIGURE</u>	<u>PAGE</u>
A-1. VIP SEAT FIXTURE.....	A-11
A-2. SUBJECT LEG AND THIGH RESTRAINTS.....	A-12
A-3. DYNAMIC PRELOAD DEVICE BLADE.....	A-13
A-4. DYNAMIC PRELOAD DEVICE BLADE.....	A-14
A-5. SHEAR SAMPLE AND SHEAR SAMPLE HOLDER.....	A-15
A-6. DYNAMIC PRELOAD DEVICE.....	A-16
A-7. AL/CFBE COORDINATE SYSTEM.....	A-17
A-8. MANIKIN COORDINATE SYSTEM.....	A-18
A-9. HUMAN HEAD ACCELEROMETER PACKAGE.....	A-19
A-10. CHEST ACCELEROMETER PACKAGE.....	A-20
A-11. TRANSDUCER LOCATIONS AND DIMENSIONS	
A-11a. PAGE 1 OF 2.....	A-21
A-11b. PAGE 2 OF 2.....	A-22
A-12. LOAD LINK INSTRUMENTATION.....	A-23
A-13. SEAT PAN INSTRUMENTATION.....	A-24
A-14. HEADREST AND SHOULDER LOAD CELL INSTRUMENTATION.....	A-25
A-15. ADACS INSTALLATION.....	A-26
A-16. AUTOMATIC DATA ACQUISITION AND CONTROL SYSTEM.....	A-27
A-17. DATA ACQUISITION AND STORAGE SYSTEM BLOCK DIAGRAM.....	A-28
A-18. KODAK EKTAPRO 1000 VIDEO SYSTEM.....	A-29
A-19. PROGRAM DP2VDTOA FLOWCHART	
A-19a. PAGE 1 OF 3.....	A-30
A-19b. PAGE 2 OF 3.....	A-31
A-19c. PAGE 3 OF 3.....	A-32
A-20. PROGRAM DP2VDTOB FLOWCHART	
A-20a. PAGE 1 OF 8.....	A-33
A-20b. PAGE 2 OF 8.....	A-34
A-20c. PAGE 3 OF 8.....	A-35
A-20d. PAGE 4 OF 8.....	A-36
A-20e. PAGE 5 OF 8.....	A-37
A-20f. PAGE 6 OF 8.....	A-38
A-20g. PAGE 7 OF 8.....	A-39
A-20h. PAGE 8 OF 8.....	A-40

## INTRODUCTION

This report was prepared by DynCorp for the Armstrong Laboratory (AL/CFBE) under Air Force Contract F33615-91-C-0531.

The information provided herein describes the test facility, seat fixture, dynamic preload device, restraint configuration, test subjects, data acquisition and instrumentation procedures that were used in the Verification of the Dynamic Preload Principle using Human Test Subjects During +Gz Impact Accelerations (DP2 Study) Test Program. Ninety-one tests were conducted during April through June 1992 on the Vertical Deceleration Tower Test Facility.

### 1. TEST FACILITY

The AAMRL Vertical Deceleration Tower was used for all of the tests.

The facility consists of a 60 foot vertical steel tower which supports a guide rail system, an impact carriage supporting a plunger, a hydraulic deceleration device and a test control and safety system. The impact carriage can be raised to a maximum height of 42 feet prior to release. After release, the carriage free falls until the plunger, attached to the undercarriage, enters a water filled cylinder mounted at the base of the tower. The deceleration profile produced as the plunger displaces the water in the cylinder is determined by the free fall distance, the carriage and test specimen mass, the shape of the plunger and the size of the cylinder orifice. A rubber bumper is used to absorb the final impact as the carriage stops. For these tests, plunger number 102 was mounted under the carriage. Drop height varied depending on the test cell requirements which ranged from 5'6" to 11'8".

### 2. SEAT FIXTURE

The VIP seat fixture, as shown in Figure A-1, was used for all of the tests. The seat was designed to withstand vertical impact accelerations up to 50 G. Its adjustable seat back and seat pan were not adjusted during this study as all of the tests were run at the 0 degree seat back angle. When positioned in the seat, the subject's upper legs were bent 90 degrees outward to a horizontal position with his lower legs bent 90 degrees downward to a vertical position. The subject was secured in the seat with a conventional two-strap shoulder harness and lap belt. The lap belt and shoulder strap were preloaded to  $20 \pm 5$  pounds as required in the test plan.

Each of the subject's legs were restrained by a strap that encircled the subject's ankle and was attached to the carriage. Another strap crossed the subject's thighs and attached to the seat pan posterior to the knees. The subject's hands were placed under the thigh restraint. These restraints are illustrated by Figure A-2.

### 3. DYNAMIC PRELOAD DEVICE

The dynamic preload device consisted of a blade, shear sample holder and shear sample. Attached to each side of the carriage is a blade. The blade has a vertical adjustment capability of  $\pm 2$  inches. Figure A-3 illustrates the dynamic preload device blade and Figure A-4 shows the blade installed on the side of the carriage.

Attached to each rail is a magazine containing a shear sample holder and a shear sample. The shear samples were made from 7075-T6 aluminum blocks 6.8 inches long. The block cross section was 1.50 inches by 0.75 inches. A 0.75 inch wide channel was milled out of the length of the block leaving a web thickness of 0.55 inches. Figure A-5 shows a shear sample and shear sample holder. Attached to the bottom of the shear sample holder in Figure A-5 are shims which allow an adjustment of the vertical position of the shear sample of up to 1.75 inches.

Figure A-6 shows the complete test setup. The blades on the carriage are just entering the tops of the sample holders (which serve to guide the blades) prior to shearing the sample.

### 4. TEST SUBJECTS

Both manikin and human test subjects were used during this test program.

A 95th percentile Alderson manikin, designated VIP-95, and a GARD manikin, designated CG-95 were used for structural and equipment proof tests.

An ADAM manikin representative of the "large" flying population was also used during this test program to measure the dynamic response for various preload conditions.

Human test subjects were dressed in a flight suit, gloves, and boots. In addition, they wore goggles and a HGU-26/P helmet (visor down).

### 5. INSTRUMENTATION

The electronic data collected during this test program is described in Sections 5.1 and 5.2. Section 5.1 discusses accelerometers while Section 5.2 discusses load transducers. Section 5.3 discusses the calibration procedures that were used. The measurement instrumentation used in this test program is listed in Tables A-1a through A-1d. These figures designate the manufacturer, type, serial number, sensitivity and other pertinent data on each transducer used. Table A-2 lists the manufacturer's typical transducer specifications.

Accelerometers and load transducers were chosen to provide the optimum resolution over the expected test load range. Full scale data ranges were chosen to provide the expected full scale range plus 50% to assure the capture of peak signals. All transducer bridges were balanced for zero



output prior to the start of each test. The accelerometers were adjusted for the effect of gravity using computer processing software. The component of a 1 G vector in line with the force of gravity that lies along the accelerometer axis was added to each accelerometer.

The accelerometer and load transducer coordinate systems are shown in Figure A-7. The seat coordinate system is right-handed with the z axis parallel to the seat back and positive upward. The x axis is perpendicular to the z axis and positive eyes forward from the subject. The y axis is perpendicular to the x and z axes according to the right hand rule. The origin of the seat coordinate system is designated as the seat reference point (SRP). The SRP is at the midpoint of the line segment formed by the intersection of the seat pan and seat back. All vector components (for accelerations, angular accelerations, forces, moments, etc.) were positive when the vector component (x, y and z) was in the direction of the positive axis.

The linear accelerometers were wired to provide a positive output voltage when the acceleration experienced by the accelerometer was applied in the +x, +y and +z directions, as shown in Figure A-7.

The angular  $R_y$  accelerometers were wired to provide a positive output voltage when the angular acceleration experienced by the angular accelerometer was applied in the +y direction according to the right hand rule, as shown in Figure A-7.

The load cells and load links were wired to provide a positive output voltage when the force exerted by the load cell on the subject was applied in the +x, +y or +z direction as shown in Figure A-7.

All transducers except the carriage accelerometers and the carriage velocity tachometer were referenced to the seat coordinate system. The carriage tachometer was wired to provide a positive output voltage during freefall. The carriage accelerometers were referenced to the carriage coordinate system, as shown in Figure A-7.

The ADAM manikin internal transducers were referenced to the manikin coordinate system which is shown in Figure A-8.

The manikin neck and lumbar load cells were wired to provide a positive output voltage when the force exerted by the load cell, on the neck or lumbar, was applied in the +x, +y or +z directions as shown in Figure A-8.

The manikin  $M_y$  torque transducers were wired to provide a positive output voltage when the torque experienced by the transducers was applied in the +y direction according to the right hand rule, as shown in Figure A-8.

Carriage velocity was measured using a Globe Industries tachometer Model 22A672-2. The rotor of the tachometer was attached to an aluminum wheel with a rubber "O" ring around its circumference to assure good rail contact. The wheel contacted the track rail and rotated as the carriage moved, producing an output voltage proportional to the velocity.

### 5.1 Accelerometers

This section describes the accelerometer instrumentation as required in the AL/CFBE test plan.

Human head accelerations were measured using three Endevco Model 7264-200 linear accelerometers and one Endevco Model 7302A angular (Ry) accelerometer. The accelerometers were mounted to the external edge of a plastic dental bite block. Each subject had his own set of custom fitted dental inserts that were used to support the bite block in his mouth. Figure A-9 illustrates the human head accelerometer package.

Head accelerations for manikin tests were measured using three Endevco Model 2264-200 linear accelerometers and one Endevco Model 7302B angular (Ry) accelerometer. These accelerometers were internally mounted in the head of the manikins.

The chest accelerometer package consisted of three Endevco Model 7264-200 linear accelerometers mounted to a 1/2 x 1/2 x 1/2 inch aluminum block. An Endevco Model 7302A angular (Ry) accelerometer was mounted on a bracket adjacent to the triaxial chest block. The accelerometer packages were inserted into a steel protection shield to which a length of Velcro fastener strap was attached. The package was placed over the subject's sternum at the level of the xiphoid and was held there by fastening the Velcro strap around the subject's chest. Figure A-10 illustrates the chest accelerometer package attached to a human subject.

Carriage accelerations were measured using three Endevco linear accelerometers: one model 2262A-200 for acceleration in the z direction and two models 2264-200 for accelerations in the x and y directions. The three accelerometers were mounted on a small acrylic block and located behind the seat on the VIP seat structure.

Seat accelerations were measured using three Endevco linear accelerometers: two Models 2264-150 for accelerations in the x and z directions and one model 2264-200 for acceleration in the y direction. The three linear accelerometers were attached to a 1 x 1 x 3/4 inch acrylic block and were mounted near the center of the load cell mounting plate.

### 5.2 Load Transducers

This section describes the load transducer instrumentation as required in the AL/CFBE test plan.

The load transducer locations and dimensions are shown in Figures A-11a and A-11b.

Shoulder/anchor forces were measured using one GM/DYN 3D-SW and two AAMRL/DYN 3D-SW triaxial load cells, each capable of measuring forces in the x, y and z directions. The parameters measured are indicated below:

- Shoulder x, y and z force

- Left lap belt x, y and z force

- Right lap belt x, y and z force

The lap/vertical anchor force triaxial load cells were located on separate brackets mounted on the side of the seat frame parallel to the seat pan. The shoulder strap force triaxial load cell was mounted on the seat frame between the seat back support plate and the headrest.

Left, right and center seat forces were measured using three load cells and three load links. The three load cells included three Strainert Model FL2.5U-2SPKT load cells. The three load links, as shown in Figure A-12, were fabricated by DynCorp using Micro Measurement Model EA-06-062TJ-350 strain gages. All six measurement devices were located under the seat pan support plate. The load links were used for measuring loads in the x and y directions, two in the x direction and one in the y direction. Each load link housed a swivel ball which acted as a coupler between the seat pan and load cell mounting plate. The Strainert load cells were used for measuring loads in the z direction. The seat pan instrumentation and the lap belt anchor load cells can be seen in Figure A-13.

Upper and lower headrest x forces were measured using two Strainert Model FL1U-2SG load cells. The load cells were mounted on a rectangular mounting plate which was attached to the upper seat back. The headrest was attached directly to the load cells. The mounting plate/load cells/headrest was adjusted up or down depending on the location of the subjects head. The headrest and shoulder belt anchor load cells can be seen in Figure A-14.

For large ADAM manikin tests, Lumbar x, y and z forces and My torque, and Neck x, y and z forces and My torque were each measured using Denton Model 1914 and 1716 load cells respectively. These load cells were internally mounted in the manikins.

### 5.3 Calibration

Calibrations were performed before and after testing to confirm the accuracy and functional characteristics of the transducers. Pre-program and post-program calibrations are given in Tables A-3a through A-3e.

The calibration of all Strainert load cells was performed by the Precision Measurement Equipment Laboratories (PMEL) at Wright-Patterson Air Force Base. PMEL calibrated these devices on a periodic basis and provided current sensitivity and linearity data.

The calibration of the accelerometers was performed by DynCorp using the comparison method (Ensor, 1970). A laboratory standard accelerometer, calibrated on a yearly basis by Endevco with standards traceable to the National Bureau of Standards, and a test accelerometer were mounted on a shaker table. The frequency response and phase shift of the test accelerometer were determined by driving the shaker table with a random noise generator and analyzing the outputs of the accelerometers with a Zenith 248/12 computer using Fourier analysis. The natural frequency and the damping factor of the test accelerometer were determined, recorded and compared to previous calibration data for that test accelerometer. Sensitivities were calculated at a 40 G/100 Hertz level. The sensitivity of the test accelerometer was determined by comparing its output to the output of the standard accelerometer.

The angular accelerometers were calibrated by DynCorp by comparing their output to the output of a linear standard accelerometer. The angular accelerometer is mounted parallel to the axis of rotation of a Honeywell low inertia D. C. motor. The standard accelerometer is mounted perpendicular to the axis of rotation at a radius of one inch to measure the tangential acceleration. The D. C. motor motion is driven at a constant sinusoidal angular acceleration of 100 Hertz and the sensitivity is calculated by comparing the rms output voltages of the angular and linear accelerometers.

The shoulder/lap triaxial load cells and load links were calibrated by DynCorp. These transducers were calibrated to a laboratory standard load cell in a special test fixture. The sensitivity and linearity of each test load cell were obtained by comparing the output of the test load cell to the output of the laboratory standard under identical loading conditions. The laboratory standard load cell, in turn, is calibrated by PMEL on a periodic basis.

The velocity wheel is calibrated periodically by DynCorp by rotating the wheel at approximately 2000, 4000 and 6000 revolutions per minute (RPM) and recording both the output voltage and the RPM.

## 6. DATA ACQUISITION

Data acquisition was controlled by a comparator on the Master Instrumentation Control Unit in the Instrumentation Station. The test was initiated when the comparator countdown clock reached zero. The comparator was set to start data collection at a preselected time.

A reference mark pulse was generated to mark the ADACS electronic data at a preselected time after test initiation to place the reference mark close to the impact point. The reference mark time was used as the start time for data processing of the electronic data.

Prior to each test and prior to placing the subject in the seat, data were recorded to establish a zero reference for all data transducers. These data were stored separately from the test data and were used in the processing of data.

### 6.1 Automatic Data Acquisition and Control System (ADACS)

Installation of the ADACS instrumentation is shown in Figure A-15. The three major components of the ADACS system are the power conditioner, signal conditioners and the encoder. A block diagram of the ADACS is shown in Figure A-16. The signal conditioners contain forty-eight amplifiers with programmable gain and filtering.

Bridge excitation for load cells and accelerometers was 10 VDC. Bridge completion and balance resistors were added as required to each module input connector.

The forty-eight module output data signals were digitized and encoded into forty-eight 11-bit digital words. Two additional 11-bit synchronization (sync) words were added to the data frame making a fifty word capability.

Three synchronization pulse trains (bit sync, word sync and frame sync) along with the NRZL data were sent to the computer via a junction box data cable.

The PDP 11/34 minicomputer received serial data from the ADACS. The serial data coming from the carriage are converted to parallel data in the data formatter. The data formatter inputs data by direct memory access (DMA) into the computer memory via a buffered data channel where data are temporarily stored on disk. Data are later transferred to the VAX 11/750 and output to magnetic tape for permanent storage. The interrelationships among the data acquisition and storage equipment are shown in Figure A-17.

Test data could be reviewed immediately after each test by using the "quick look" SCAN routine. SCAN was used to produce a plot of the data stored on any channel as a function of time. The routine determined the minimum and maximum values of any data plot. It was also used to calculate the rise time, pulse duration and carriage acceleration and create a disk file containing significant test parameters.

## 6.2 Selspot Motion Analysis System

The AL/CFBE test plan did not require photogrammetric data to be collected for this test program. Therefore, the Selspot Motion Analysis System was not used.

However, a Kodak Ektapro 1000 video system was used to provide offboard coverage of each test. This video recorder and display unit is capable of recording high-speed motion up to a rate of 1000 frames per second. The Kodak Ektapro 1000 Video System (less camera) is shown in Figure A-18. Immediate replay of the impact is possible in real time or in slow motion.

## 7. PROCESSING PROGRAMS

The executable images for the ADACS processing programs are located in directory PROCESS of the VAX 11/750 and the test data is assumed to be stored in logical directory DATADIR. All plots and the test summary sheet are output to the LN03 laser printer. The test base file is output to directory PROCESS.

### 7.1 ADACS Program Operation

The two Fortran programs that process the ADACS test data for the DP2 Study (Vertical Deceleration Tower facility) are named DP2VDT0A and DP2VDT0B. The DCL file which controls the execution of these programs is named DP2VDT. The character string 'DP2' identifies the study, 'VDT' identifies the facility (Vertical Deceleration Tower), '0' is the revision number and the last character determines the program order of execution.

DP2VDT0A accepts user input and creates a temporary DCL file which controls the sequential batch processing of a specified number of tests. DP2VDT0A requests the user to enter the total number of tests to be processed and the test number of each test. Logical directory DATADIR is assumed to contain a zero reference file named '<test no>Z.VDT', a test data file named '<test no>D.VDT' and a sensitivity file named '<test no>S.VDT'.

DP2VDT0A requests the user to enter the total number of tests to be processed and the test number for each test. The default test parameters are retrieved from the header block of the test data file and displayed as a menu on the screen. The user may specify new values for any of the displayed test parameters. The test parameters include the subject ID, weight, age, height and sitting height. Additional parameters include the cell type, nominal G level, subject type (manikin or human) and belt preload status (computed or not computed). If the belt preloads were computed, then the left lap, right lap and shoulder strap preloads are also displayed.

DP2VDT0B generates time histories for the carriage x, y and z axis accelerations; the carriage velocity; the seat x, y and z axis accelerations; the head x, y, z, Ry and resultant accelerations; the chest x, y, z, Ry and resultant acceleration; and the ADAM internal chest x, y, z, Ry and resultant accelerations. The dynamic response of the DRI model is computed for the seat Z axis acceleration.

Time histories are also generated for the shoulder x, y, z and resultant forces; the headrest upper and lower x axis forces and their sum; the left lap x, y, z and resultant forces; the right lap x, y, z and resultant forces; the left, right and center seat z forces, and their sum; the left and right seat x axis forces, and their sum; the seat y axis force; and the seat resultant. The seat z force is corrected to subtract out the force due to the mass of the seat pan. If the ADAM manikin is used as the subject, the ADAM neck and lumbar x, y and z axis forces, resultant, and My torque are also computed.

The impact rise time, duration and velocity change are computed and stored in the test base file. Values for the preimpact level and the extrema for each time history are stored in the test base file and printed out as a summary sheet for each test. The time histories are also plotted.

## 7.2 ADACS Program Flowcharts

Flowcharts of the two programs, DP2VDT0A and DP2VDT0B are shown in Figures A-19 and A-20 respectively. Each flowchart identifies the files used and the subroutines called by the program. Some of the subroutines which are not flowcharted are located in user libraries. Others have such a simple structure that they do not require flowcharting.



DIGI AL INSTRUMENTATION REQUIREMENTS										DYNCORP													
PROGRAM		DYNAMIC PRELOA		2		DATE		22 APR 92		THRU		08 JUN 92		THRU		2757							
FACILITY		VERTICAL DECEL		RATTION TOWER		RUN		2667		THRU													
DATA CHANNEL	DATA POINT	XDUCER MFG & TYPE	SERIAL NUMB-R	XDUCER SENS	EXCITE V	FILTER SERIES	AMP GAIN	S/M	SAMPLE RATE	FULL SCALE SENS.	FILTER HZ	XDUCER ZERO RANGE	BRIDGE BALANCE RESISTORS	BRIDGE COMP RESISTORS	SPECIAL NOTATIONS								
15	LEFT SEAT x FORCE	NM/DYN EA-06-06 2TJ-350	003	11.08 uv/LB	10.00	60	201	13	1K	1123 LB	120	2.5 +5.0 0.0	68K +IN GND	-									
16	RIGHT SEAT x FORCE	NM/DYN EA-06-06 2TJ-350	3	10.79 uv/LB	10.00	60	201	5	1K	1153 LB	120	2.5 +5.0 0.0	26K -IN GND	-									
17	CENTER SEAT y FORCE	NM/DYN EA-06-06 2TJ-350	1	10.57 uv/LB	10.00	60	201	17	1K	1177 LB	120	2.5 +5.0 0.0	22K +IN GND	-									
18	LEFT LAP x FORCE	AMRL/DYN 3D-SW	24X	7.40 uv/LB	10.00	60	201	11	1K	1681 LB	120	2.5 +5.0 0.0	24K +IN GND	-									
19	LEFT LAP y FORCE	AMRL/DYN 3D-SW	24Y	7.08 uv/LB	10.00	60	201	4	1K	1757 LB	120	2.5 +5.0 0.0	47K +IN GND	-									
20	LEFT LAP z FORCE	AMRL/DYN 3D-SW	24Z	7.94 uv/LB	10.00	60	201	14	1K	1566 LB	120	2.5 +5.0 0.0	47K +IN GND	-									
21	RIGHT LAP x FORCE	AMRL/DYN 3D-SW	15X	5.48 uv/LB	10.00	60	201	8	1K	2270 LB	120	2.5 +5.0 0.0	17K -IN GND	-									
22	RIGHT LAP y FORCE	AMRL/DYN 3D-SW	15Y	5.42 uv/LB	10.00	60	402	8	1K	1147 LB	120	2.5 +5.0 0.0	14K +IN GND	-									
23	RIGHT LAP z FORCE	AMRL/DYN 3D-SW	15Z	6.38 uv/LB	10.00	60	201	3	1K	1950 LB	120	2.5 +5.0 0.0	3.9K -IN GND	-									
24	VELOCITY	GLOBE 22A6T 2-2	4	.0643 V/F/S	-	30	1	-	1K	77.8 F/8	60	0.0 +5.0 0.0	-	-	SIGNAL ATTENUATED BY 7.65 SENSITIVITY=0.492+7.65-.0643								
25	SHOULDER x FORCE	GM/DYN 3D-SW	20Z	6.36 uv/LB	10.00	60	402	4	1K	978 LB	120	2.5 +5.0 0.0	36K +IN GND	-									
26	SHOULDER y FORCE	GM/DYN 3D-SW	20Y	5.34 uv/LB	10.00	60	803	5	1K	585 LB	120	2.5 +5.0 0.0	33K +IN GND	-									
27	SHOULDER z FORCE	GM/DYN 3D-SW	20X	4.93 uv/LB	10.00	60	402	9	1K	1261 LB	120	2.5 +5.0 0.0	62K +IN GND	-									
28	SEAT x ACCEL.	ENDEVCO 2264-1 50	BN39	3.130 mv/G	10.00	60	25	29	1K	32.0 G	120	2.5 +5.0 0.0	-	1.65K									

PAGE 2 OF 4

PAGE 2 OF 4

TABLE A-1b: INSTRUMENTATION REQUIREMENTS



DIG TAL INSTRUMENTATION REQUIREMENTS																	DYNACORP	
PROGRAM		DYNAMIC PRELO/ 2		DATE 22 APR 92		THRU 08 JUN 92		THRU 2757		THRU 2757		THRU 2757		THRU 2757		THRU 2757		
FACILITY		VERTICAL DECEL		HATION TOWER		RUN 2667		THRU 2667		THRU 2667		THRU 2667		THRU 2667		THRU 2667		
DATA CHANNEL	DATA POINT	XOUCI NFG & TYPE	SERIAL NUMBER	XOUCER SENS	EXCITE V	CHAN	FILTER SERIES	AMP GAIN	SAMPLE RATE	SCALE	FULL SCALE SENS.	FILTER HZ	XOUCER ZERO RANGE	BRIDGE BALANCE RESISTORS	BRIDGE COMP RESISTORS	SPECIAL NOTATIONS		
29	SEAT y ACCEL.	ENDEVCO 2264-2 00	BX17	2.715 mv/g	10.00	29	60	50	1K	18.4 G	18.4 G	120	2.5 +5.0 0.0	92K +IN GND	1.65K			
30	SEAT z ACCEL.	ENDEVCO 2264-150	BB32	2.602 mv/g	10.00	30	60	25	1K	38.4 G	38.4 G	120	2.5 +5.0 0.0	110K +IN GND	1.65K			
31	UPPER HEADREST x FORCE	STRAINSEN FLIU-29G	206	20.43 uv/LB	10.00	31	60	201	1K	609 LB	609 LB	120	2.5 +5.0 0.0	-	-			
32	LOWER HEADREST x FORCE	STRAINSEN FLIU-29G	209	20.11 uv/LB	10.00	32	60	201	1K	618 LB	618 LB	120	2.5 +5.0 0.0	390K +IN GND	-			
33	NECK x FORCE	DENTON 1716	086 FX	8.17 uv/LB	10.00	33	60	100	1K	3060 LB	3060 LB	120	2.5 +5.0 0.0	-	-			
34	NECK y FORCE	DENTON 1716	086 FY	8.71 uv/LB	10.00	34	60	100	1K	2870 LB	2870 LB	120	2.5 +5.0 0.0	-	-			
35	NECK z FORCE	DENTON 1716	086 FZ	4.69 uv/LB	10.00	35	60	201	1K	2652 LB	2652 LB	120	2.5 +5.0 0.0	-	-			
36	NECK My FORCE	DENTON 1716	086 MY	6.74 uv/LB-IN	10.00	36	60	100	1K	3709 LB-IN	3709 LB-IN	120	2.5 +5.0 0.0	-	-			
37	LUMBAR x FORCE	DENTON 1914	040 FX	6.43 uv/LB	10.00	37	60	50	1K	7776 LB	7776 LB	120	2.5 +5.0 0.0	-	-			
38	LUMBAR y FORCE	DENTON 1914	040 FY	6.43 uv/LB	10.00	38	60	50	1K	7776 LB	7776 LB	120	2.5 +5.0 0.0	-	-			
39	LUMBAR z FORCE	DENTON 1914	040 FZ	2.738 uv/LB	10.00	39	60	100	1K	9130 LB	9130 LB	120	2.5 +5.0 0.0	-	-			
40	LUMBAR My FORCE	DENTON 1914	040 MY	5.11 uv/LB-IN	10.00	40	60	50	1K	9785 LB-IN	9785 LB-IN	120	2.5 +5.0 0.0	-	-			
45	EVENT	-	-	1.0 VOLT	-	45	1000	2.5	1K	2.5 VOLT	2.5 VOLT	2000	5.0 +5.0 0.0	-	-			
46	T = Ø	-	-	1.0 VOLT	-	46	1000	1	1K	5.0 VOLT	5.0 VOLT	2000	5.0 +5.0 0.0	-	-			

PAGE 3 OF 4

PAGE 3 OF 4

TABLE A-1c: INSTRUMENTATION REQUIREMENTS



MANUFACTURER	MODEL	RANGE	SENSITIVITY (mv)	RESONANCE FREQ (Hz)	FREQUENCY RESPONSE (Hz.)	EXCITATION (Volt)	2 ARM or 4 ARM	ADDITIONAL NOTES
Endevco	2264-150	± 150 G	2.5/G	3400	0-800	10	2 arm	Linear accelerometer
Endevco	2264-200	± 200 G	2.5/G	4700	0-1200	10	2 arm	Linear accelerometer
Endevco	7264-200	± 200 G	2.5/G	6000	0-1200	10	2 arm	Linear accelerometer, 1000 G overrange
Endevco	2262A-200	± 200 G	2.5/G	7000	0-2000	10	4 arm	Linear accelerometer, .7 damping ratio
Endevco	7302A	± 50,000 Rad/Sec <sup>2</sup>	.0055 /Rad/Sec <sup>2</sup>	2500	1-600	10	4 arm	Angular accelerometer, X10 overrange
Endevco	7302B	± 50,000 Rad/Sec <sup>2</sup>	.004 /Rad/Sec <sup>2</sup>	3000	1-600	10	4 arm	Angular accelerometer, X10 overrange
Straininsert	FL2.5U- 2SPKT	± 2500 LB	.008/LB	3600	0-2000	10	4 arm	Load cell; 15 V max exc.; 5 K LB max. overrange
Straininsert	FL1U-2SG	± 1000 LB	.020/LB	3600	0-2000	10	4 arm	Load cell; 15 V max exc.; 2 K LB max. overrange
Denton	1914	± 5000 LB	-	N/A	N/A	10	4 arm	6 axis load cell; 15 V max. exc.
Denton	1716	± 3000 LB	-	N/A	N/A	10	4 arm	6 axis load cell; 15 V max. exc.

TABLE A-2: TYPICAL TRANSDUCER SPECIFICATIONS

# **DYNCORP PROGRAM CALIBRATION LOG**

PROGRAM Dynamic Preload 2 DATES: 22 APR 92 - 08 JUN 92  
 FACILITY Vertical Deceleration Tower RUN NUMBERS: 2667 - 2757

DATA POINT	TRANSDUCER MFG. & MODEL	SERIAL NUMBER	PRE-CAL		POST-CAL		XCHANGE	NOTES
			DATE	SENS	DATE	SENS		
CARRIAGE z ACCEL.	ENDEVCO 2262A-200	FR31	07APR92	5.122 mv/G	10JUN92	5.119 mv/G	-0.1	
CARRIAGE x ACCEL.	ENDEVCO 2264-200	BP10	06APR92	2.483 mv/G	10JUN92	2.474 mv/G	-0.4	
CARRIAGE y ACCEL.	ENDEVCO 2264-200	BN61	04APR92	2.870 mv/G	10JUN92	2.879 mv/G	+0.3	
DUMMY HEAD x ACCEL.	ENDEVCO 2264-200	CH74	08APR92	2.959 mv/G	10JUN92	3.013 mv/G	+1.8	
DUMMY HEAD y ACCEL.	ENDEVCO 2264-200	BQ42	08APR92	2.729 mv/G	10JUN92	2.703 mv/G	-1.0	
DUMMY HEAD z ACCEL.	ENDEVCO 2264-200	CH73	08APR92	2.741 mv/G				Damaged between end of testing and re- moval from facility. Cal. cannot be done.
DUMMY HEAD Ry ANGULAR ACCEL.	ENDEVCO 7302B	TJ75	09APR92	3.904 uv/RAD/ SEC2	11JUN92	3.766 uv/RAD/ SEC2	-3.5	
CHEST x ACCEL.	ENDEVCO 7264-200	BH76H	08APR92	3.182 mv/G	10JUN92	3.189 mv/G	+0.2	
CHEST y ACCEL.	ENDEVCO 7264-200	BH81H	08APR92	3.252 mv/G	10JUN92	3.262 mv/G	+0.3	
CHEST z ACCEL.	ENDEVCO 7264-200	BH87H	08APR92	2.980 mv/G	10JUN92	2.988 mv/G	+0.3	

PAGE 1 OF 5

**TABLE A-3a: TRANSDUCER PRE- AND POST-CALIBRATION**

# DYNCORP PROGRAM CALIBRATION LOG

**PROGRAM** Dynamic Preload 2      **DATES:** 22 APR 92 - 08 JUN 92  
**FACILITY** Vertical Deceleration Tower      **RUN NUMBERS:** 2667 - 2757

DATA POINT	TRANSDUCER MFG. & MODEL	SERIAL NUMBER	PRE-CAL		POST-CAL		XCHANGE	NOTES
			DATE	SENS	DATE	SENS		
SEAT x ACCEL.	ENDEVCO 2264-200	BN39	07APR92	3.130 mv/G	10JUN92	3.129 mv/G	0.0	
SEAT y ACCEL.	ENDEVCO 2264-200	BX17	07APR92	2.715 mv/G	10JUN92	2.626 mv/G	-3.3	
SEAT z ACCEL.	ENDEVCO 2264-150	BB32	07APR92	2.602 mv/G	10JUN92	2.680 mv/G	+3.0	
HUMAN HEAD x ACCEL.	ENDEVCO 7264-200	CL39H	31MAR92	3.197 mv/G				Tests 2667-2705 dam- aged during testing.
HUMAN HEAD y ACCEL.	ENDEVCO 7264-200	CL83H	31MAR92	2.929 mv/G	10JUN92	2.924 mv/G	-0.2	
HUMAN HEAD z ACCEL.	ENDEVCO 7264-200	CL86H	31MAR92	2.870 mv/G	10JUN92	2.865 mv/G	-0.2	
HUMAN HEAD ANGULAR	ENDEVCO 7302A	H74P	09APR92	3.800 uv/RAD/ SEC2	11JUN92	3.805 uv/RAD/ SEC2	+0.1	
HUMAN HEAD x ACCEL.	ENDEVCO 7264-200	CD85H	19AUG91	2.692 mv/G	10JUN92	2.674 mv/G	-0.7	Tests 2705-2757.

PAGE 2 OF 5

TABLE A-3b: TRANSDUCER PRE- AND POST-CALIBRATION

# **DYNCORP PROGRAM CALIBRATION LOG**

**PROGRAM** Dynamic Preload 2      **DATES:** 22 APR 92 - 08 JUN 92  
**FACILITY** Vertical Deceleration Tower      **RUN NUMBERS:** 2667 - 2757

DATA POINT	TRANSDUCER MFG. & MODEL	SERIAL NUMBER	PRE-CAL		POST-CAL		XCHANGE	NOTES
			DATE	SENS	DATE	SENS		
LEFT SEAT z FORCE	STRAINSERT FL2.5U-2SPKT	3294-3	26AUG91	8.08 uv/LB				Calibrated period- ically by PMEL.
RIGHT SEAT z FORCE	STRAINSERT FL2.5U-2SPKT	7135-3	04NOV91	7.92 uv/LB				Calibrated period- ically by PMEL.
CENTER SEAT z FORCE	STRAINSERT FL2.5U-2SPKT	7588-2	20DEC91	8.04 uv/LB				Calibrated period- ically by PMEL.
LEFT SEAT x FORCE	MM/DYN EA-06-062TJ-350	003	10APR92	11.08 uv/LB	16JUN92	11.16 uv/LB	+ .7	
RIGHT SEAT x FORCE	MM/DYN EA-06-062TJ-350	3	10APR92	10.79 uv/LB	16JUN92	10.77 uv/LB	-0.2	
CENTER SEAT y FORCE	MM/DYN EA-06-062TJ-350	1	10APR92	10.57 uv/LB	16JUN92	10.66 uv/LB	+ .8	
LEFT LAP x FORCE	AAMRL/DYN 3D-SW	24X	10APR92	7.40 uv/LB	11JUN92	7.39 uv/LB	- .1	
LEFT LAP y FORCE	AAMRL/DYN 3D-SW	24Y	10APR92	7.08 uv/LB	11JUN92	7.02 uv/LB	- .8	
LEFT LAP z FORCE	AAMRL/DYN 3D-SW	24Z	10APR92	7.94 uv/LB	11JUN92	7.84 uv/LB	-1.1	
RIGHT LAP x FORCE	AAMRL/DYN 3D-SW	15X	10APR92	5.48 uv/LB	11JUN92	5.39 uv/LB	-2.0	

**TABLE A-3c: TRANSDUCER PRE- AND POST-CALIBRATION**

# DYNCORP PROGRAM CALIBRATION LOG

**PROGRAM** Dynamic Perload 2      **DATES:** 22 APR 92 - 08 JUN 92  
**FACILITY** Vertical Deceleration Tower      **RUN NUMBERS:** 2667 - 2757

DATA POINT	TRANSDUCER MFG. & MODEL	SERIAL NUMBER	PRE-CAL		POST-CAL		XCHANGE	NOTES
			DATE	SENS	DATE	SENS		
RIGHT LAP y FORCE	AAMRL/DYN 3D-SW	15Y	10APR92	5.42 uv/LB	11JUN92	5.39 uv/LB	- .5	
RIGHT LAP z FORCE	AAMRL/DYN 3D-SW	15Z	10APR92	6.38 uv/LB	11JUN92	6.30 uv/LB	-1.3	
SHOULDER x FORCE	GM/DYN 3D-SW	20Z	10APR92	6.36 uv/LB	11JUN92	6.30 uv/LB	- .9	
SHOULDER y FORCE	GM/DYN 3D-SW	20Y	10APR92	5.34 uv/LB	11JUN92	5.32 uv/LB	- .4	
SHOULDER z FORCE	GM/DYN 3D-SW	20X	10APR92	4.93 uv/LB	11JUN92	4.89 uv/LB	- .8	
UPPER HEADREST x FORCE	STRAINERT FL1U-2SG	206	06SEP89	20.43 uv/LB				Calibrated period- ically by PMEL.
LOWER HEADREST x FORCE	STRAINERT FL1U-2SG	209	06SEP89	20.11 uv/LB				Calibrated period- ically by PMEL.

PAGE 4 OF 5

TABLE A-3d: TRANSDUCER PRE- AND POST-CALIBRATION

# DYNCORP PROGRAM CALIBRATION LOG

**PROGRAM** Dynamic Preload 2      **DATES:** 22 APR 92 - 08 JUN 92  
**FACILITY** Vertical Deceleration Tower      **RUN NUMBERS:** 2667 - 2757

DATA POINT	TRANSDUCER MFG. & MODEL	SERIAL NUMBER	PRE-CAL		POST-CAL		XCHANGE	NOTES
			DATE	SENS	DATE	SENS		
NECK x FORCE	DENTON 1716	086FX	25FEB92	8.17 uv/LB				
NECK y FORCE	DENTON 1716	086FY	25FEB92	8.71 uv/LB				
NECK z FORCE	DENTON 1716	086FZ	25FEB92	4.69 uv/LB				
NECK My FORCE	DENTON 1716	086MY	25FEB92	6.74 uv/ IN-LB				
LUMBAR x FORCE	DENTON 1914	040FX	10OCT91	6.43 uv/LB				
LUMBAR y FORCE	DENTON 1914	040FY	10OCT91	6.43 uv/LB				
LUMBAR z FORCE	DENTON 1914	040FZ	10OCT91	2.738 uv/LB				All transducers on this page are con- tractor SRL's respon- sibility.
LUMBAR My FORCE	DENTON 1914	040MY	10OCT91	5.11 uv/ IN-LB				

PAGE 5 OF 5

TABLE A-3e: TRANSDUCER PRE- AND POST-CALIBRATION



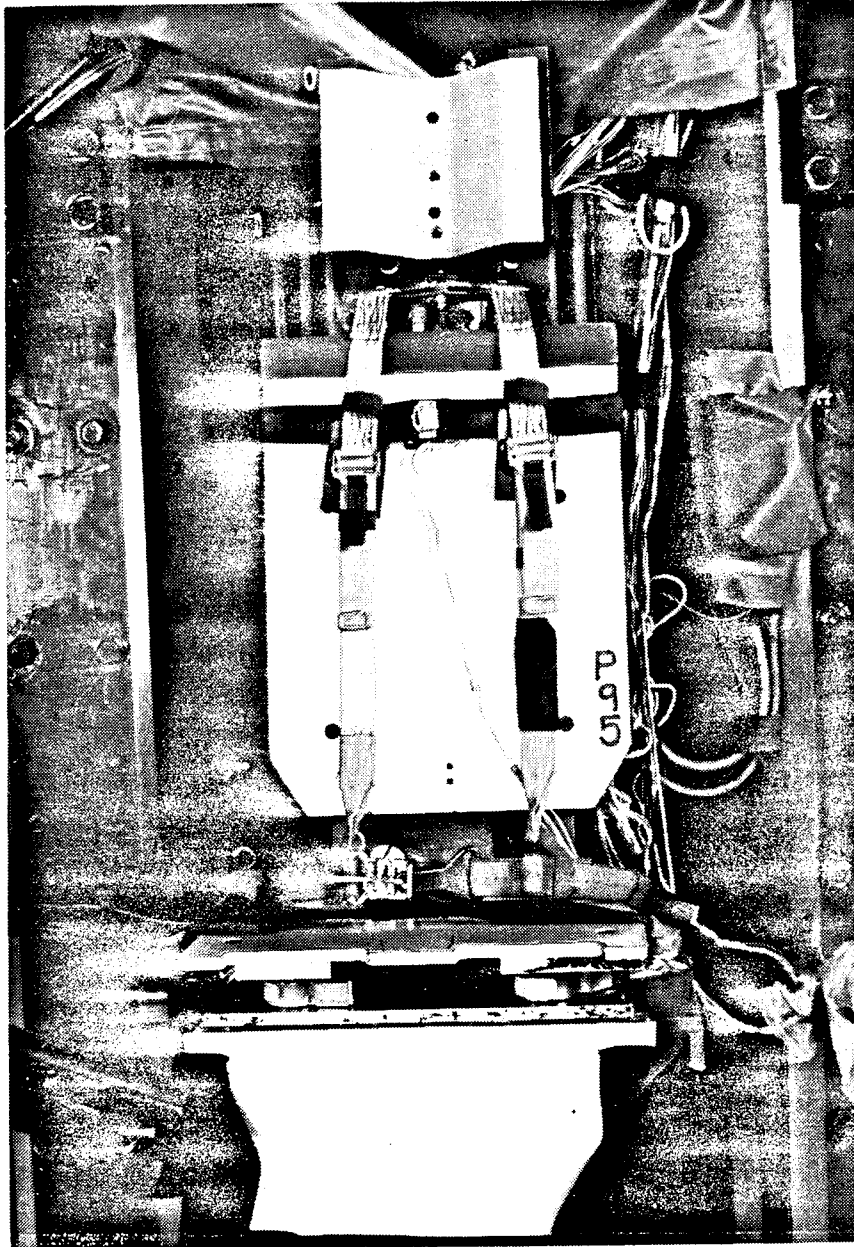


FIGURE A-1: VIP SEAT FIXTURE

A-11



FIGURE A-2: SUBJECT LEG AND THIGH RESTRAINTS

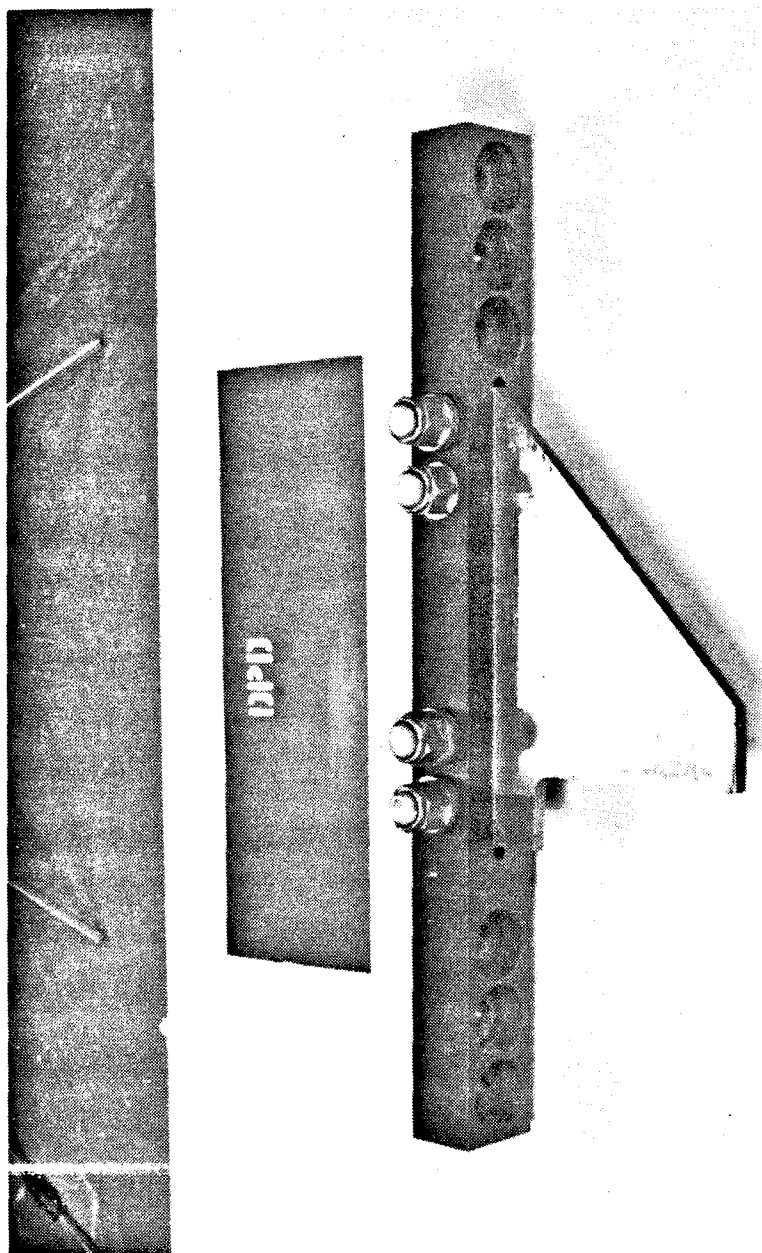


FIGURE A-3: DYNAMIC PRELOAD DEVICE BLADE

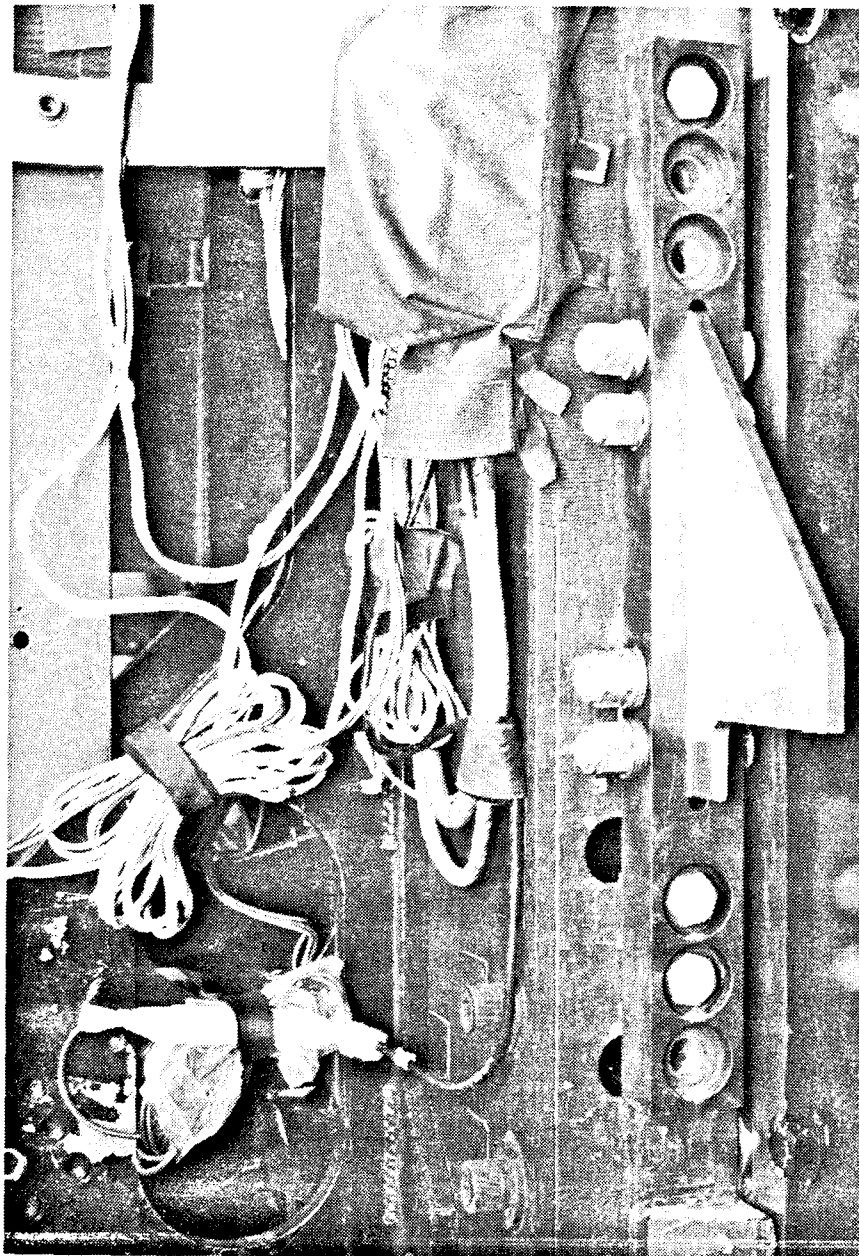


FIGURE A-4: DYNAMIC PRELOAD DEVICE BLADE

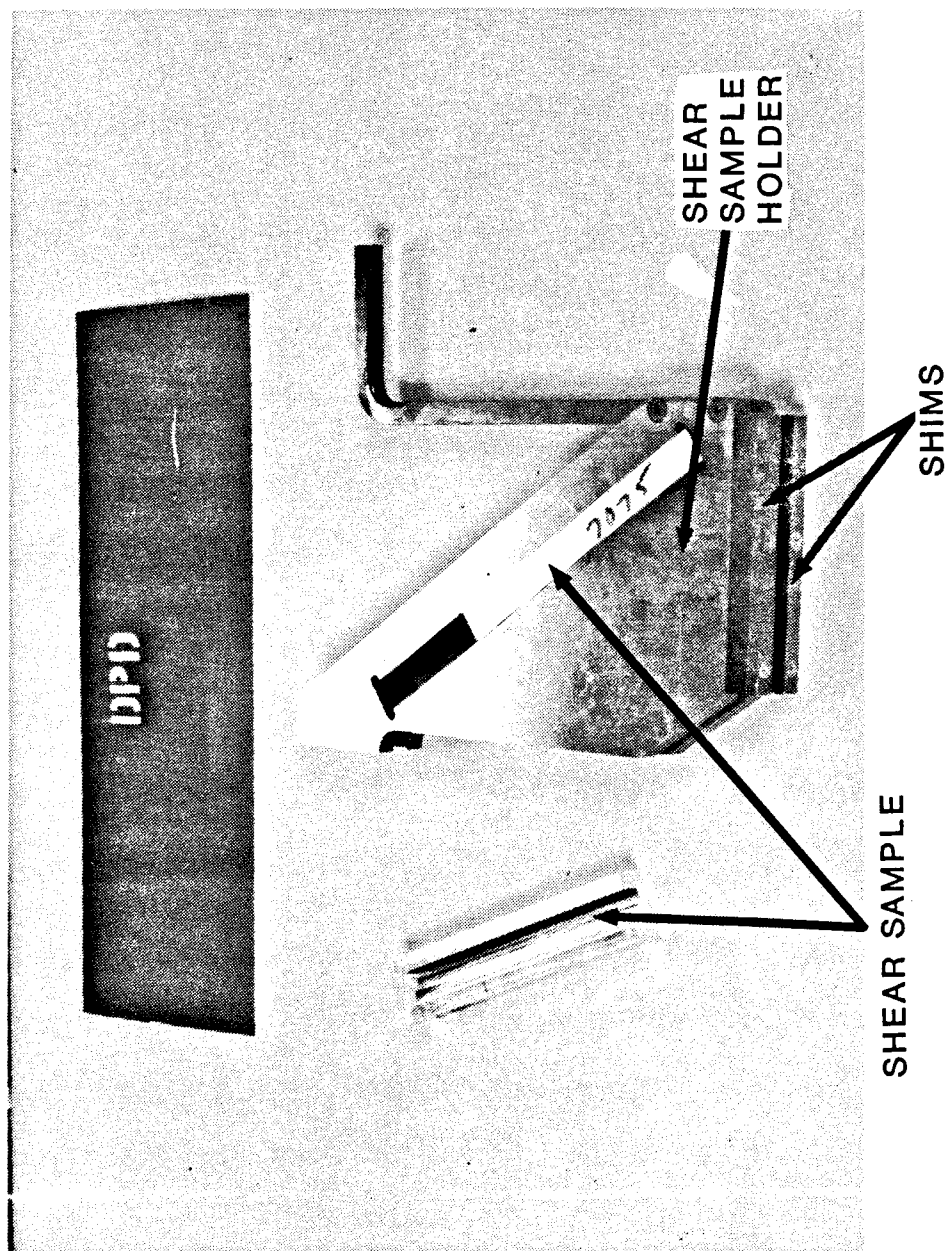
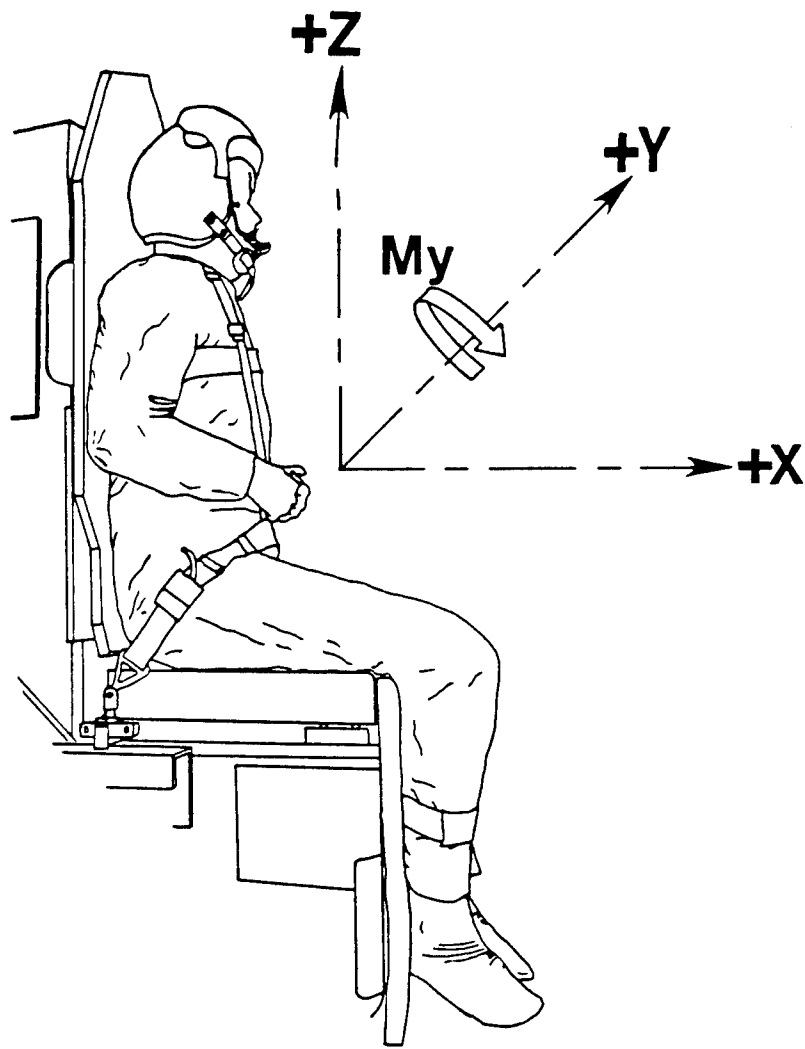


FIGURE A-5: SHEAR SAMPLE AND SHEAR SAMPLE HOLDER



1. THE ADAM MANIKIN FORCES AND TORQUES WERE REFERENCED TO THE MANIKIN COORDINATE SYSTEM.
2. THE NECK AND LUMBAR LOAD CELLS WERE WIRED TO PROVIDE A POSITIVE OUTPUT VOLTAGE WHEN THE FORCE EXERTED BY THE LOAD CELL, ON THE NECK OR LUMBAR, WAS APPLIED IN THE  $+x$ ,  $+y$  OR  $+z$  DIRECTION AS SHOWN.
3. THE  $M_y$  TORQUE TRANSDUCERS WERE WIRED TO PROVIDE A POSITIVE OUTPUT VOLTAGE WHEN THE TORQUE EXPERIENCED BY THE TRANSDUCERS WAS APPLIED IN THE  $+y$  DIRECTION ACCORDING TO THE RIGHT HAND RULE AS SHOWN.

FIGURE A-8: MANIKIN COORDINATE SYSTEM

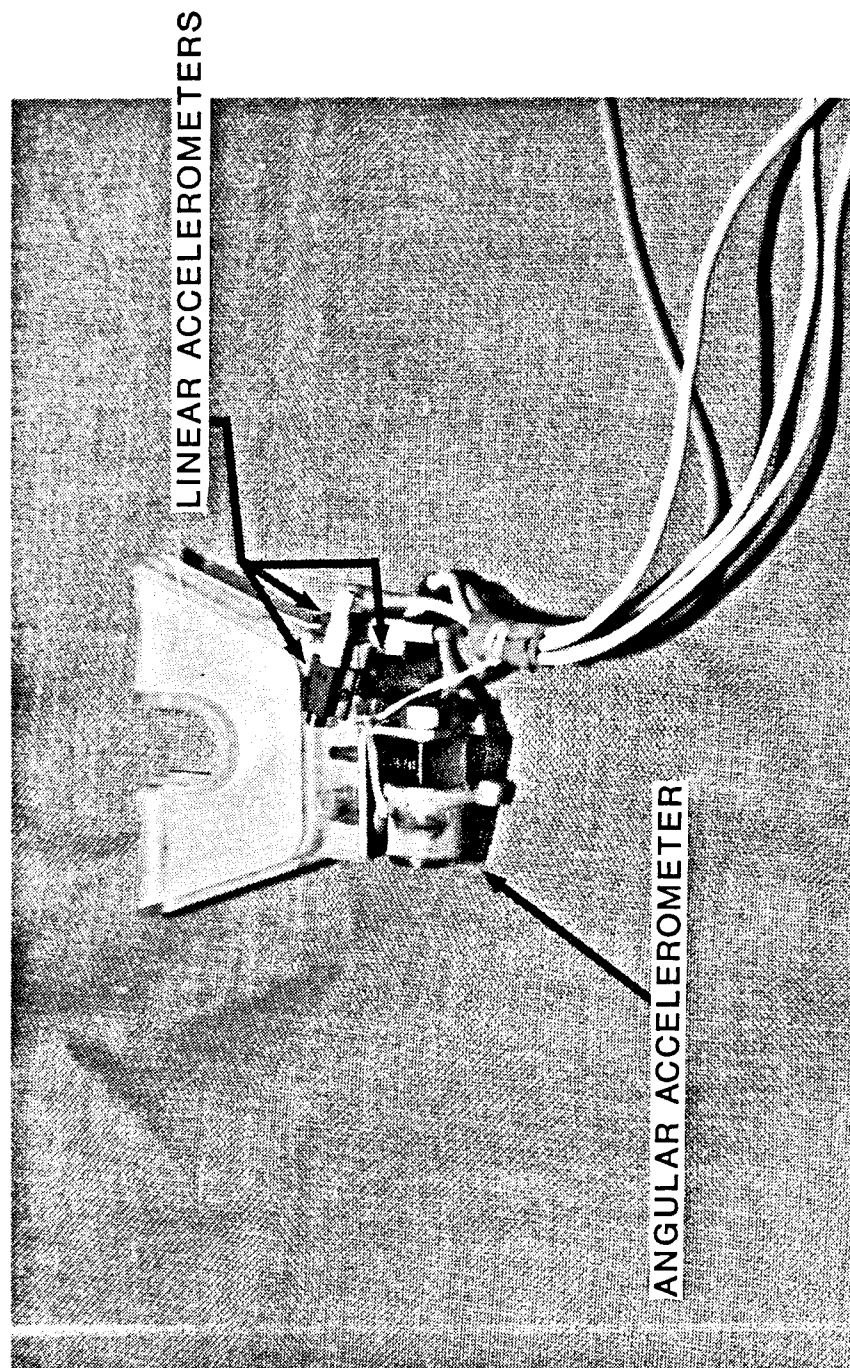


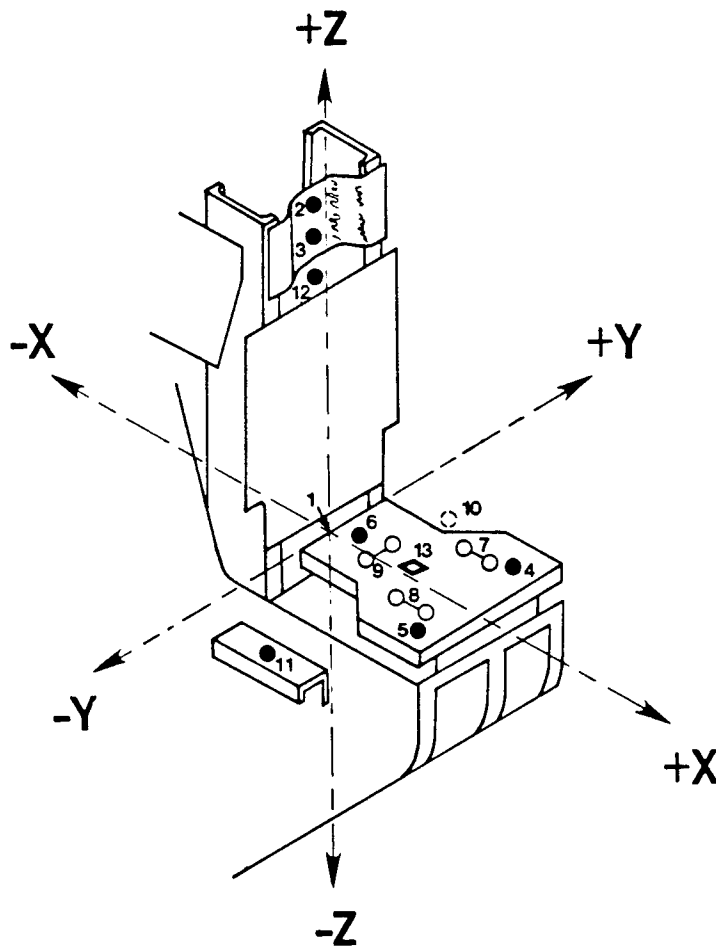
FIGURE A-9: HUMAN HEAD ACCELEROMETER PACKAGE





FIGURE A-10: CHEST ACCELEROMETER PACKAGE





<u>NO.</u>	<u>DESCRIPTION</u>	<u>NO.</u>	<u>DESCRIPTION</u>
1	SEAT REFERENCE POINT	8	RIGHT SEAT X FORCE
2	UPPER HEADREST X FORCE	9	CENTER SEAT Y FORCE
3	LOWER HEADREST X FORCE	10	LEFT LAP BELT FORCE
4	LEFT SEAT Z FORCE	11	RIGHT LAP BELT FORCE
5	RIGHT SEAT Z FORCE	12	SHOULDER FORCE
6	CENTER SEAT Z FORCE	13	SEAT X, Y & Z ACCELERATION
7	LEFT SEAT X FORCE		

ITEM 10 NOT SHOWN

THE HEADREST WAS ADJUSTABLE UP OR DOWN DEPENDING ON EACH SUBJECT. HEADREST LOAD CELL NUMBERS 2 AND 3 MOVE WITH THE HEADREST. THE MEASUREMENTS FOR THE HEADREST LOAD CELLS WERE TAKEN WHEN THE TOP MOUNTING HOLES IN THE HEAD REST WERE LINED UP WITH THE TOP HOLES IN THE FRAME SUPPORT.

FIGURE A-11a: TRANSDUCER LOCATIONS AND DIMENSIONS (PAGE 1 OF 2)

ALL DIMENSIONS ARE REFERENCED TO THE SEAT REFERENCE POINT (SRP). THE SEAT REFERENCE POINT IS LOCATED AT THE INTERSECTION OF THE SEAT PAN CENTER LINE AND THE SEAT BACK CENTER LINE (z AXIS).

CONTACT POINT DIMENSIONS IN INCHES (CM)

NO.	X	Y	Z
1	0.00 ( 0.00)	0.00 ( 0.00)	0.00 ( 0.00)
2	- 0.31 (- 0.80)	0.00 ( 0.00)	37.38 ( 94.95)
3	- 0.31 (- 0.80)	0.00 ( 0.00)	32.47 ( 82.48)
4	17.90 ( 45.46)	5.00 ( 12.70)	- 1.22 (- 3.10)
5	17.90 ( 45.46)	- 5.00 (-12.70)	- 1.22 (- 3.10)
6	6.68 ( 16.96)	0.00 ( 0.00)	- 1.22 (- 3.10)
7	10.00 ( 25.41)	6.00 ( 15.25)	- 1.85 (- 4.70)
8	10.00 ( 25.41)	- 6.00 (-15.25)	- 1.85 (- 4.70)
9	9.26 ( 23.51)	1.99 ( 5.05)	- 1.85 (- 4.70)
10	0.81 ( 2.06)	9.00 ( 22.86)	- 1.61 (- 4.10)
11	0.81 ( 2.06)	- 9.00 (-22.86)	- 1.61 (- 4.10)
12	- 5.47 (-13.90)	0.00 ( 0.00)	27.39 ( 69.58)
13	12.33 ( 31.31)	0.00 ( 0.00)	- 1.69 (- 4.30)

SEE FIGURE A-11a FOR DESCRIPTIONS OF TRANSDUCER ITEM NUMBERS

THE SEAT ACCELEROMETER MEASUREMENTS (ITEM 13) ARE TAKEN AT THE CENTER OF THE ACCELEROMETER BLOCK.

THE CONTACT POINT IS THE POINT ON THE LOAD CELL AT WHICH THE EXTERNAL FORCE IS APPLIED.

THE MEASUREMENTS FOR THE LOAD CELLS WHICH ANCHOR THE HARNESS (ITEMS 10, 11 & 12) ARE TAKEN AT THE POINT WHERE THE HARNESS IS ATTACHED TO THE LOAD CELL.

FIGURE A-11b: TRANSDUCER LOCATIONS AND DIMENSIONS (PAGE 2 OF 2)

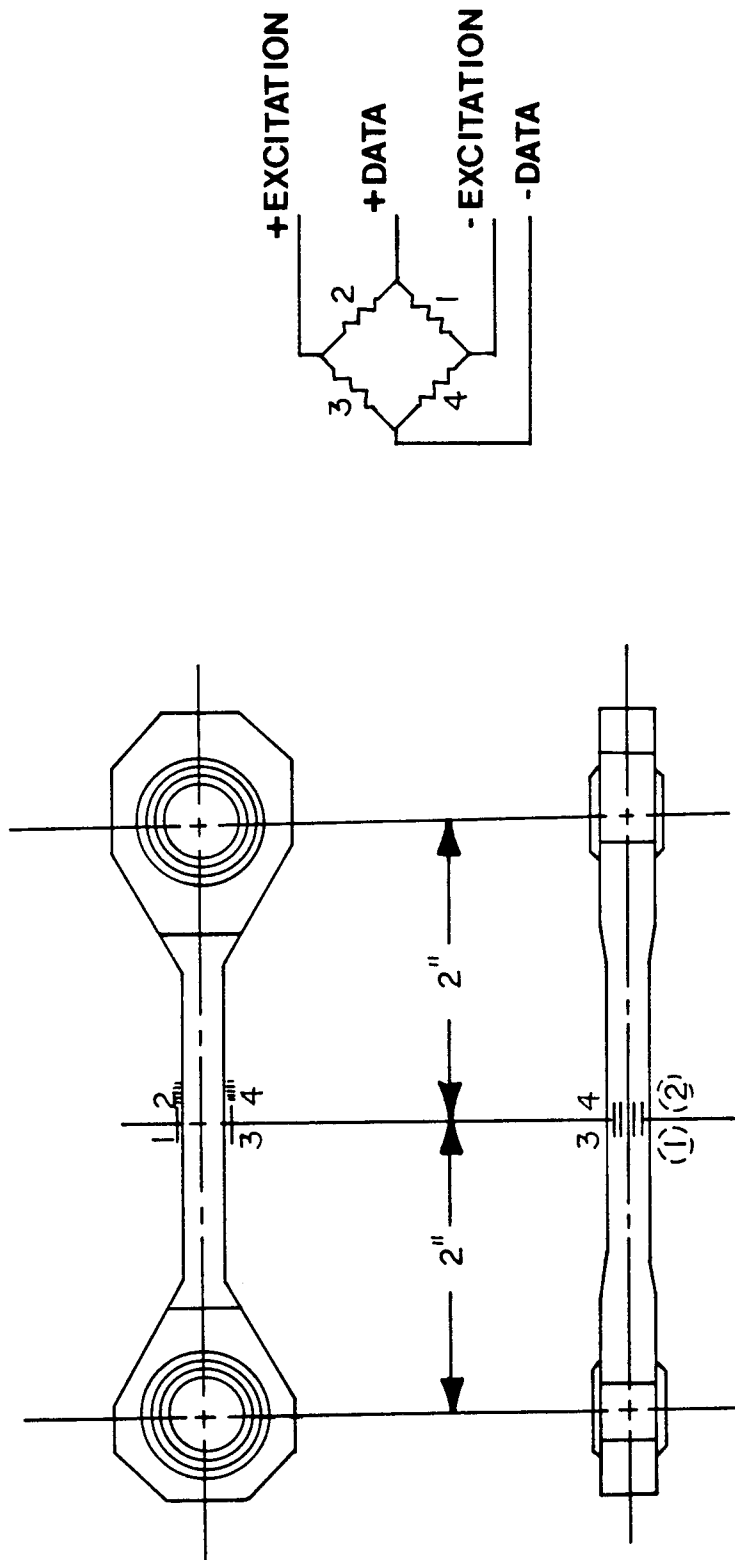
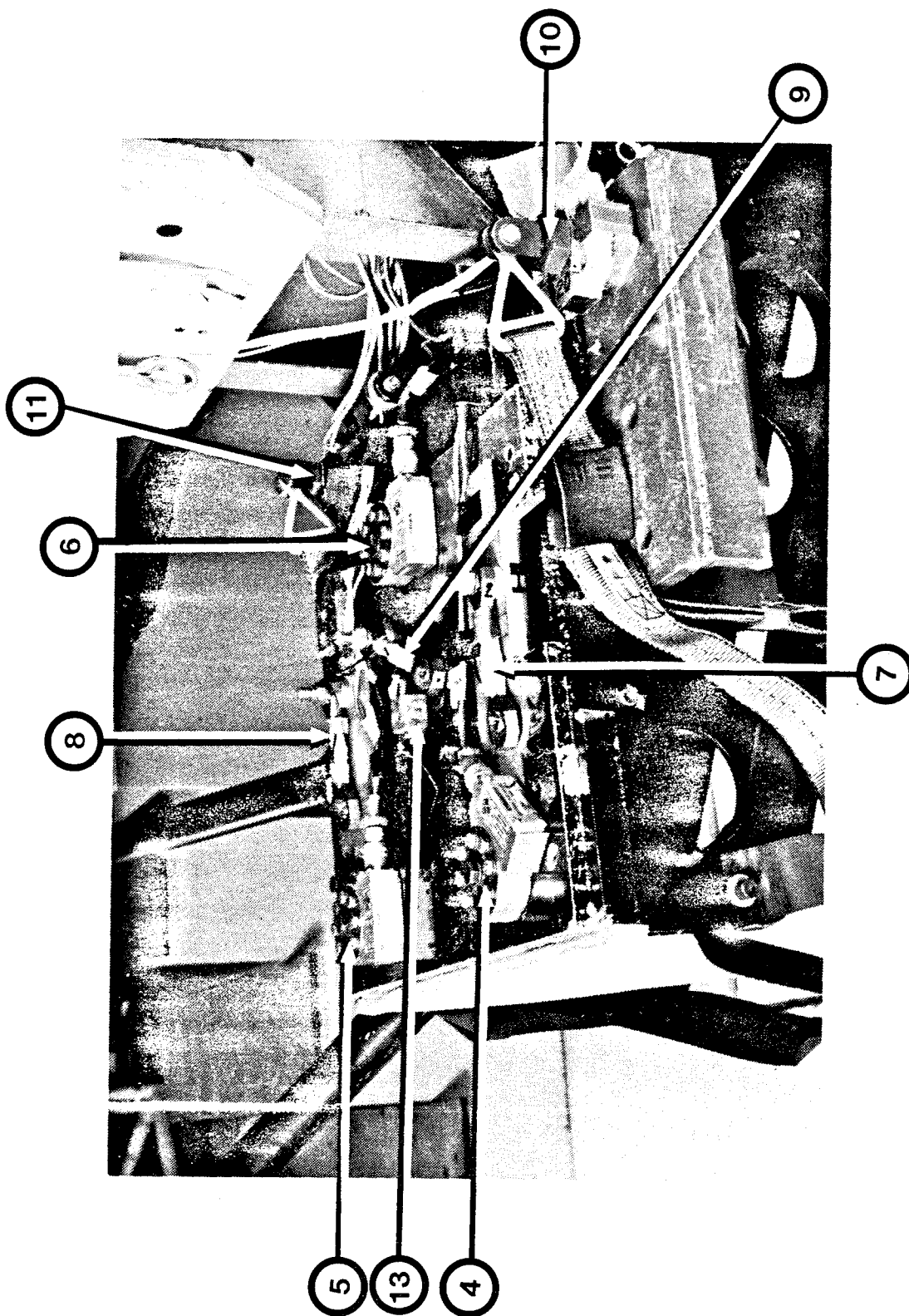
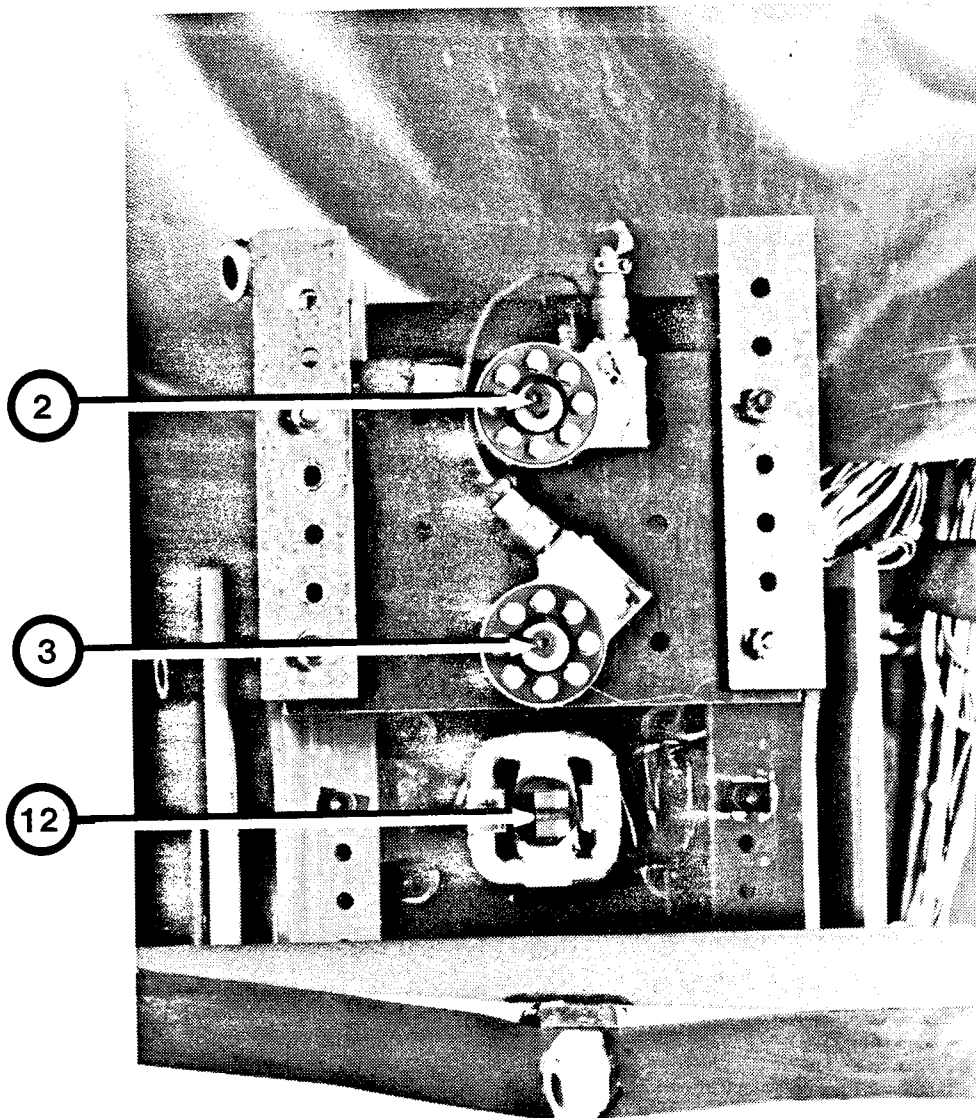


FIGURE A-12: LOAD LINK INSTRUMENTATION



NOTE: REFER TO FIGURE A-11a FOR A DESCRIPTION OF THE TRANSDUCER ITEM NUMBERS.

FIGURE A-13: SEAT PAN INSTRUMENTATION



NOTE: REFER TO FIGURE A-11a FOR A DESCRIPTION OF THE TRANSDUCER ITEM NUMBERS.

FIGURE A-14: HEADREST AND SHOULDER LOAD CELL INSTRUMENTATION

SIGNAL CONDITIONERS

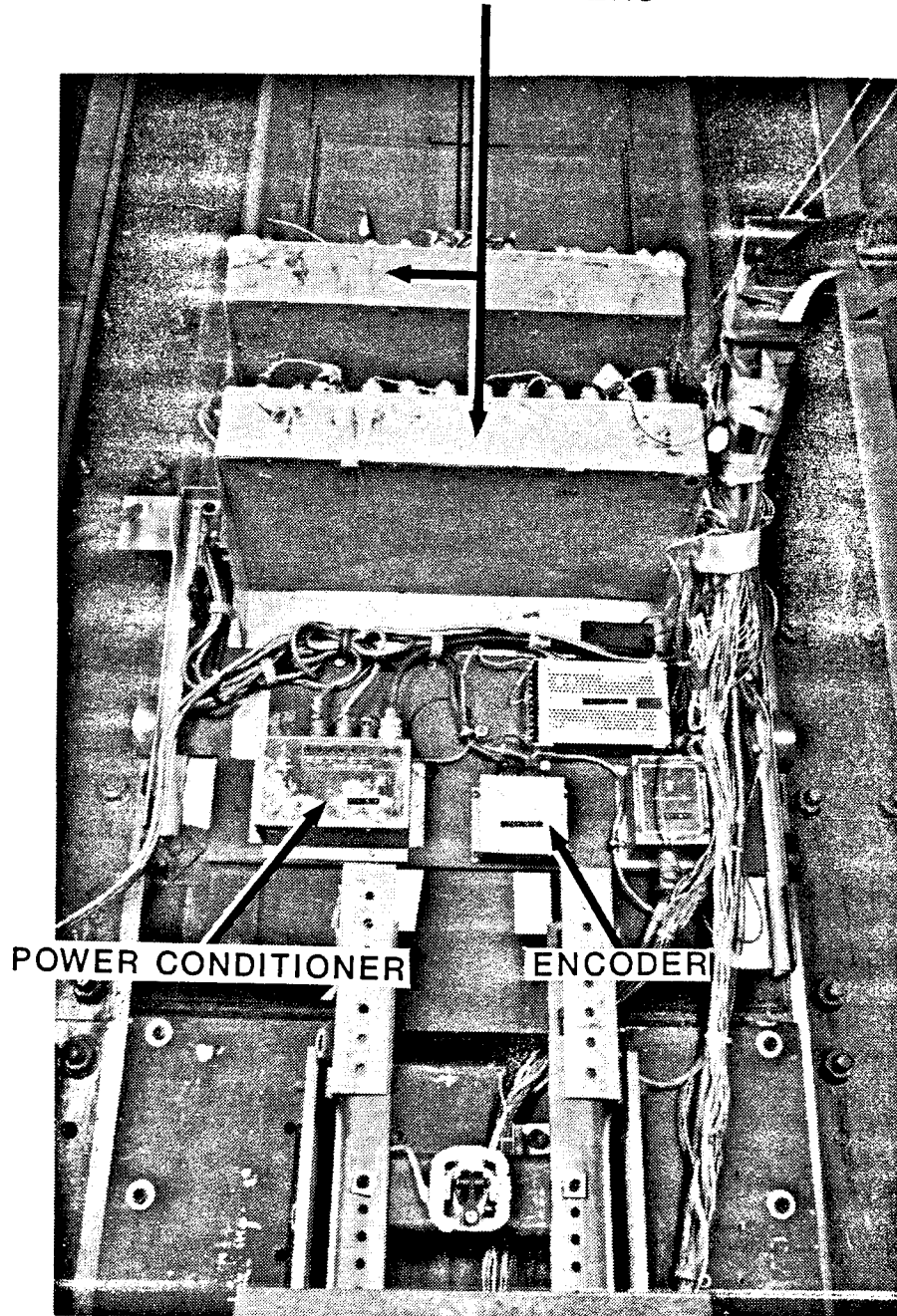
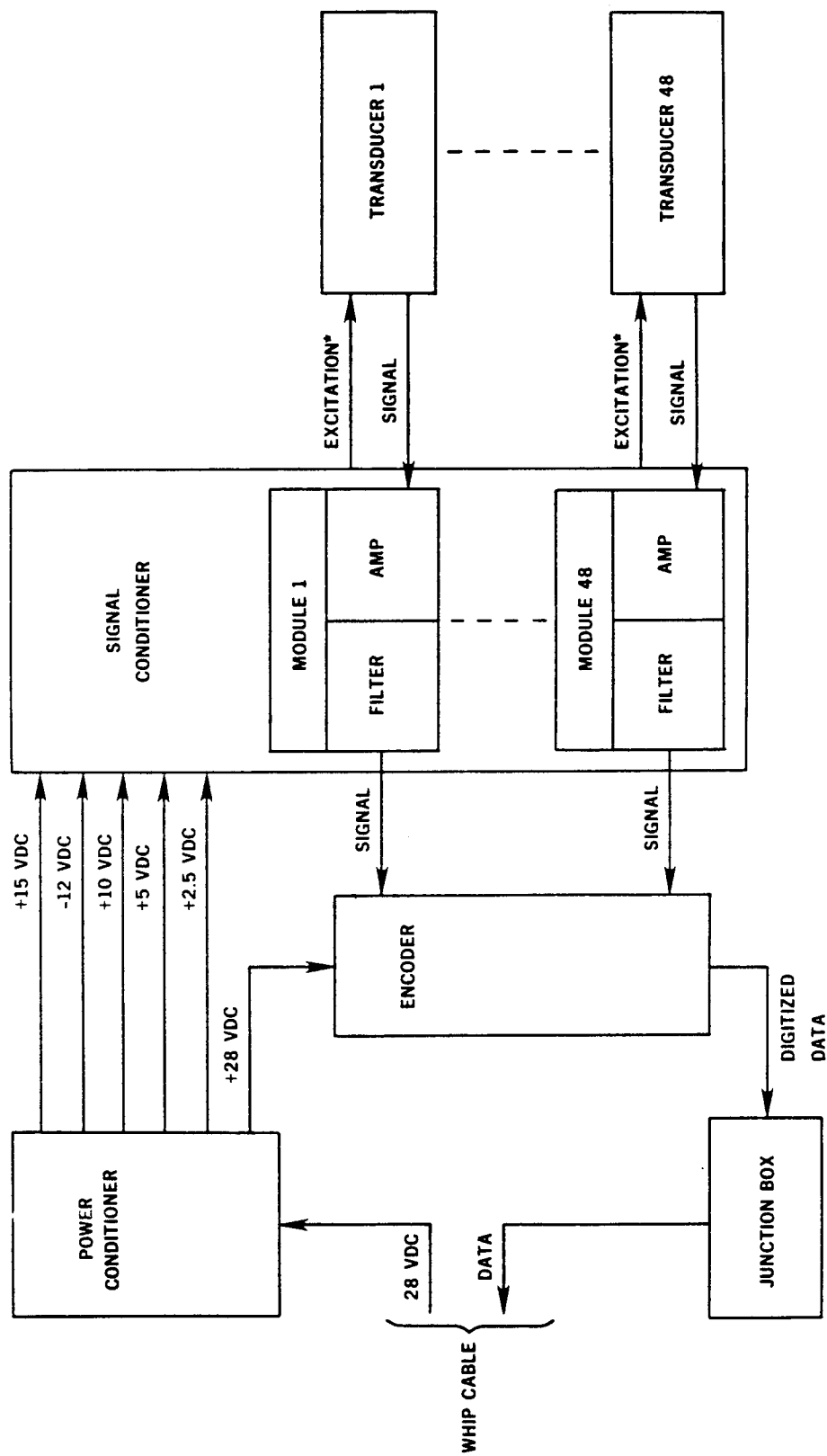


FIGURE A-15: ADACS INSTALLATION



\* +10 OR +5 VDC, FOR BRIDGE-TYPE TRANSUDCERS ONLY.

FIGURE A-16: AUTOMATIC DATA ACQUISITION AND CONTROL SYSTEM

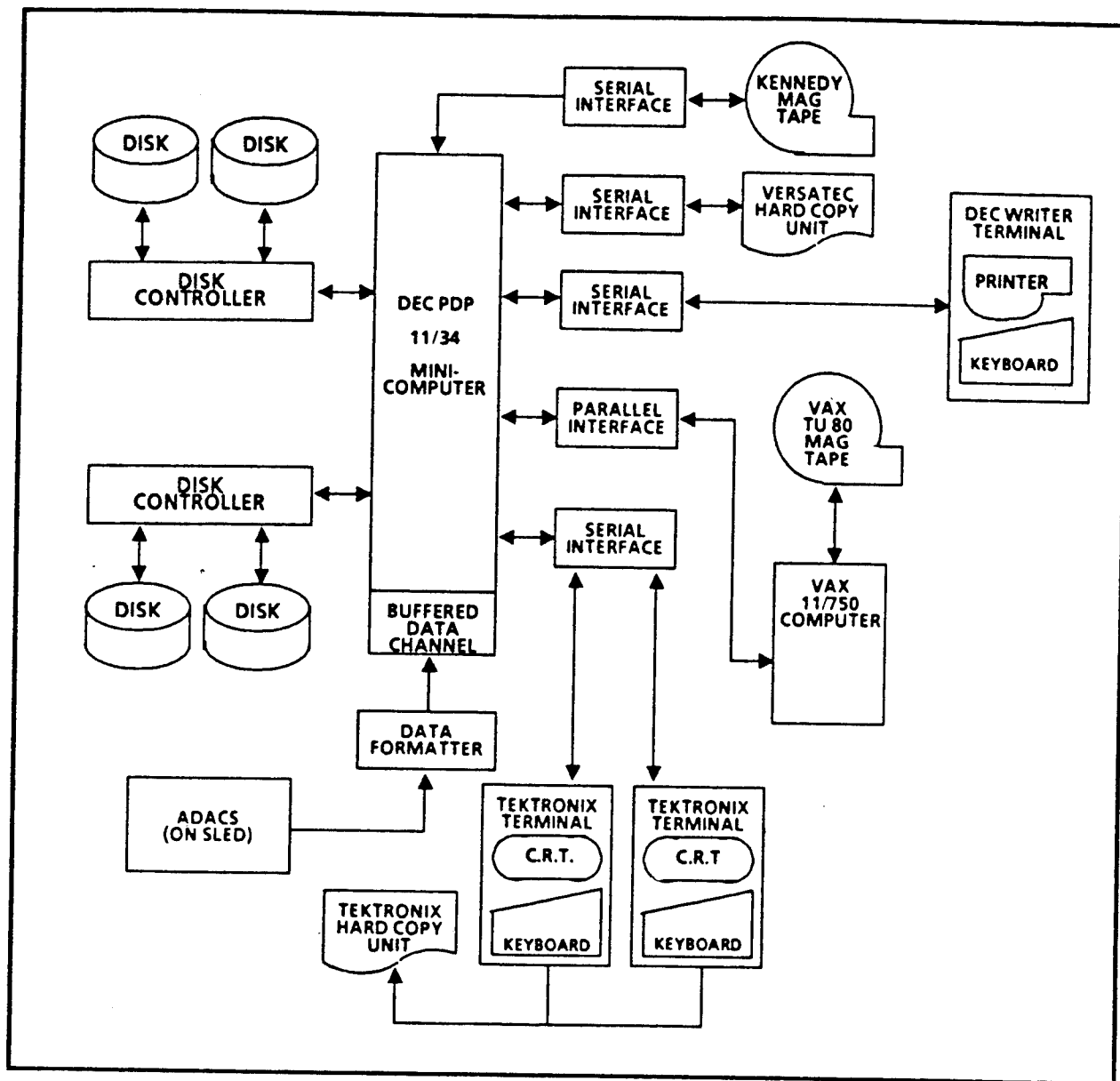


FIGURE A-17: DATA ACQUISITION AND STORAGE SYSTEM BLOCK DIAGRAM



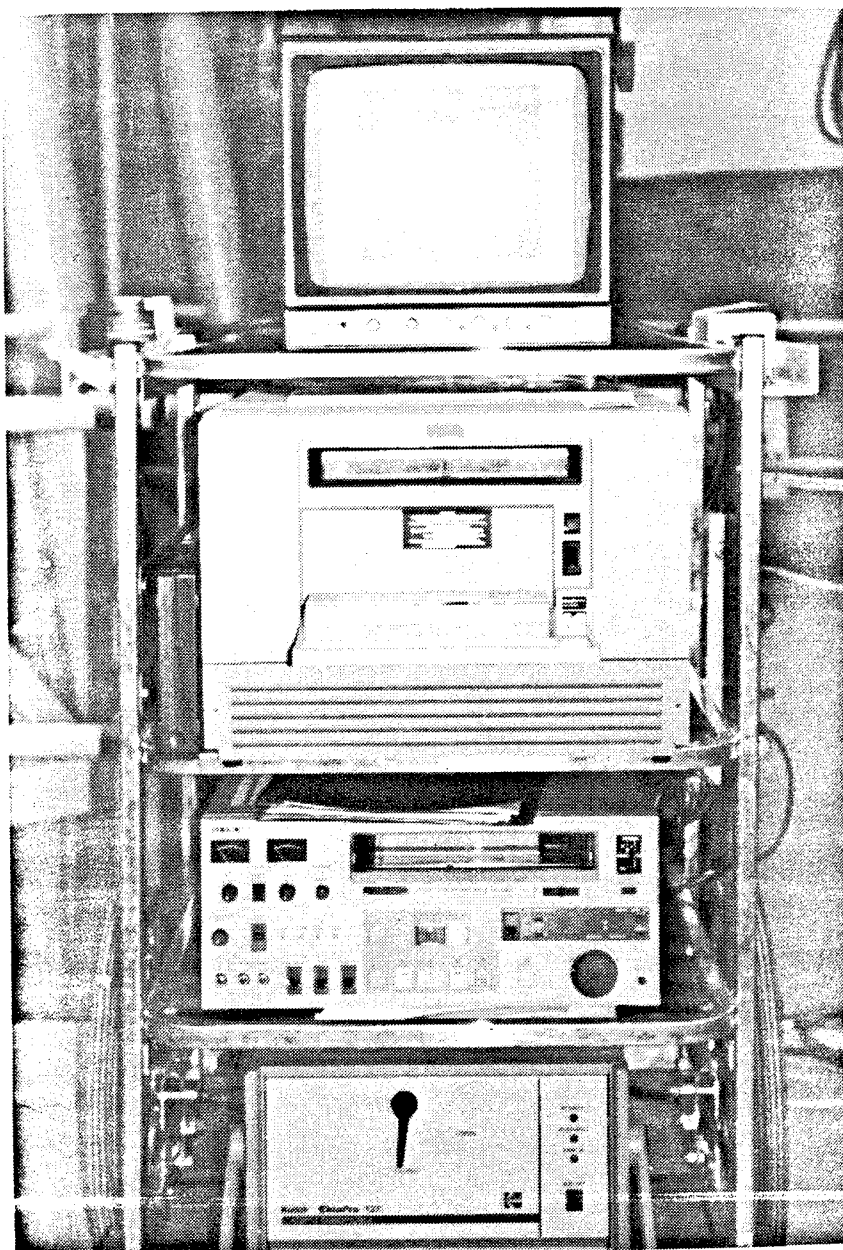


FIGURE A-18: KODAK EKTAPRO 1000 VIDEO SYSTEM

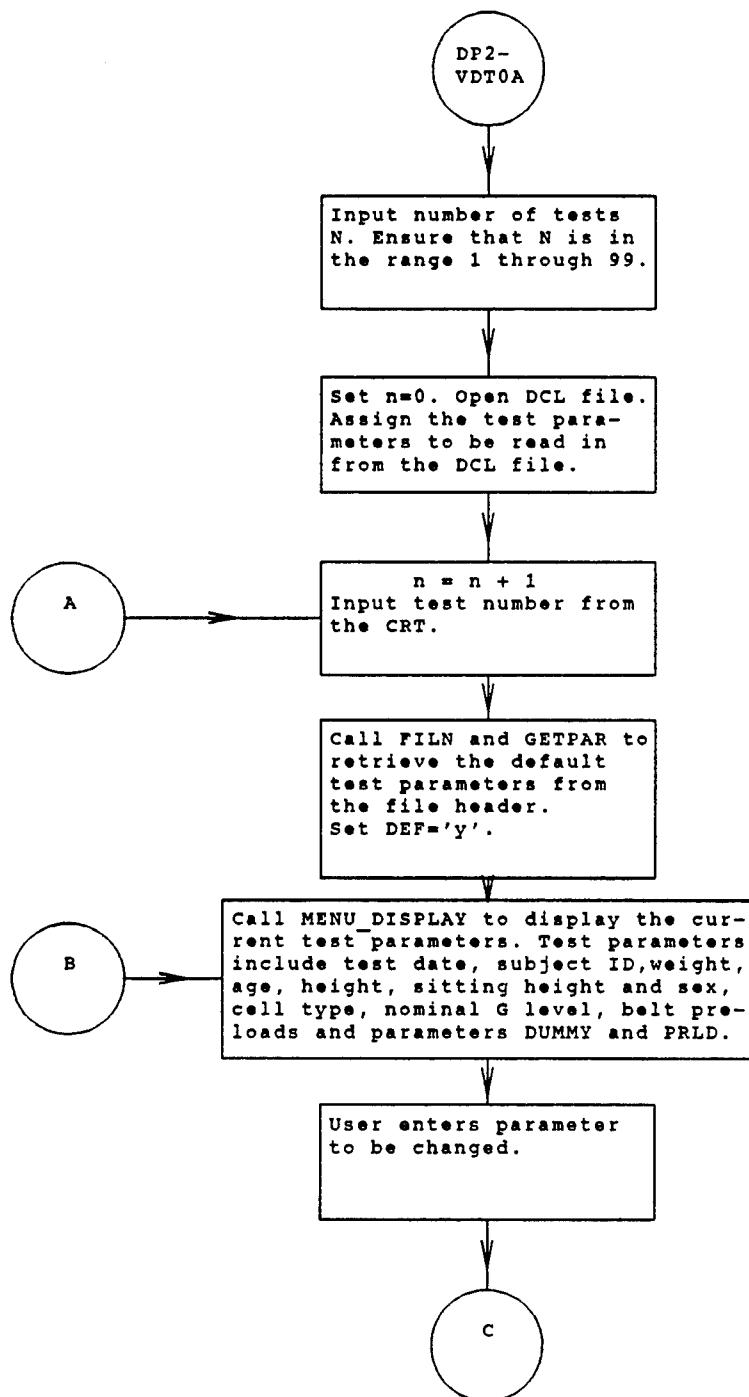


FIGURE A-19a: PROGRAM DP2VDT0A FLOWCHART (PAGE 1 OF 3)

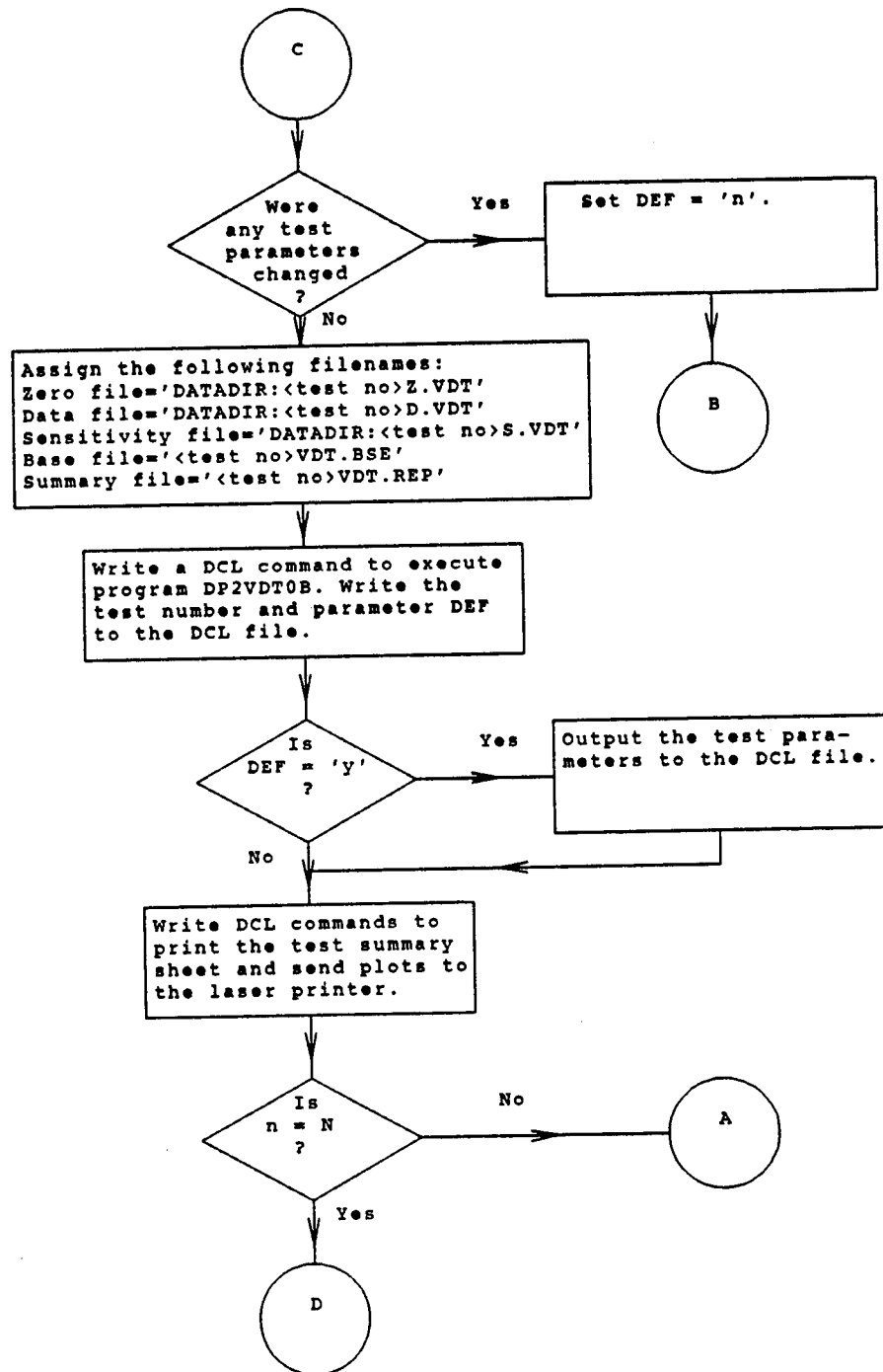


FIGURE A-19b: PROGRAM DP2VDT0A FLOWCHART (PAGE 2 OF 3)

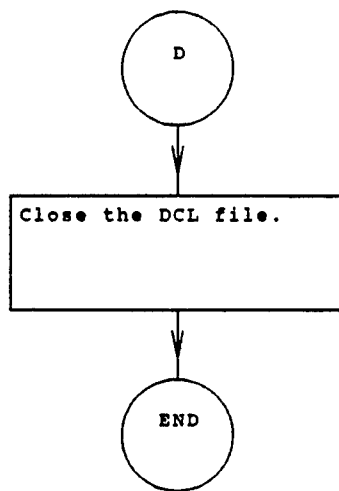


FIGURE A-19c: PROGRAM DP2VDT0A FLOWCHART (PAGE 3 OF 3)

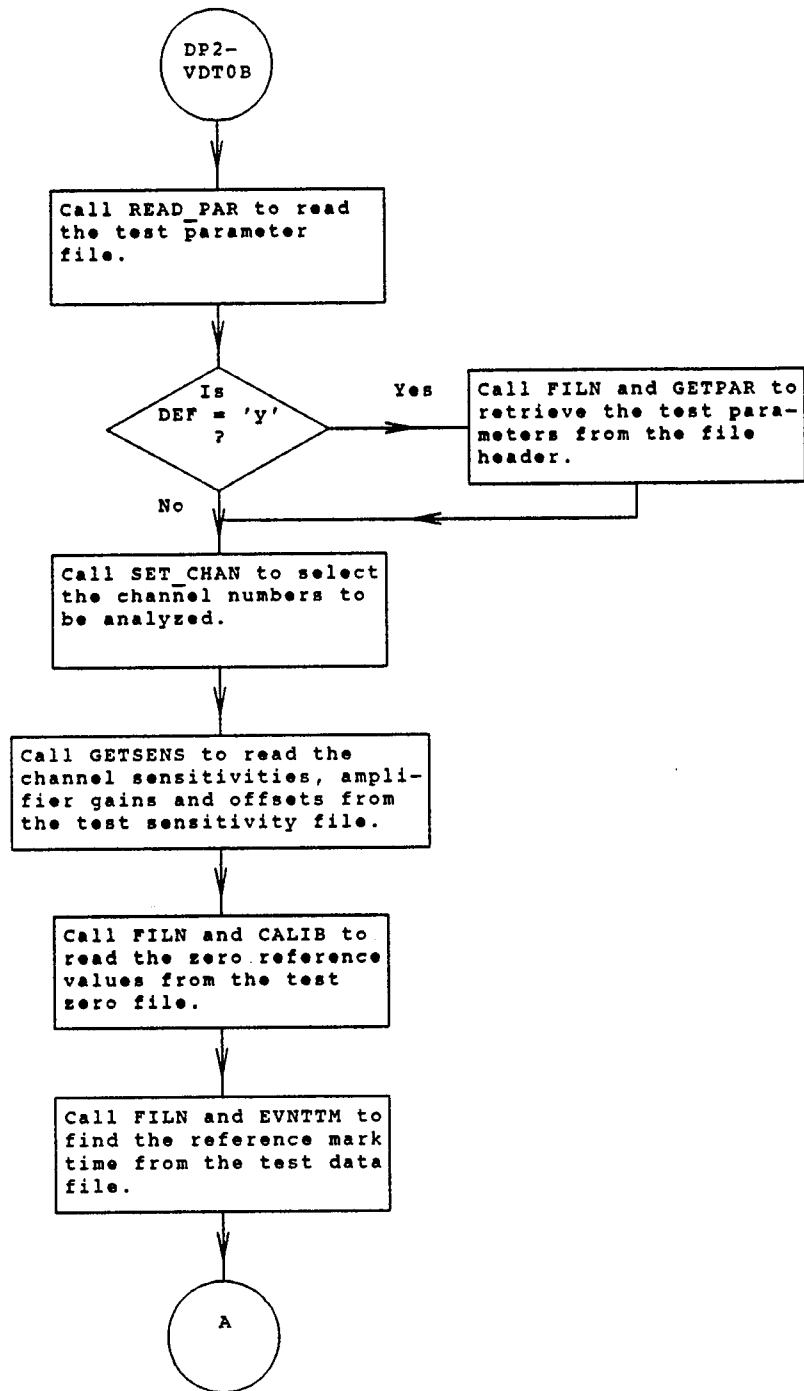


FIGURE A-20a: PROGRAM DP2VDT0B FLOWCHART (PAGE 1 OF 8)

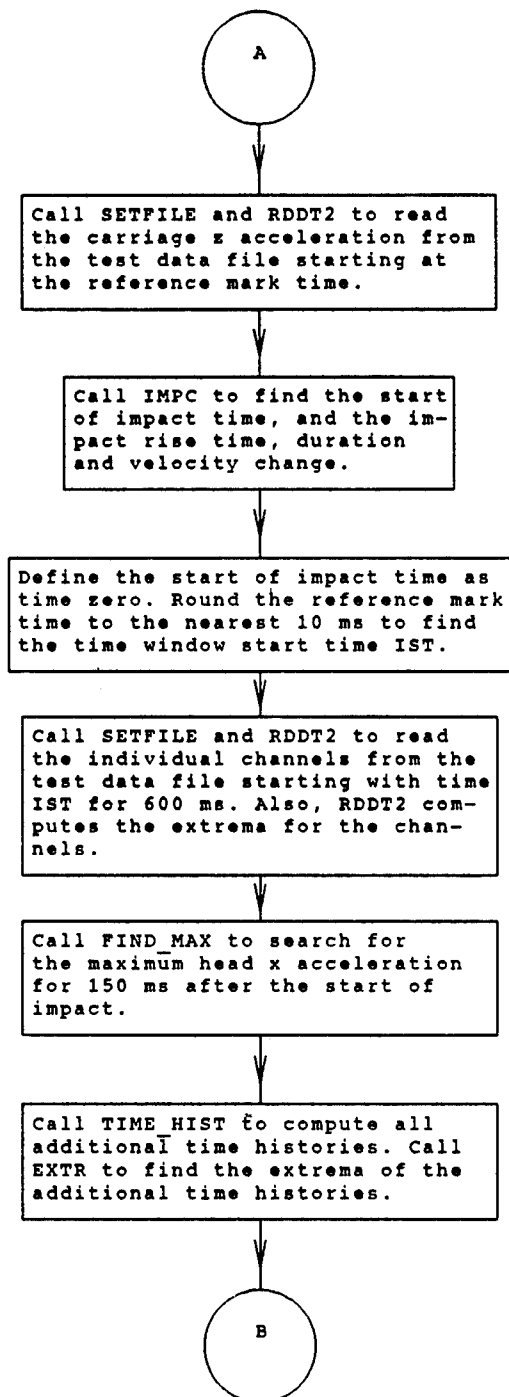


FIGURE A-20b: PROGRAM DP2VDT0B FLOWCHART (PAGE 2 OF 8)

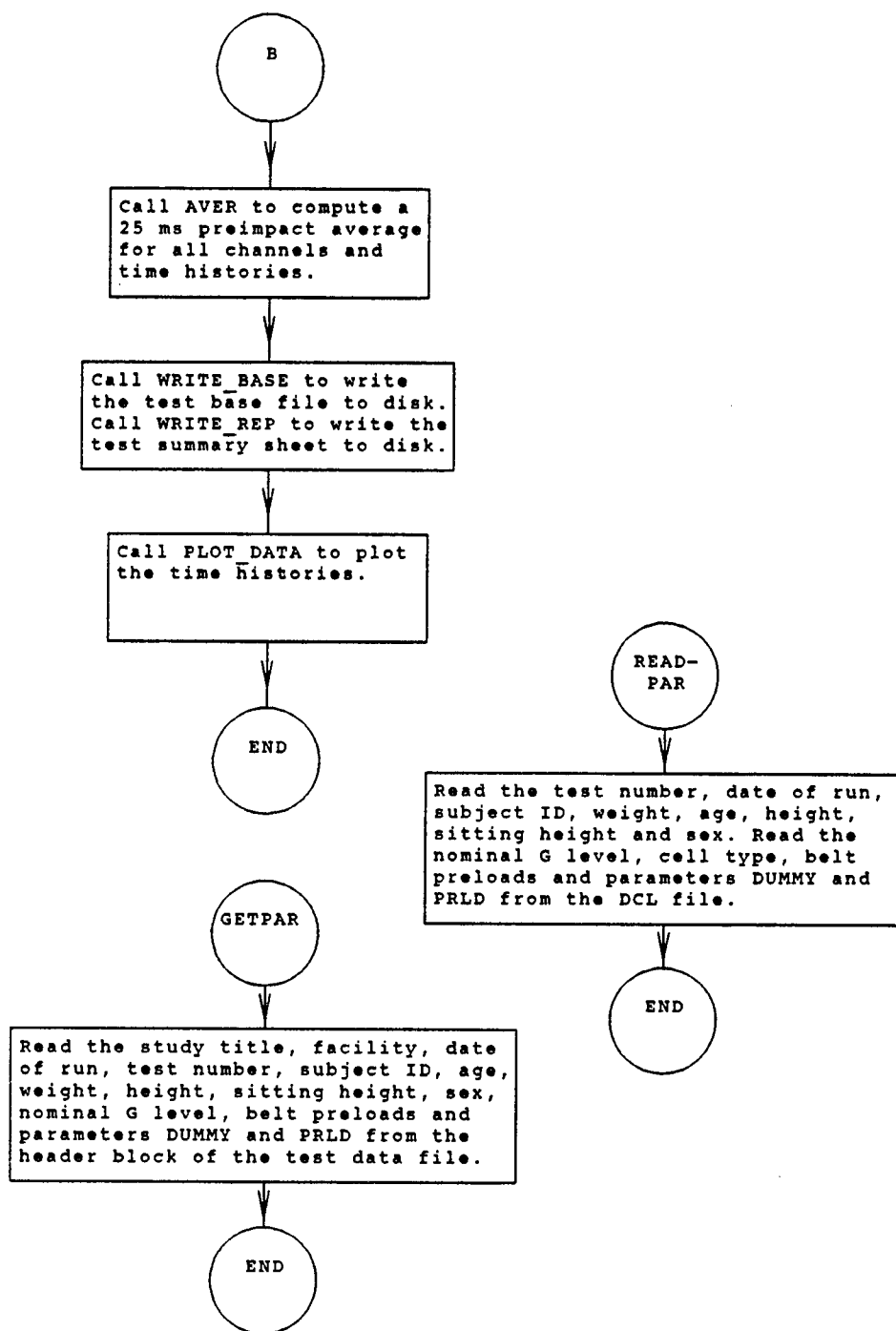


FIGURE A-20c: PROGRAM DP2VDT0B FLOWCHART (PAGE 3 OF 8)

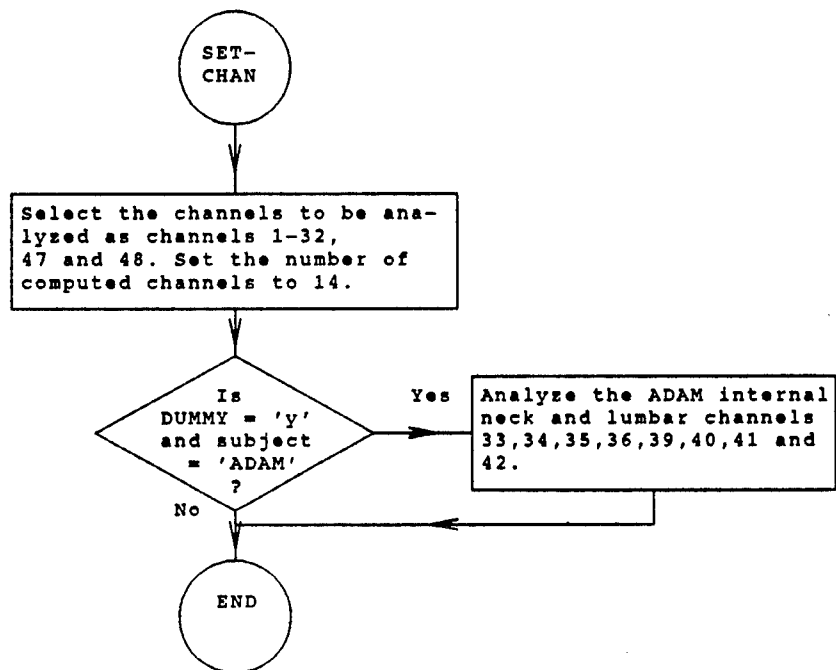


FIGURE A-20d: PROGRAM DP2VDT0B FLOWCHART (PAGE 4 OF 8)



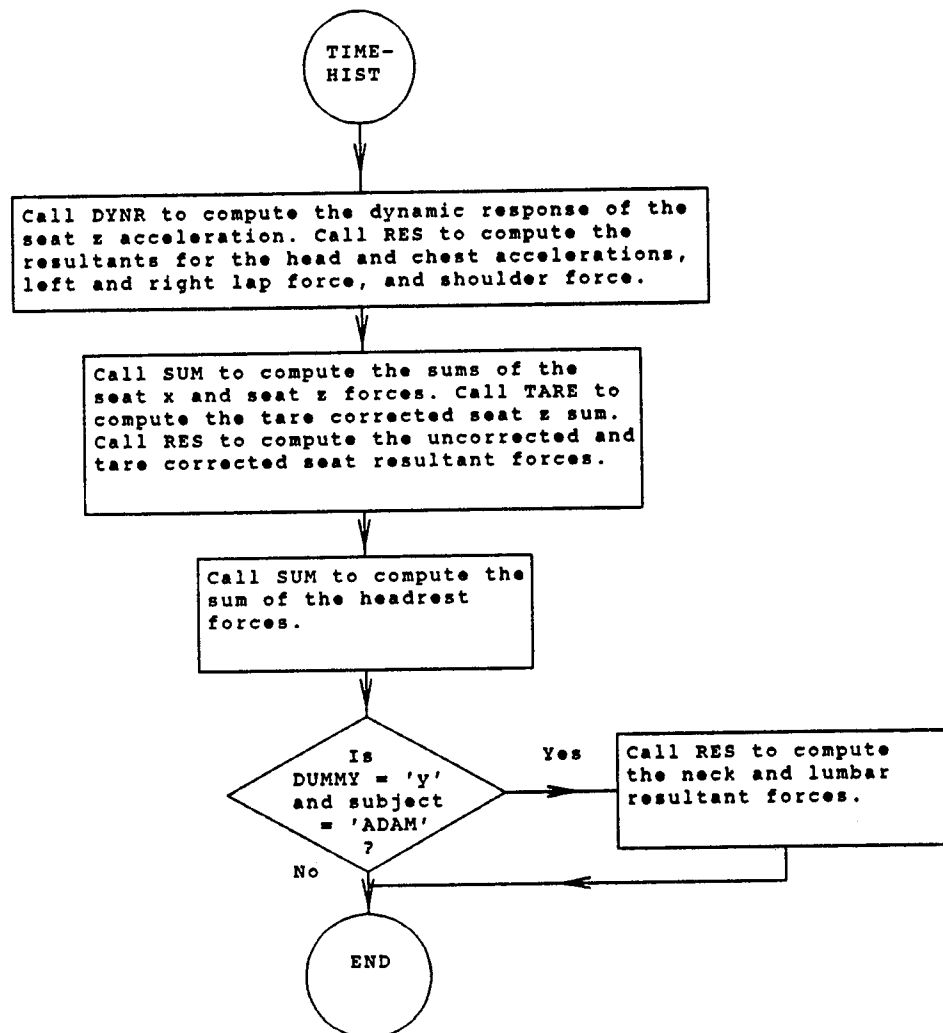


FIGURE A-20e: PROGRAM DP2VDT0B FLOWCHART (PAGE 5 OF 8)

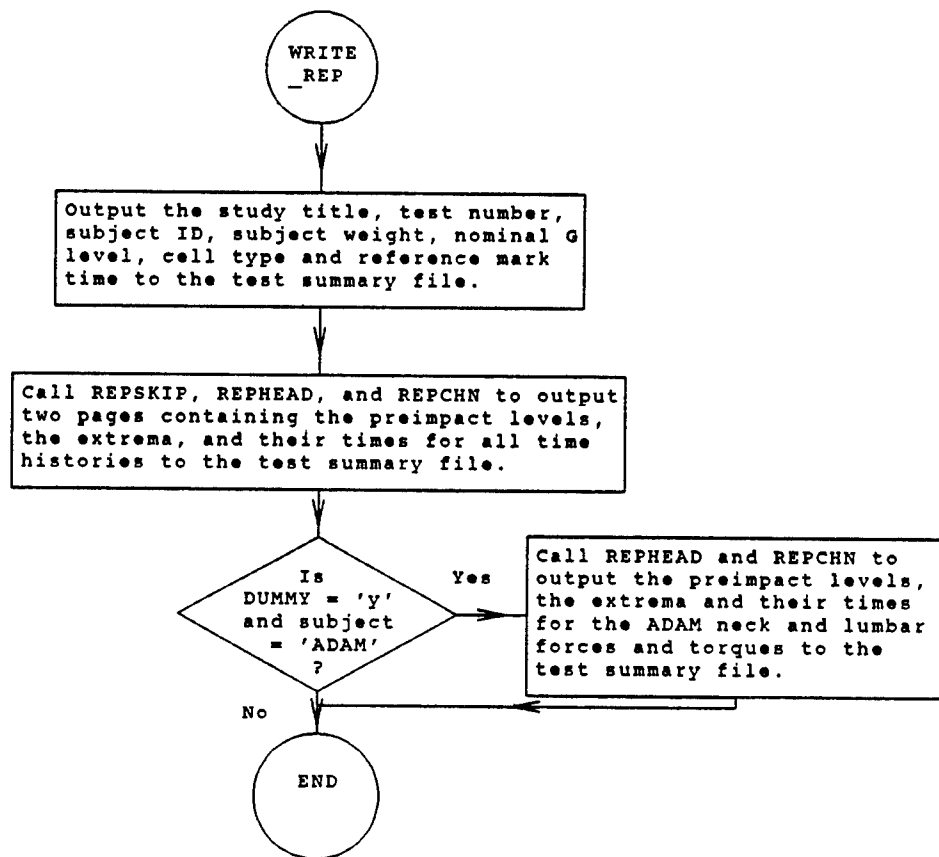


FIGURE A-20f: PROGRAM DP2VDT0B FLOWCHART (PAGE 6 OF 8)

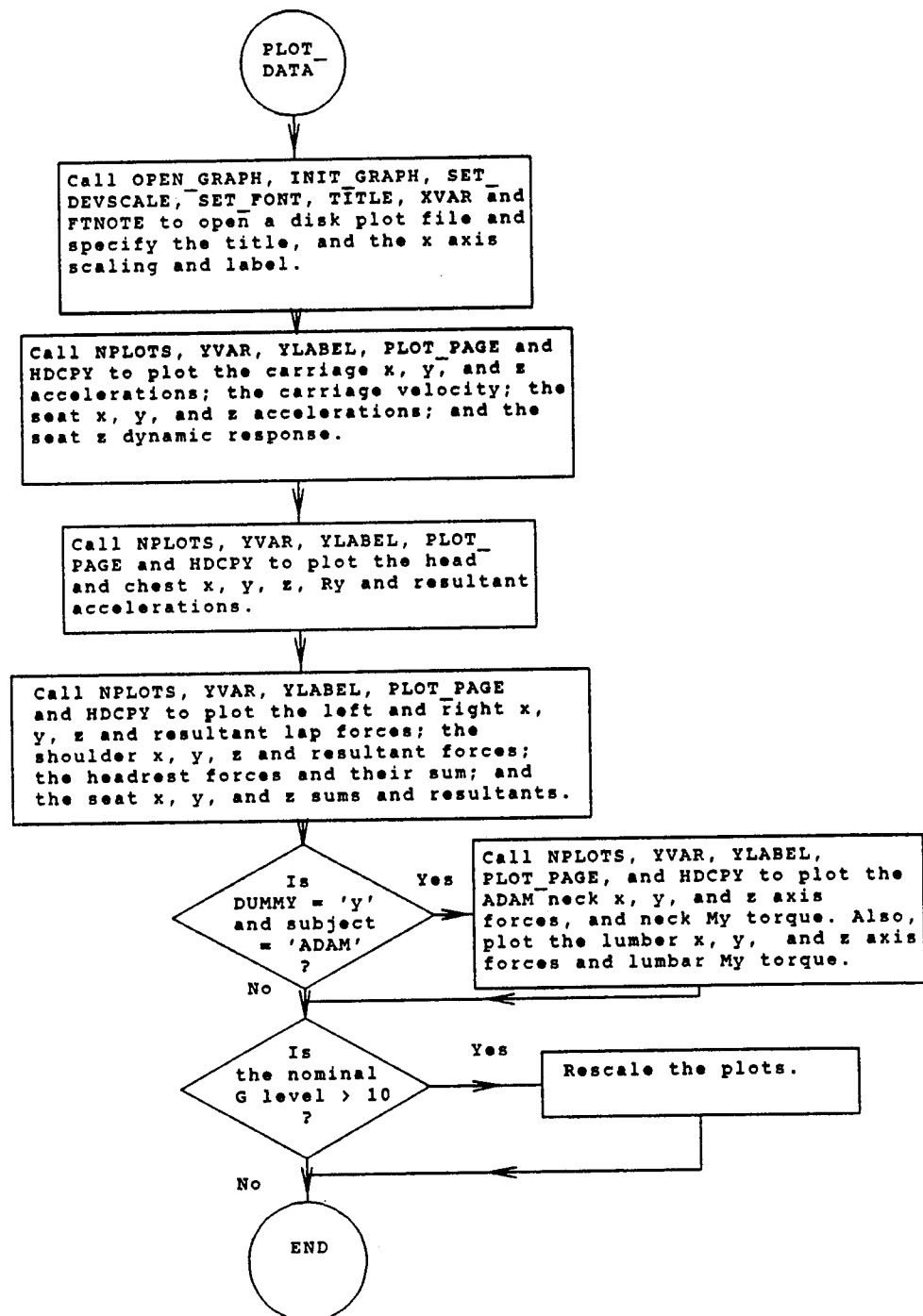


FIGURE A-20g: PROGRAM DP2VDT0B FLOWCHART (PAGE 7 OF 8)

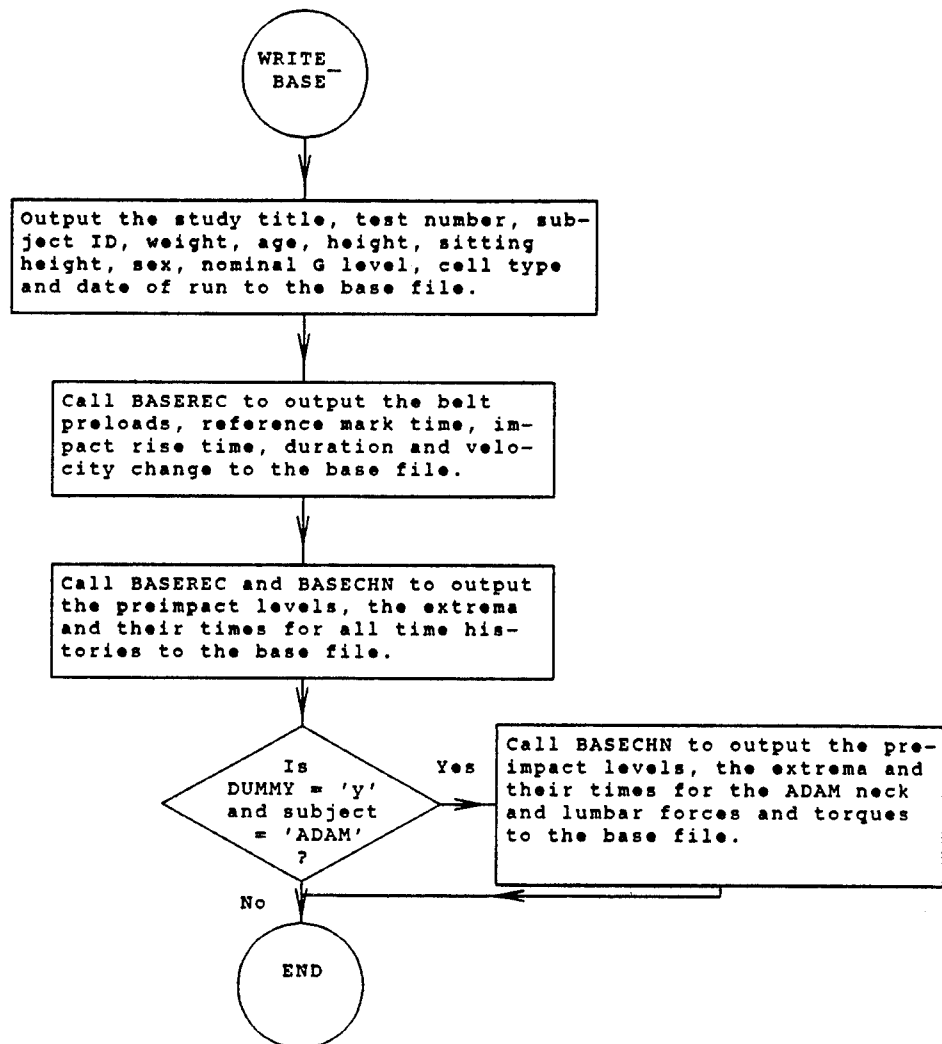


FIGURE A-20h: PROGRAM DP2VDT0B FLOWCHART (PAGE 8 OF 8)

APPENDIX B  
SAMPLE DATA SUMMARIES AND GRAPHS

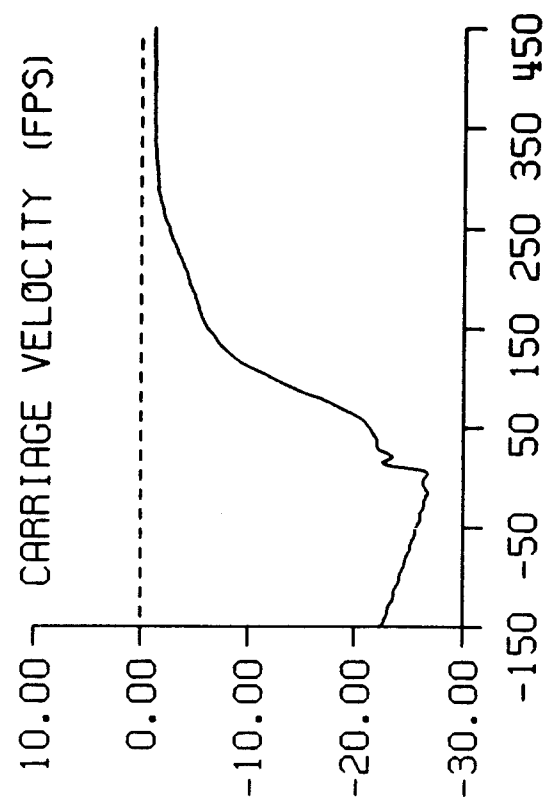
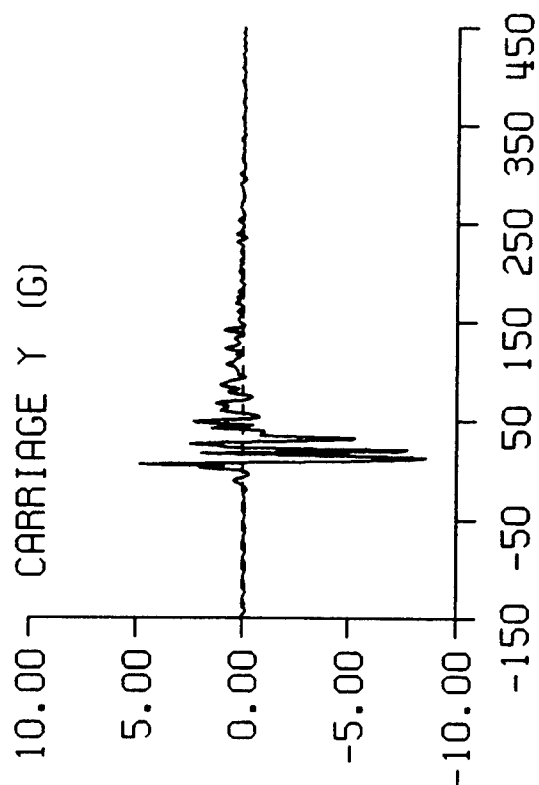
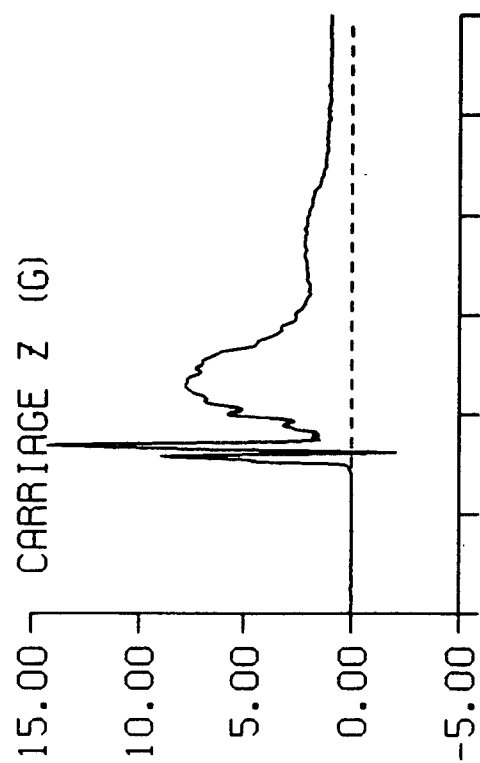
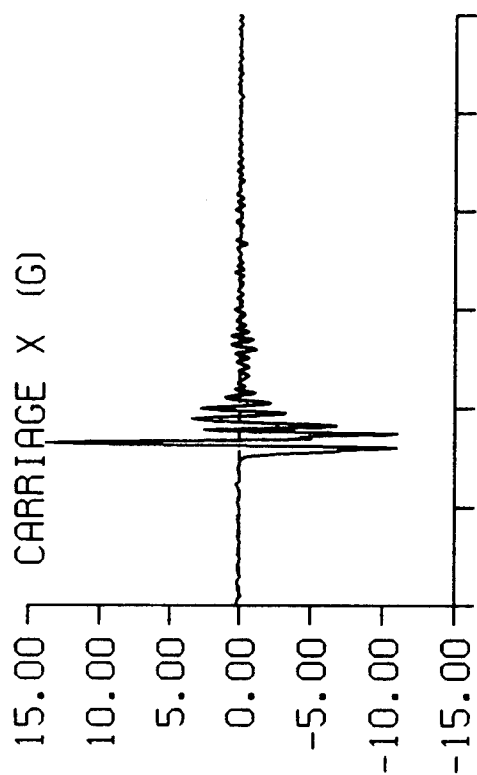
DP2 STUDY TEST: 2678 SUBJ: ADAM-L WT: 216.0 NOM G: 10.0 CELL: B

DATA ID	IMMEDIATE PREIMPACT	MAXIMUM VALUE	MINIMUM VALUE	TIME OF MAXIMUM	TIME OF MINIMUM
REFERENCE MARK TIME (MS)				-151.	
2.5V EXT PWR (VOLTS)	2.50	2.50	2.50	2.	3.
10V EXT PWR (VOLTS)	10.00	10.00	10.00	1.	0.
CARRIAGE ACCELERATION (G)					
X AXIS	0.06	13.87	-11.05	15.	24.
Y AXIS	-0.01	4.85	-8.62	6.	13.
Z AXIS	-0.01	14.27	-2.07	19.	12.
CARRIAGE VELOCITY (FPS)	-26.50	-1.17	-26.74	440.	4.
SEAT ACCELERATION (G)					
X AXIS	0.01	11.59	-5.46	11.	18.
Y AXIS	0.04	5.48	-5.29	28.	18.
Z AXIS	-0.05	11.23	-3.06	11.	44.
Z AXIS DRI	-0.05	8.92	-0.33	110.	185.
HEAD ACCELERATION (G)					
X AXIS	0.07	3.65	-1.62	39.	168.
Y AXIS	0.12	1.06	-0.52	107.	71.
Z AXIS	-0.02	15.31	-0.10	34.	1.
RESULTANT	0.16	15.39	0.11	34.	0.
RY (RAD/SEC2)	-15.14	624.24	-1110.47	45.	38.
CHEST ACCELERATION (G)					
X AXIS	0.09	4.94	-4.64	47.	34.
Y AXIS	0.18	1.03	-1.14	53.	48.
Z AXIS	-0.05	11.07	-0.08	48.	4.
RESULTANT	0.22	12.00	0.12	48.	0.
RY (RAD/SEC2)	-0.40	1937.62	-3067.68	47.	54.
SHOULDER STRAP FORCES (LB)					
X AXIS	-14.34	-3.81	-68.32	384.	126.
Y AXIS	0.54	14.45	-4.86	32.	45.
Z AXIS	2.21	54.24	1.29	100.	365.
RESULTANT	14.53	85.17	4.03	126.	402.
HEADREST FORCES (LB)					
UPPER X AXIS	0.89	17.39	-20.34	25.	19.
LOWER X AXIS	0.95	23.44	-4.38	15.	56.
X AXIS SUM	1.84	31.68	-13.02	26.	30.

DP2 STUDY TEST: 2678 SUBJ: ADAM-L WT: 216.0 NOM G: 10.0 CELL: B

DATA ID	IMMEDIATE PREIMPACT	MAXIMUM VALUE	MINIMUM VALUE	TIME OF MAXIMUM	TIME OF MINIMUM
LAP FORCES (LB)					
LEFT X AXIS	-18.08	2.02	-28.23	46.	175.
LEFT Y AXIS	1.21	5.20	-8.85	31.	41.
LEFT Z AXIS	-25.40	16.94	-34.73	17.	168.
LEFT RESULTANT	31.21	44.89	3.76	175.	38.
RIGHT X AXIS	-23.23	2.86	-28.90	28.	164.
RIGHT Y AXIS	-2.71	9.82	-6.24	31.	41.
RIGHT Z AXIS	-25.57	19.25	-29.46	16.	170.
RIGHT RESULTANT	34.66	41.37	5.27	170.	28.
SEAT FORCES (LB)					
LEFT X AXIS	0.58	43.65	-99.98	9.	46.
RIGHT X AXIS	-1.08	99.12	-123.27	28.	45.
X AXIS SUM	-0.51	106.86	-221.00	28.	45.
Y AXIS	-2.40	100.03	-68.17	35.	20.
LEFT Z AXIS	-3.53	339.78	-3.53	32.	0.
RIGHT Z AXIS	-5.27	277.98	-6.00	32.	0.
CENTER Z AXIS	44.09	1615.65	49.11	101.	0.
Z AXIS SUM	35.29	2058.61	39.58	105.	0.
RESULTANT	35.45	2059.68	40.81	105.	0.
Z SUM MINUS TARE	54.74	1921.46	19.16	101.	3.
RESULTANT MINUS TARE	54.76	1921.94	19.77	101.	3.
ADAM NECK FORCE (LB)					
X AXIS	-6.18	33.58	-24.53	37.	177.
Y AXIS	-2.35	14.86	-5.22	108.	15.
Z AXIS	-10.34	151.37	-12.99	34.	3.
RESULTANT	12.29	152.87	0.58	34.	350.
ADAM NECK MY (IN-LB)	-2.75	60.14	-62.22	36.	46.
ADAM LUMBAR FORCE (LB)					
X AXIS	-6.00	209.25	-8.39	106.	0.
Y AXIS	-2.19	24.72	-21.92	42.	33.
Z AXIS	-54.58	867.25	-72.84	34.	168.
RESULTANT	55.21	867.50	1.54	34.	397.
ADAM LUMBAR MY (IN-LB)	-7.53	136.93	-498.83	31.	107.

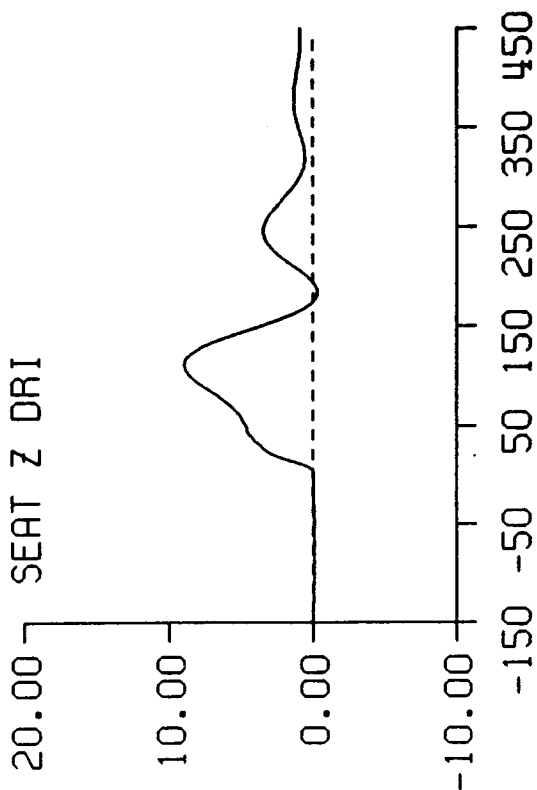
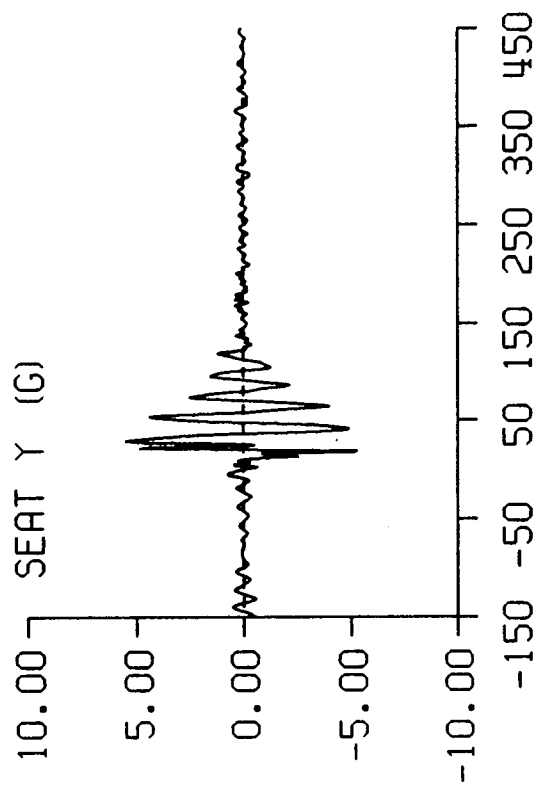
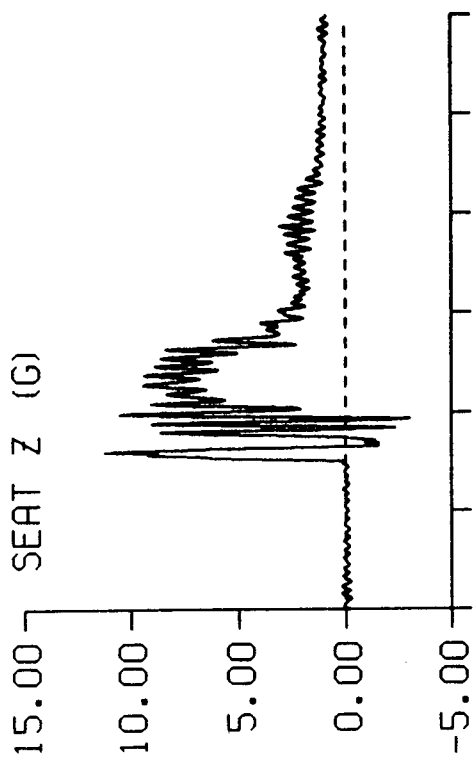
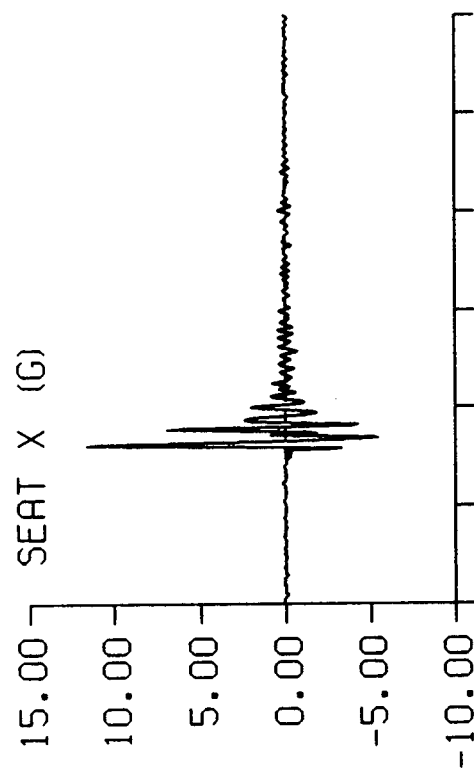
DP2 STUDY TEST: 2678 SUBJ: ADAM-L CELL: B



TIME IN MILLISECONDS

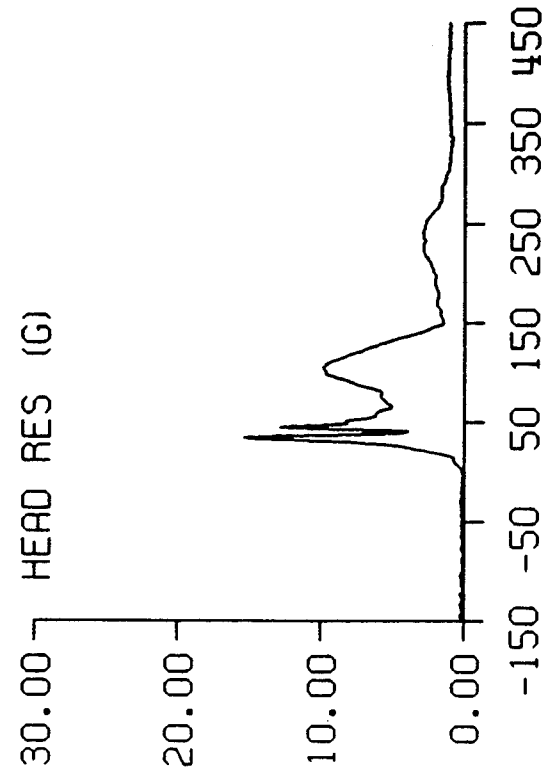
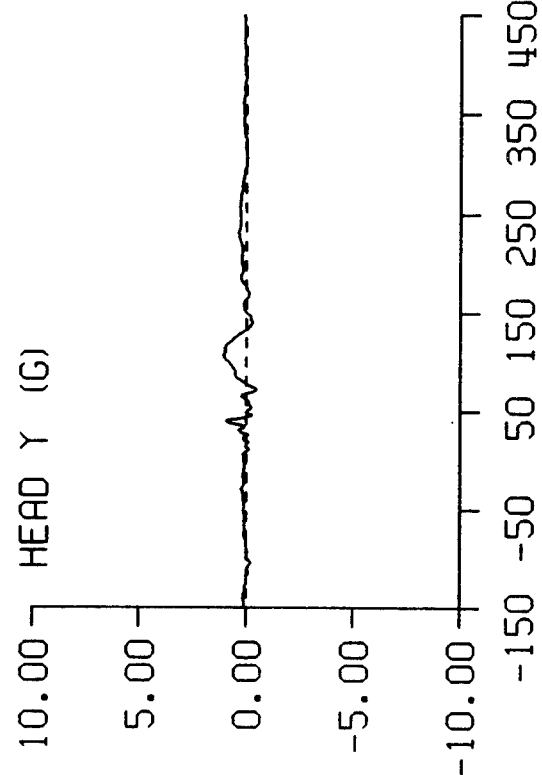
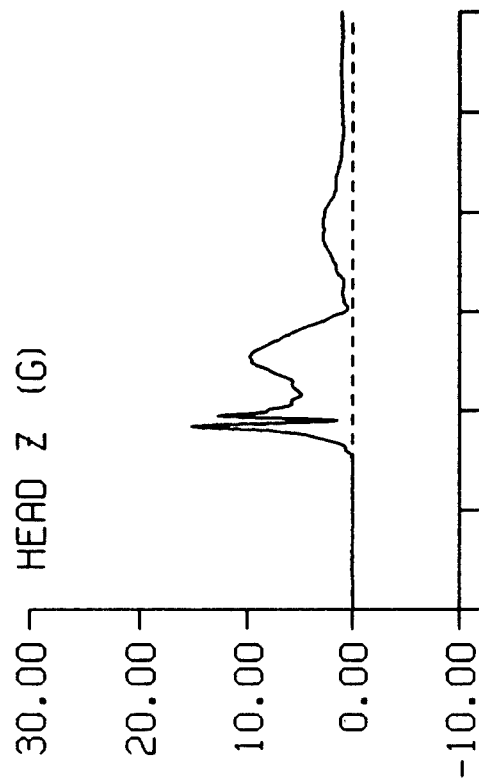
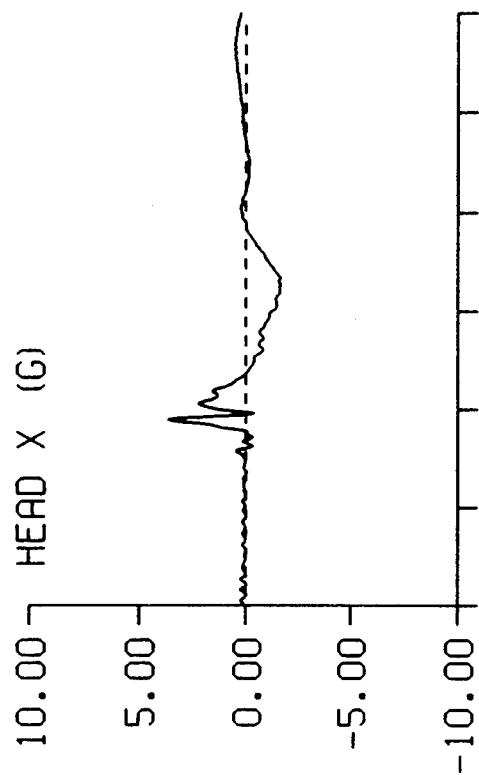


DP2 STUDY TEST: 2678 SUBJ: ADAM-L CELL: B



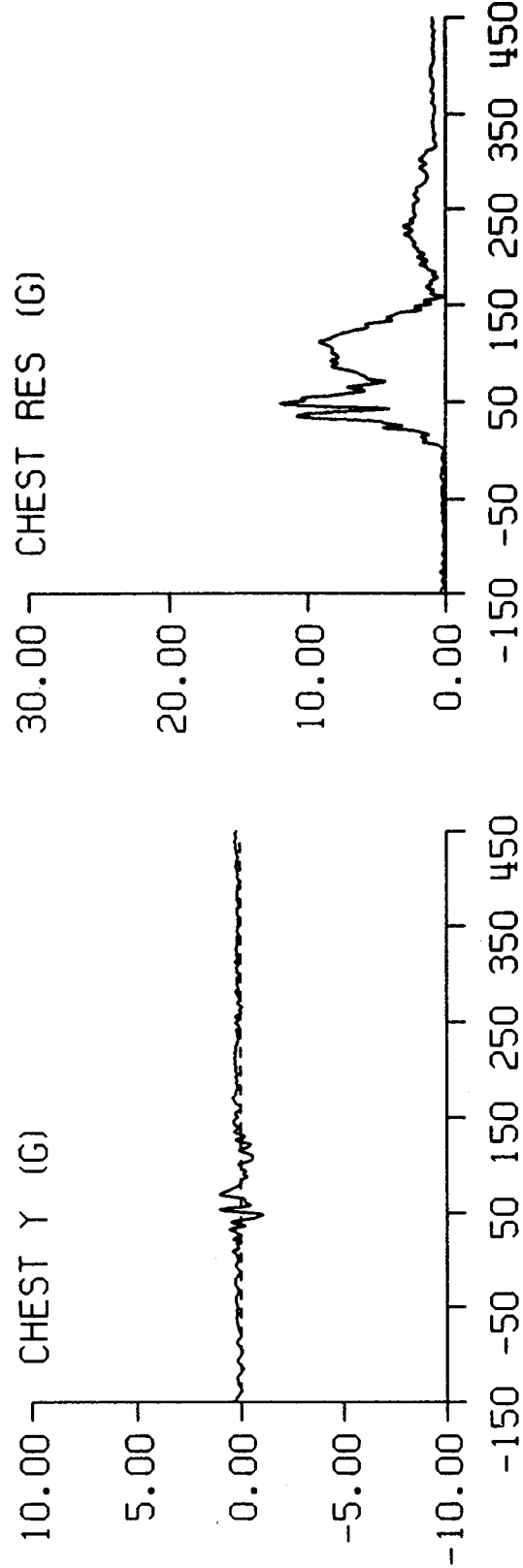
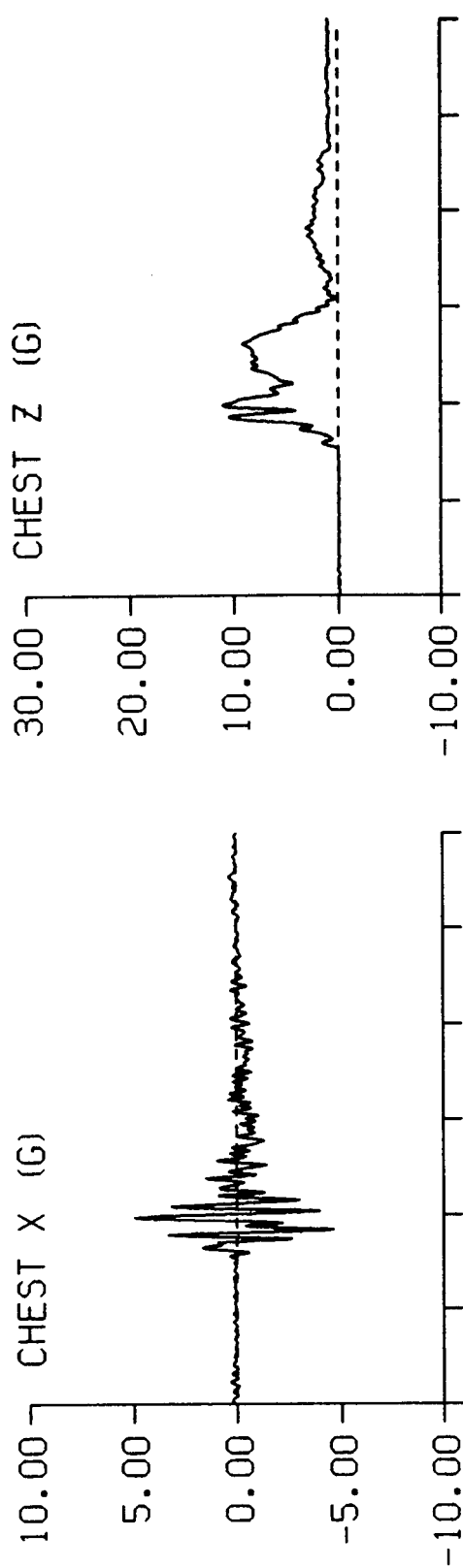
TIME IN MILLISECONDS

DP2 STUDY TEST: 2678 SUBJ: ADAM-L CELL: B



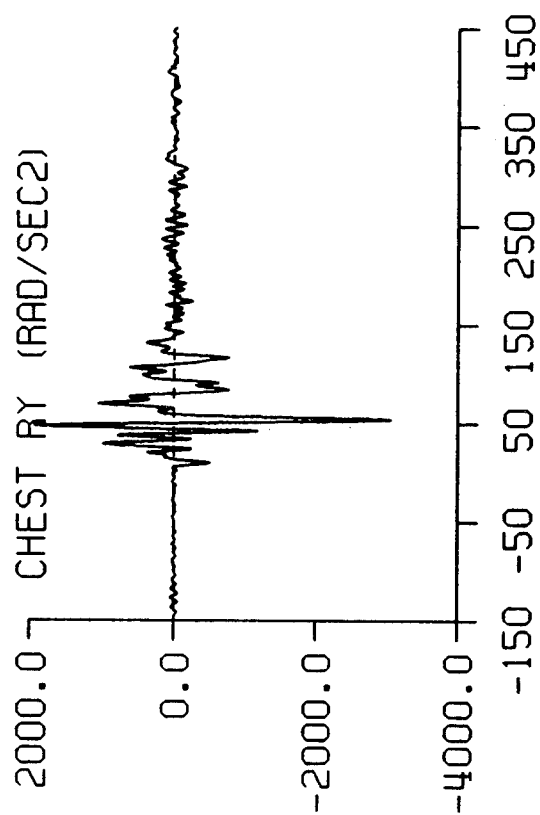
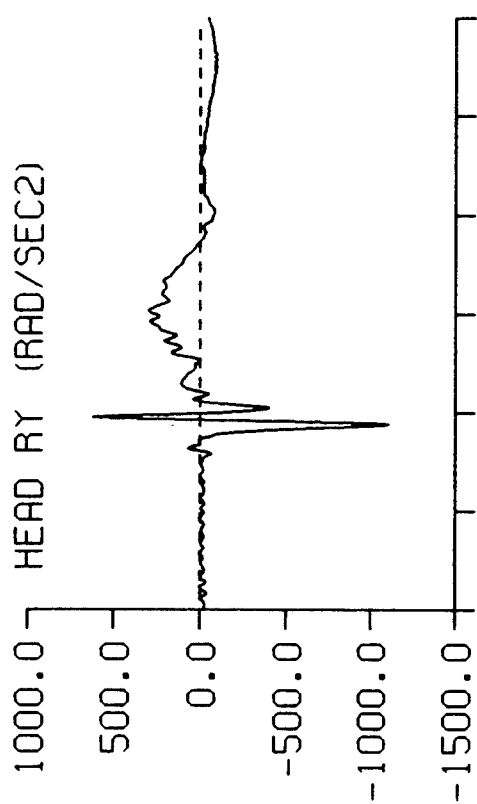
TIME IN MILLISECONDS

DP2 STUDY TEST: 2678 SUBJ: ADAM-L CELL: B



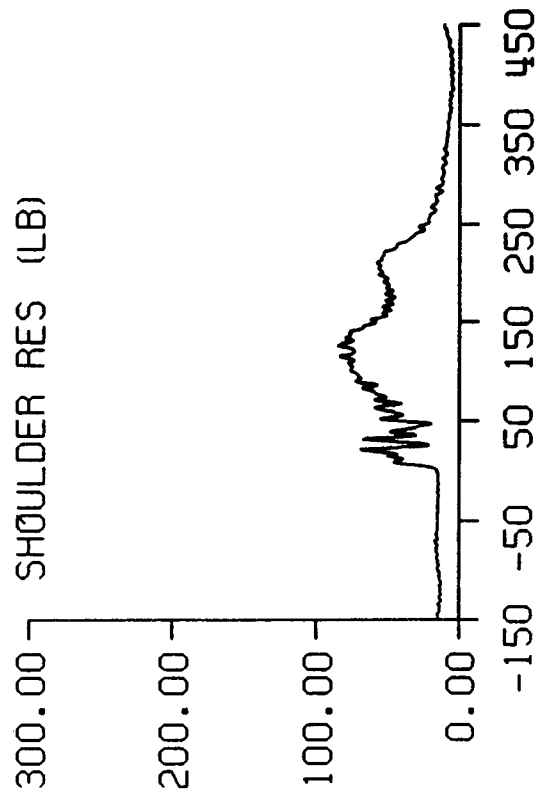
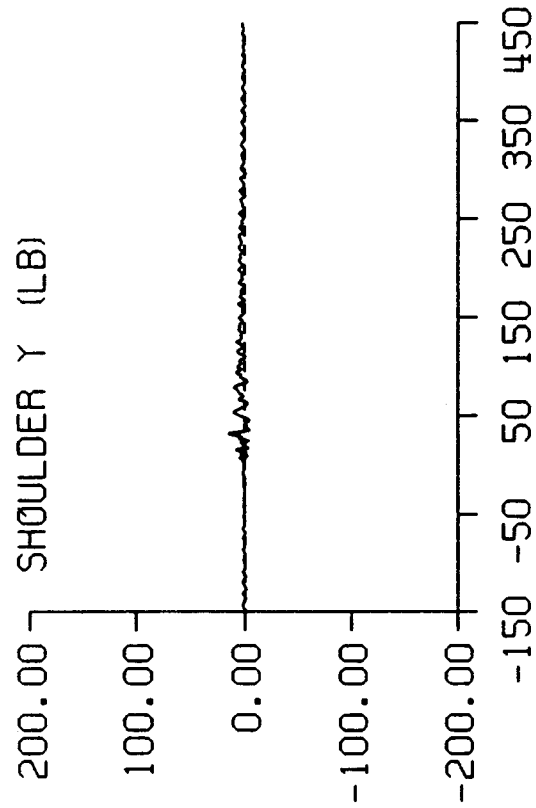
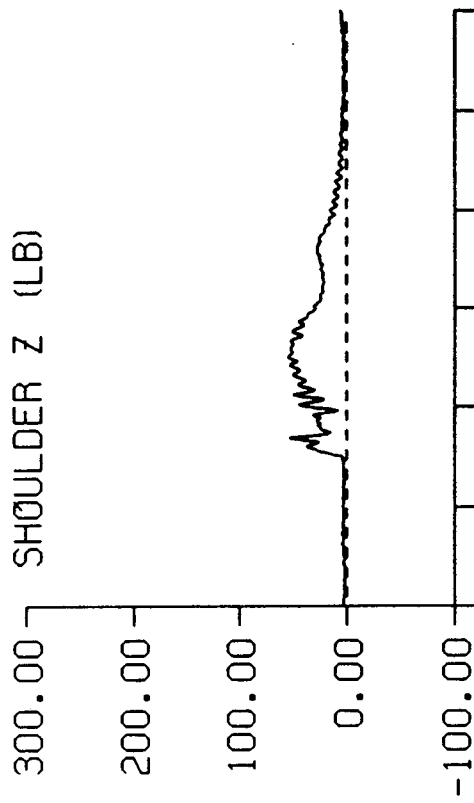
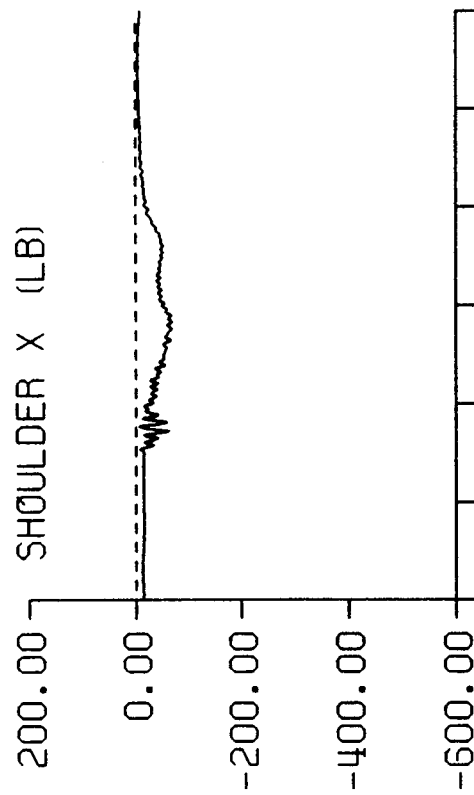
TIME IN MILLISECONDS

DP2 STUDY TEST: 2678 SUBJ: ADAM-L CELL: B



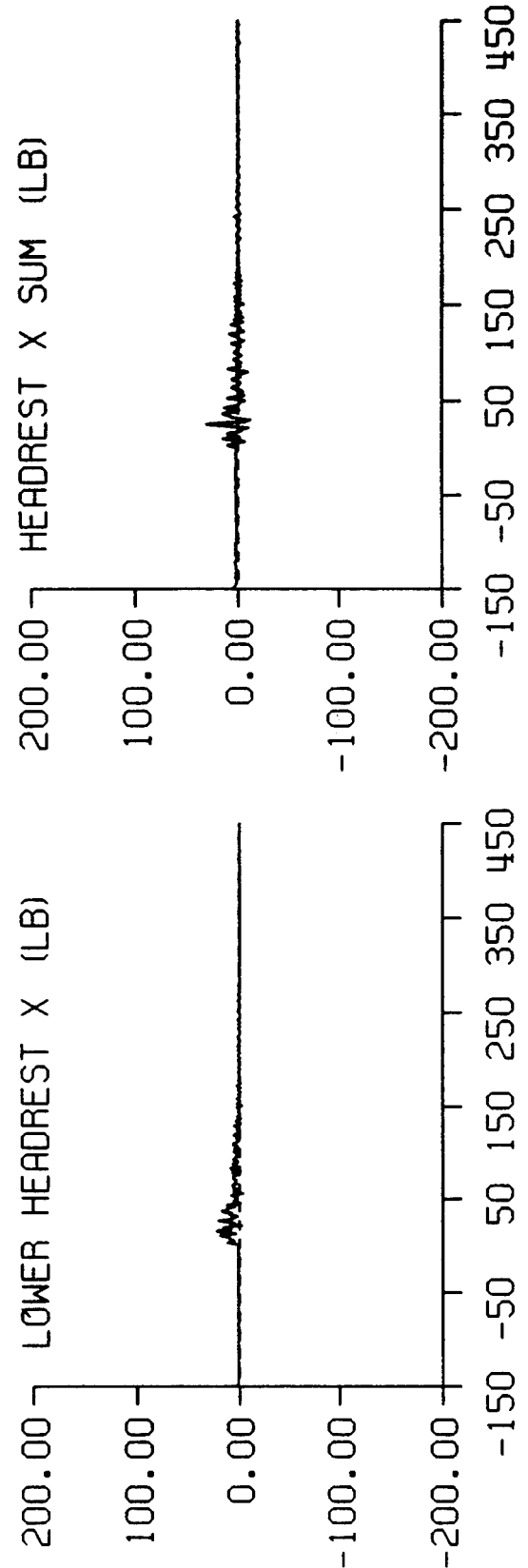
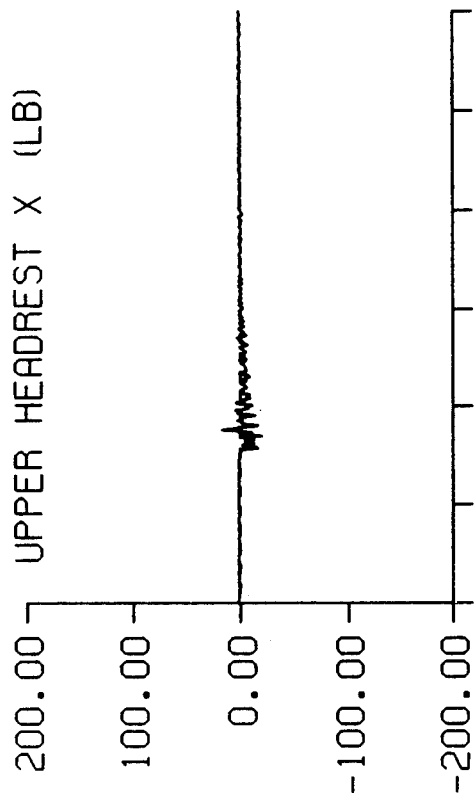
TIME IN MILLISECONDS

DP2 STUDY TEST: 2678 SUBJ: ADAM-L CELL: B



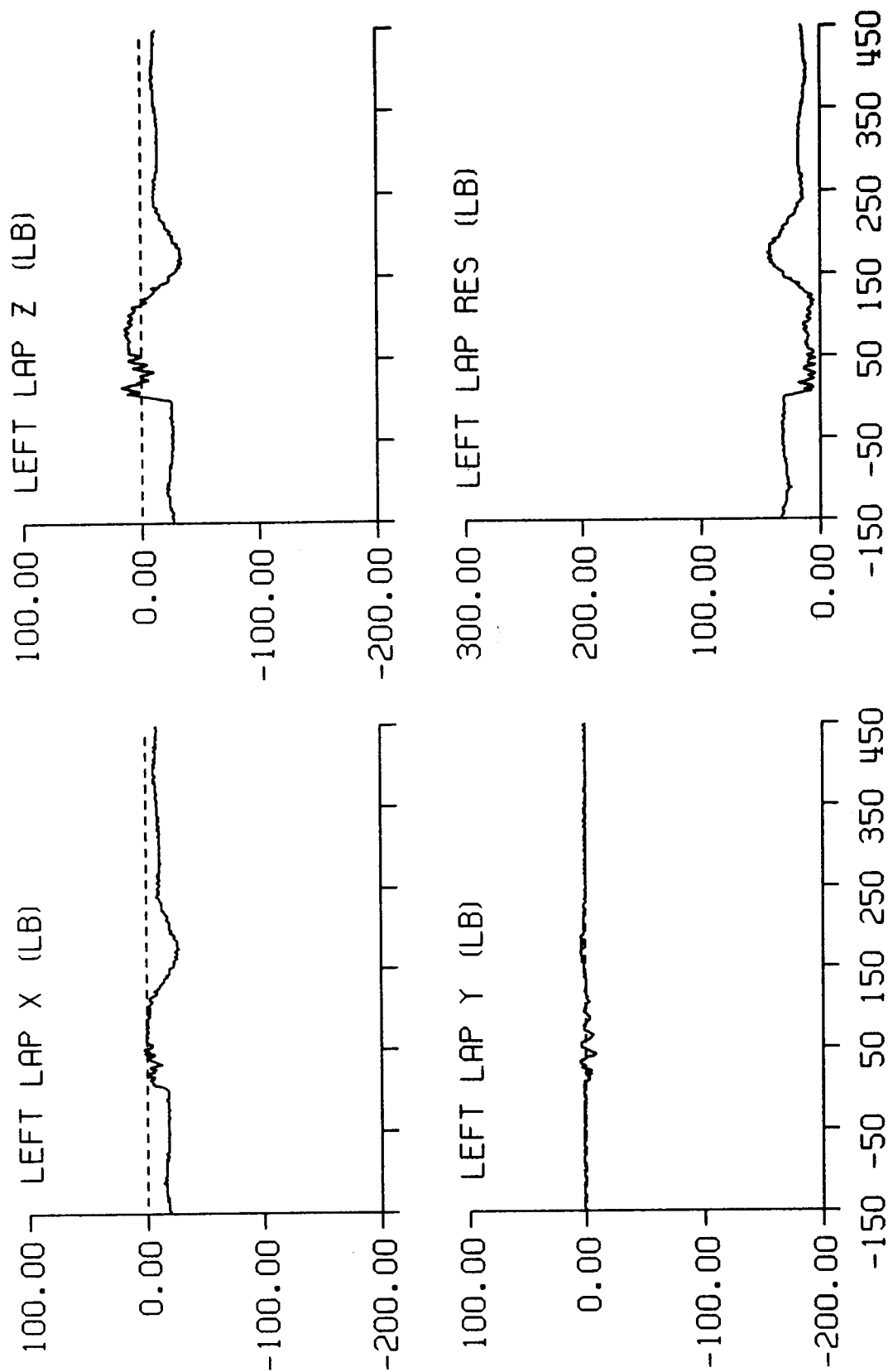
TIME IN MILLISECONDS

DP2 STUDY TEST: 2678 SUBJ: ADAM-L CELL: B



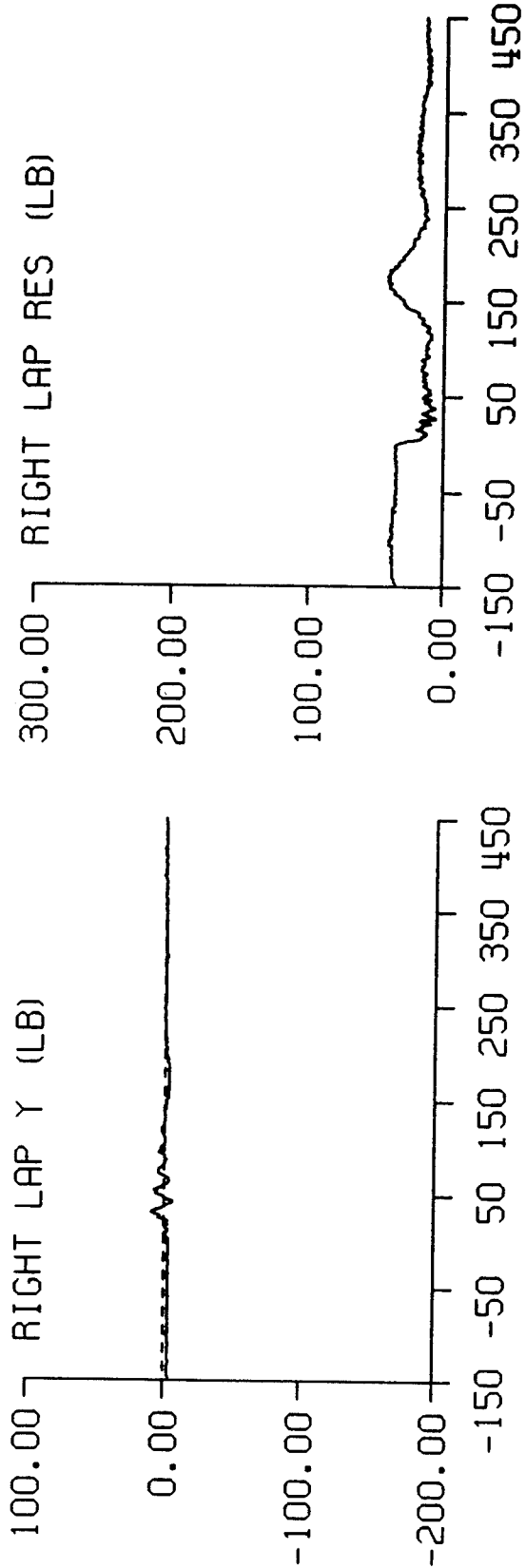
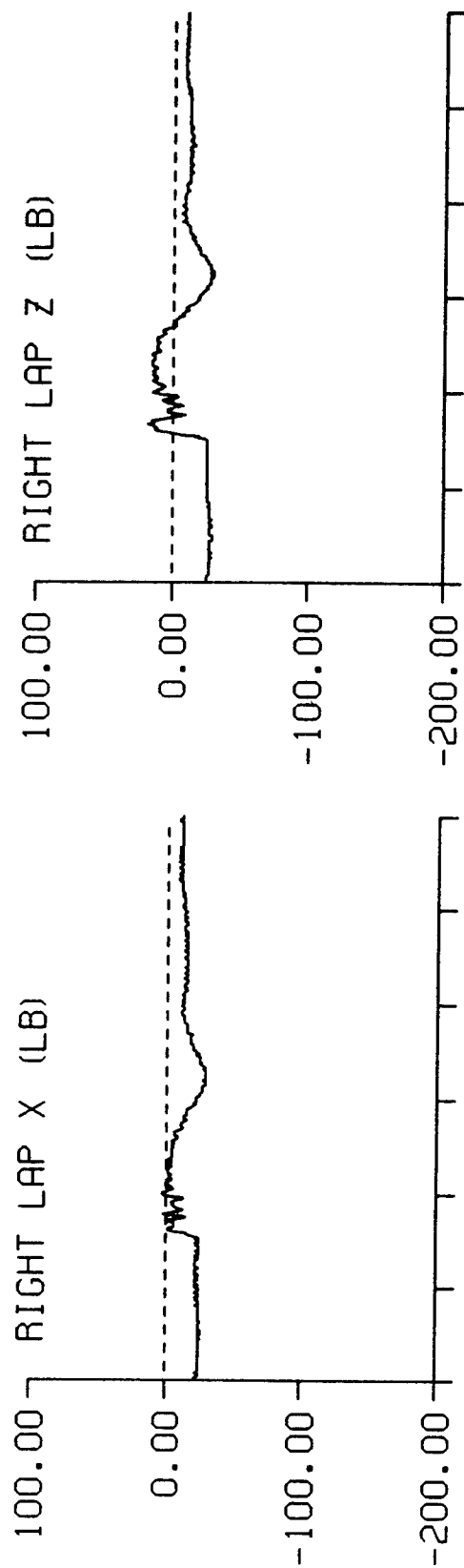
TIME IN MILLISECONDS

DP2 STUDY TEST: 2678 SUBJ: ADAM-L CELL: B



TIME IN MILLISECONDS

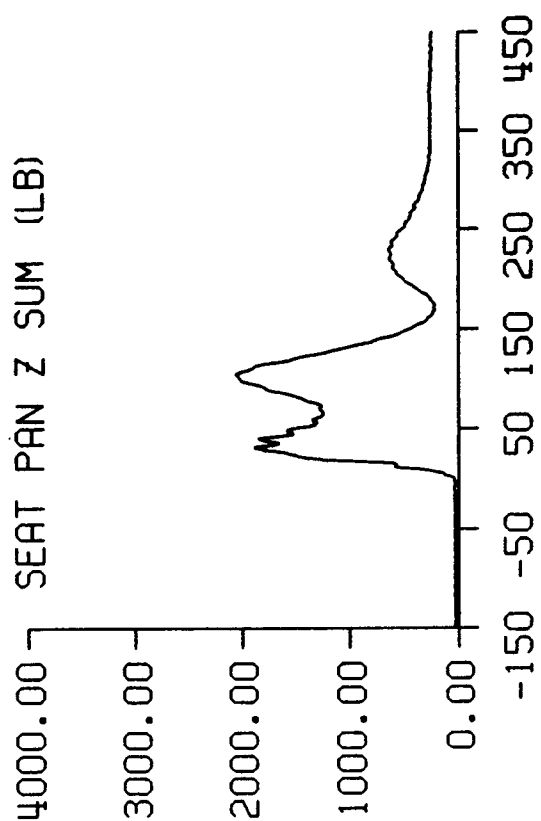
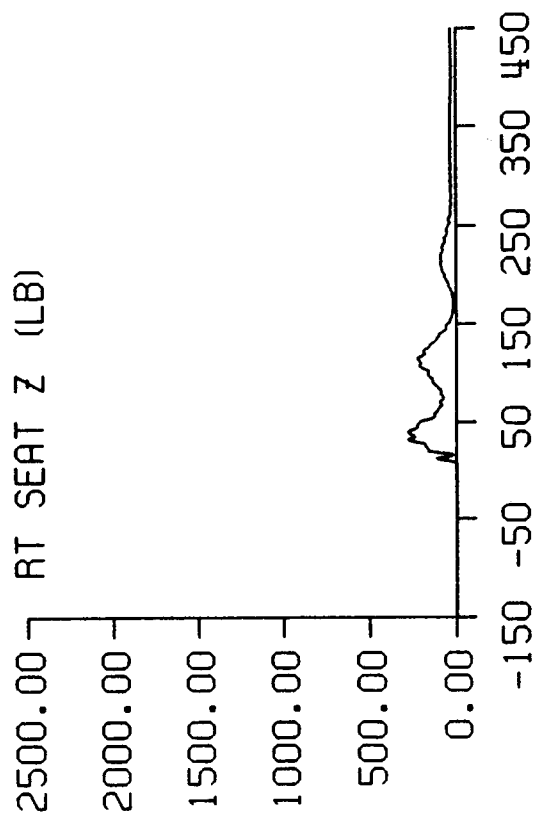
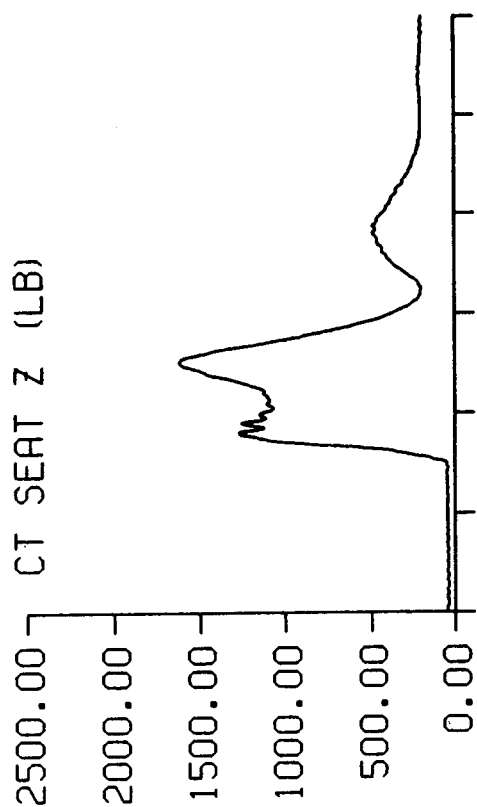
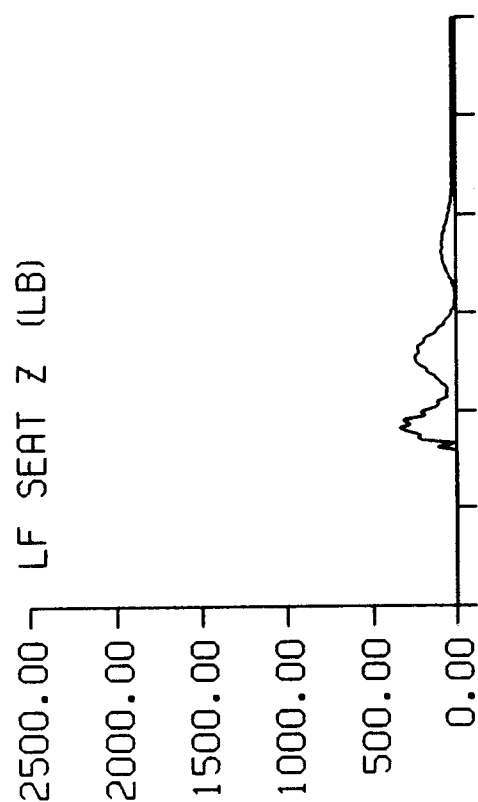
DP2 STUDY TEST: 2678 SUBJ: ADAM-L CELL: B



TIME IN MILLISECONDS

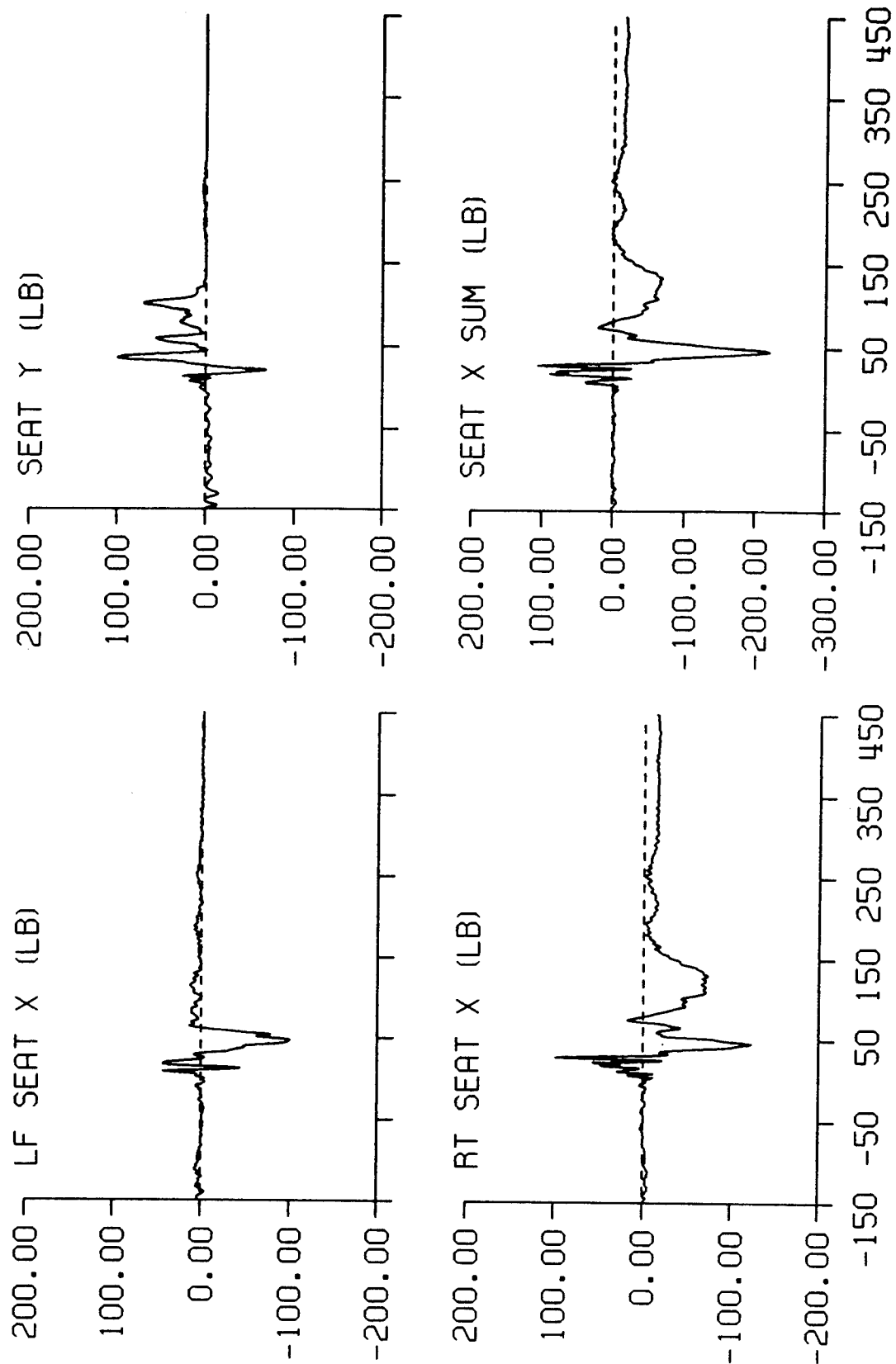


DP2 STUDY TEST: 2678 SUBJ: ADAM-L CELL: B



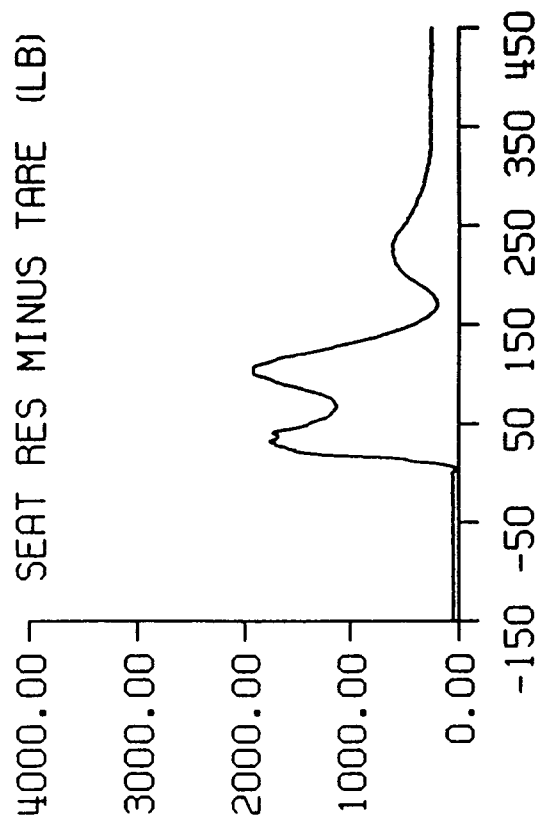
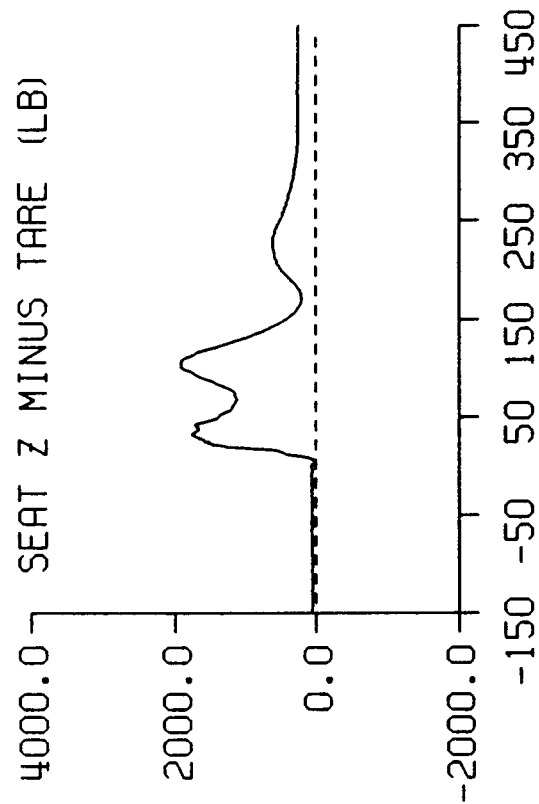
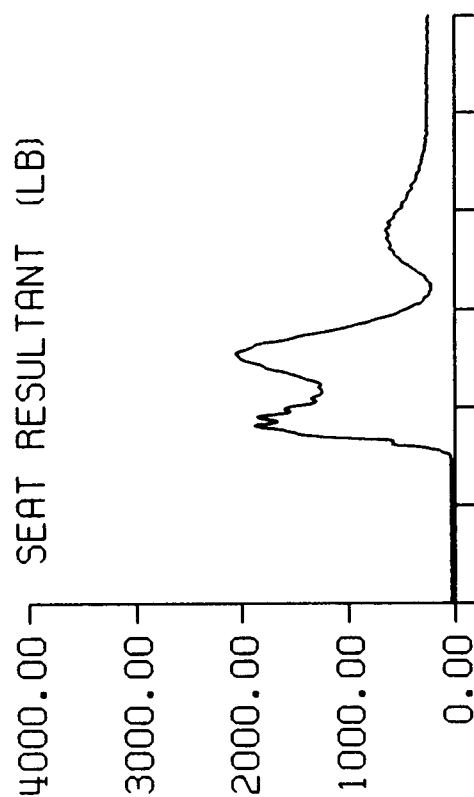
TIME IN MILLISECONDS

DP2 STUDY TEST: 2678 SUBJ: ADAM-L CELL: B



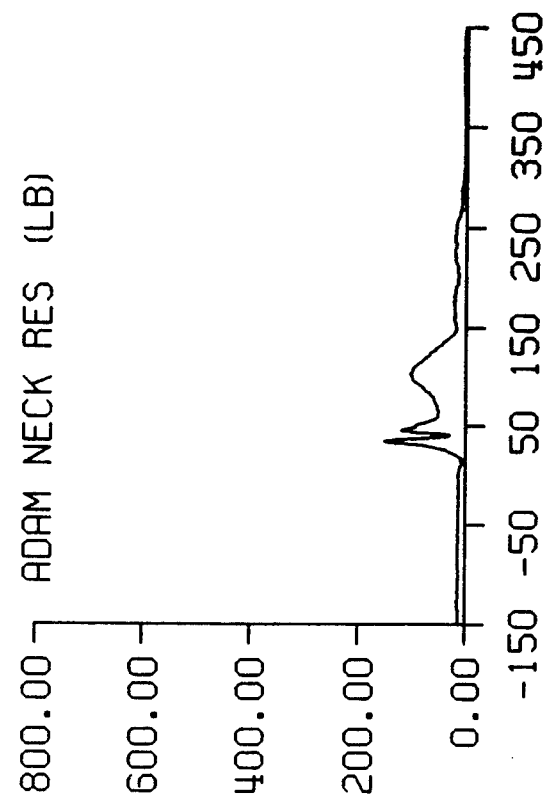
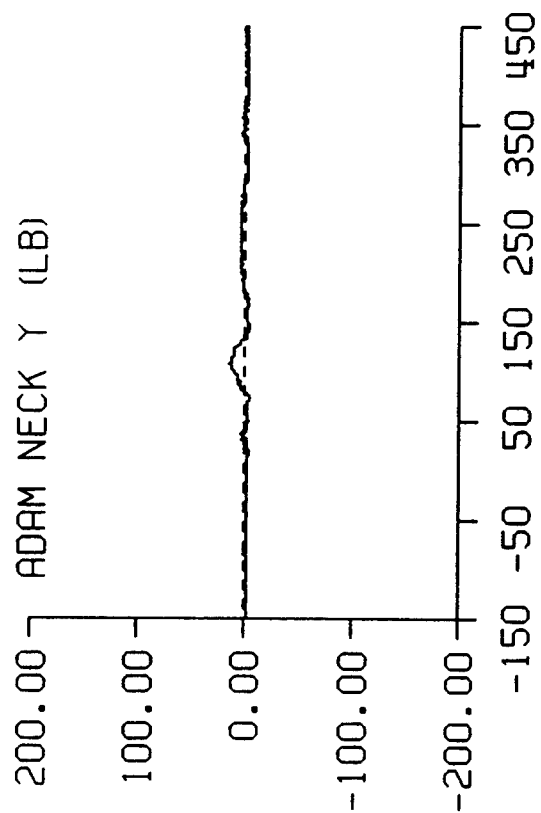
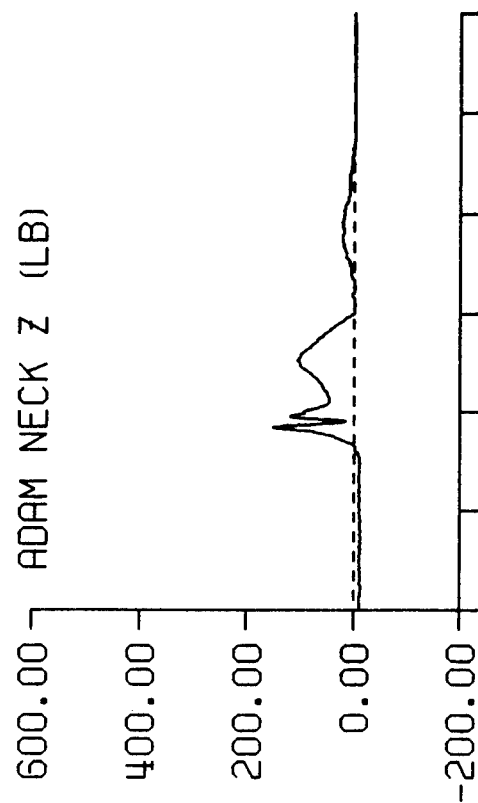
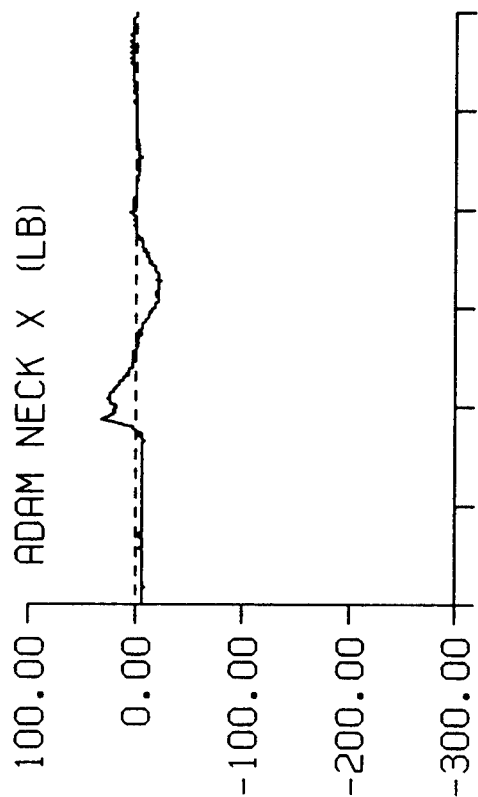
TIME IN MILLISECONDS

DP2 STUDY TEST: 2678 SUBJ: ADAM-L CELL: B



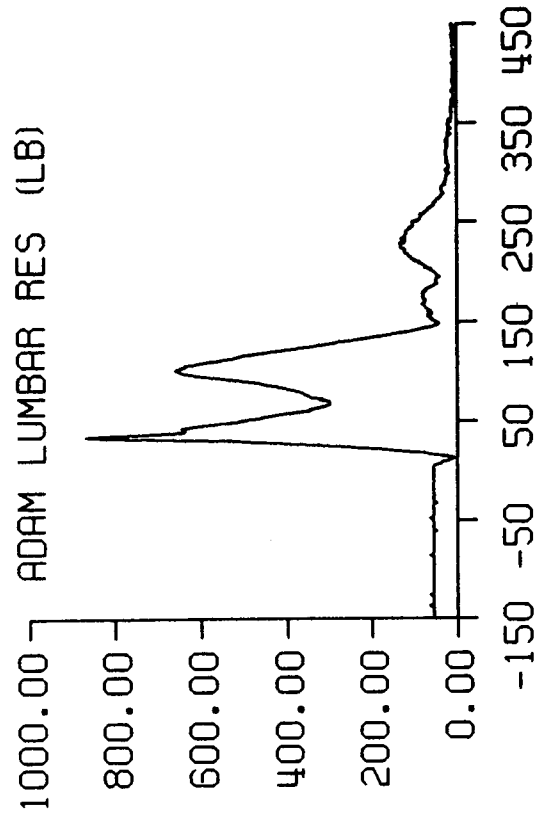
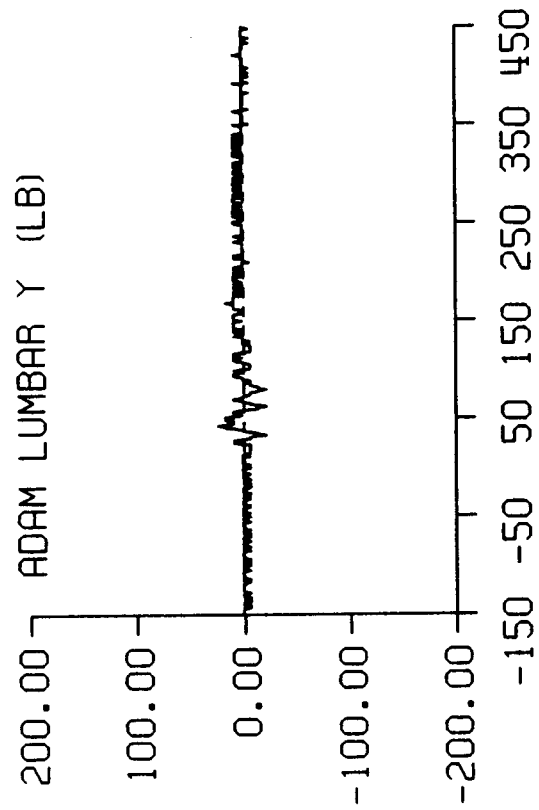
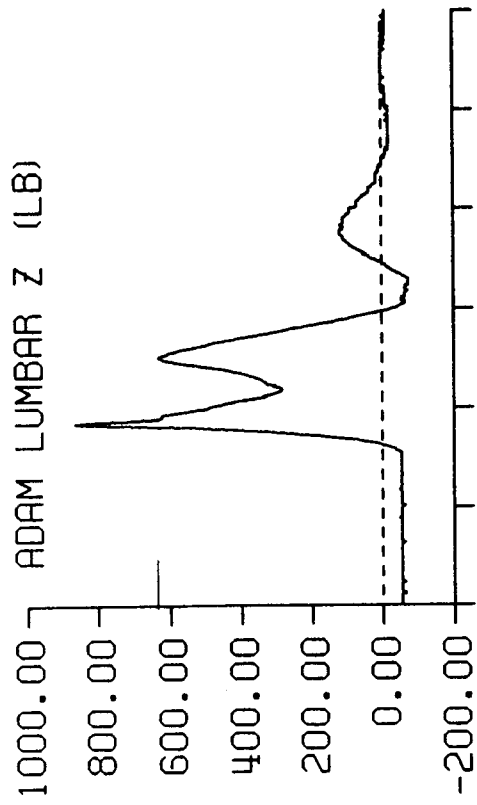
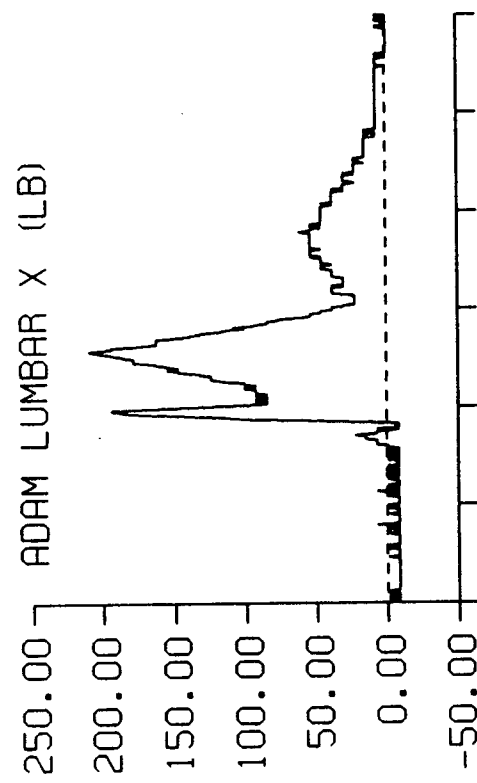
TIME IN MILLISECONDS

DP2 STUDY TEST: 2678 SUBJ: ADAM-L CELL: B



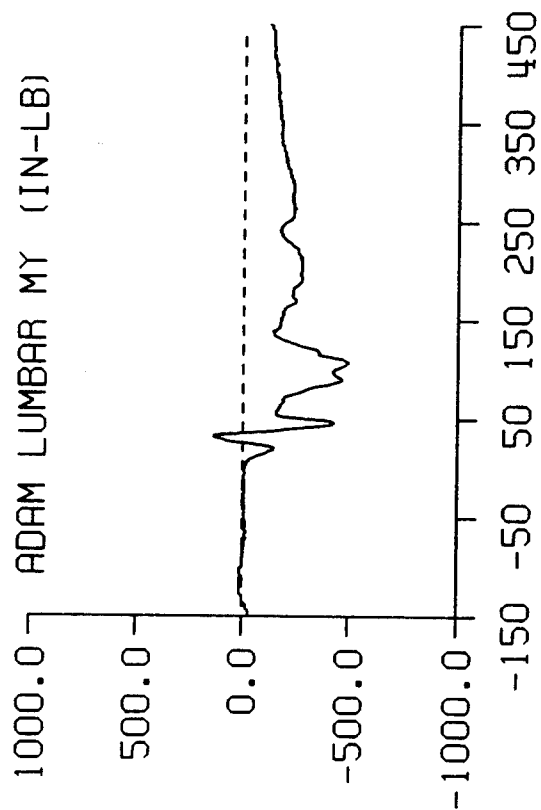
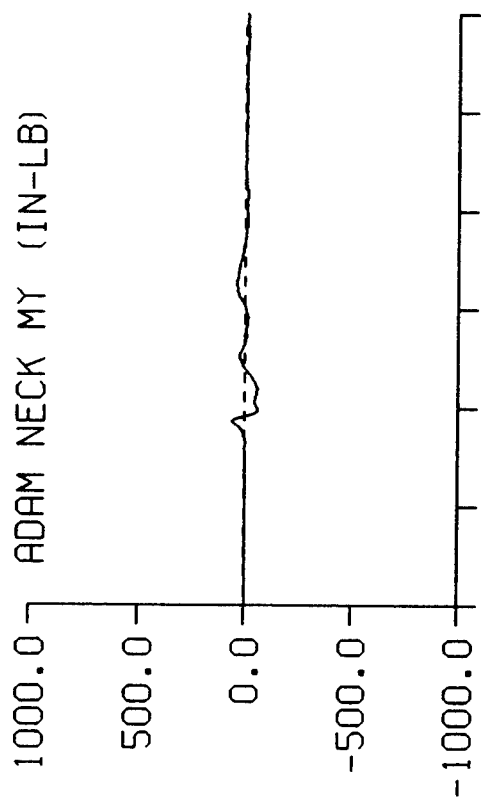
TIME IN MILLISECONDS

DP2 STUDY TEST: 2678 SUBJ: ADAM-L CELL: B



TIME IN MILLISECONDS

DP2 STUDY TEST: 2678 SUBJ: ADAM-L CELL: B



TIME IN MILLISECONDS

DP2 STUDY TEST: 2683 SUBJ: C-9 WT: 202.0 NOM G: 6.0 CELL: A

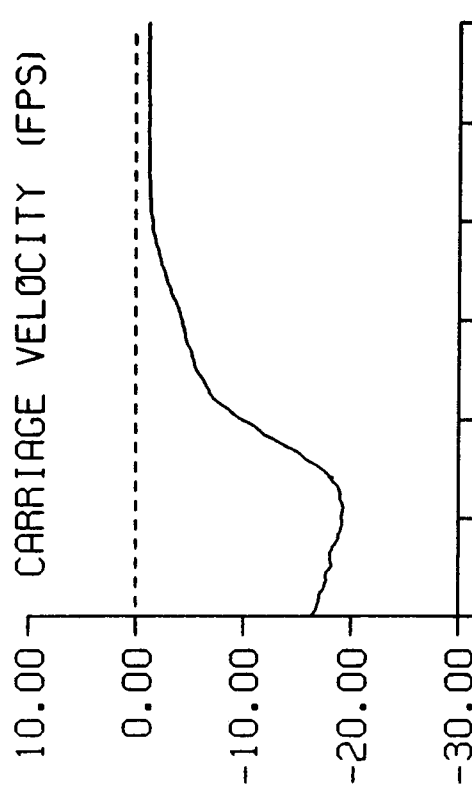
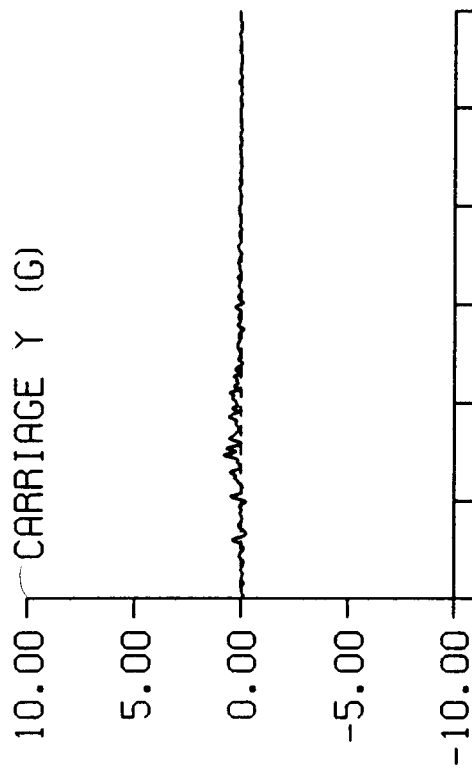
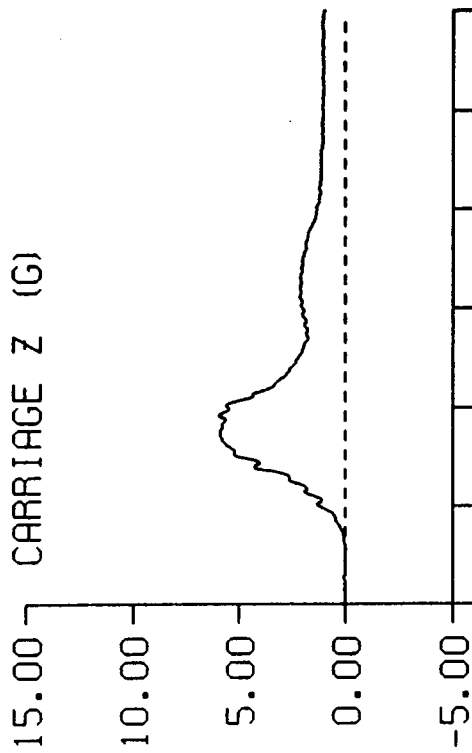
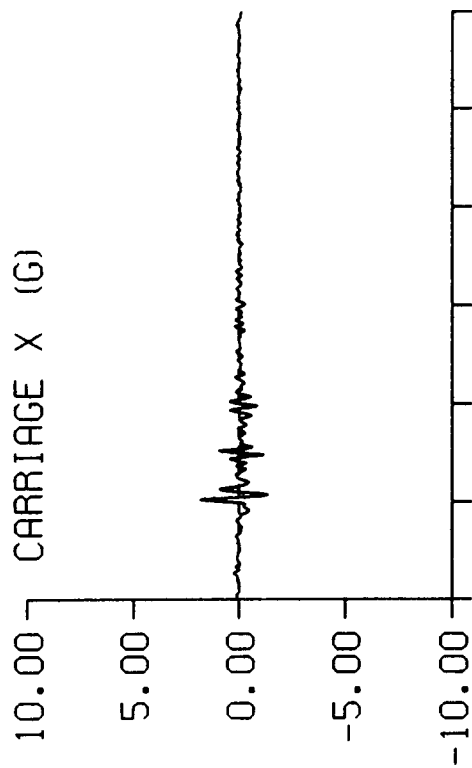
DATA ID	IMMEDIATE PREIMPACT	MAXIMUM VALUE	MINIMUM VALUE	TIME OF MAXIMUM	TIME OF MINIMUM
REFERENCE MARK TIME (MS)				-98.	
2.5V EXT PWR (VOLTS)	2.50	2.50	2.50	41.	1.
10V EXT PWR (VOLTS)	10.00	10.00	10.00	102.	0.
CARRIAGE ACCELERATION (G)					
X AXIS	0.00	1.84	-1.43	12.	17.
Y AXIS	-0.01	0.82	-0.26	56.	9.
Z AXIS	0.14	5.99	0.47	102.	0.
CARRIAGE VELOCITY (FPS)	-18.43	-1.18	-19.25	398.	20.
SEAT ACCELERATION (G)					
X AXIS	0.00	1.61	-1.20	12.	57.
Y AXIS	0.11	0.99	-1.45	25.	12.
Z AXIS	0.06	7.00	-0.15	103.	16.
Z AXIS DRI	-0.09	7.41	0.00	107.	0.
HEAD ACCELERATION (G)					
X AXIS	-0.22	0.88	-1.12	70.	139.
Y AXIS	0.15	0.22	-0.26	0.	86.
Z AXIS	1.71	9.03	1.83	93.	0.
RESULTANT	1.73	9.05	1.84	93.	1.
RY (RAD/SEC2)	54.74	229.29	-13.95	116.	159.
CHEST ACCELERATION (G)					
X AXIS	0.11	1.64	-0.15	89.	11.
Y AXIS	0.18	0.41	-0.54	15.	110.
Z AXIS	-0.12	6.95	-0.01	99.	5.
RESULTANT	0.26	7.09	0.21	99.	3.
RY (RAD/SEC2)	-10.12	189.41	-186.35	145.	53.
SHOULDER STRAP FORCES (LB)					
X AXIS	-102.03	-35.27	-151.58	505.	114.
Y AXIS	6.09	15.65	1.03	88.	339.
Z AXIS	6.72	50.46	6.33	114.	3.
RESULTANT	102.44	160.41	35.99	114.	505.
HEADREST FORCES (LB)					
UPPER X AXIS	1.12	1.12	-7.40	1.	57.
LOWER X AXIS	0.27	8.67	-3.08	60.	58.
X AXIS SUM	1.39	5.53	-8.62	60.	57.

DP2 STUDY TEST: 2683 SUBJ: C-9 WT: 202.0 NOM G: 6.0 CELL: A

DATA ID	IMMEDIATE PREIMPACT	MAXIMUM VALUE	MINIMUM VALUE	TIME OF MAXIMUM	TIME OF MINIMUM
LAP FORCES (LB)					
LEFT X AXIS	-85.01	-16.77	-92.37	487.	5.
LEFT Y AXIS	39.11	42.15	7.02	1.	469.
LEFT Z AXIS	-128.64	-23.49	-136.23	495.	1.
LEFT RESULTANT	159.07	169.90	30.17	5.	495.
RIGHT X AXIS	-74.52	-15.88	-77.14	493.	0.
RIGHT Y AXIS	-31.06	-3.44	-32.11	478.	0.
RIGHT Z AXIS	-105.50	-19.53	-111.12	477.	2.
RIGHT RESULTANT	132.85	139.03	25.40	2.	493.
SEAT FORCES (LB)					
LEFT X AXIS	20.46	39.36	12.43	23.	98.
RIGHT X AXIS	-0.46	19.17	-5.02	61.	204.
X AXIS SUM	20.00	50.56	16.45	13.	7.
Y AXIS	-2.44	1.18	-18.82	87.	345.
LEFT Z AXIS	81.61	317.14	54.25	79.	413.
RIGHT Z AXIS	13.65	176.63	15.71	79.	0.
CENTER Z AXIS	154.32	1037.77	148.82	96.	374.
Z AXIS SUM	249.58	1512.89	218.78	88.	509.
RESULTANT	250.40	1513.11	220.11	88.	509.
Z SUM MINUS TARE	267.03	1415.14	222.29	96.	509.
RESULTANT MINUS TARE	267.78	1415.36	222.91	96.	509.

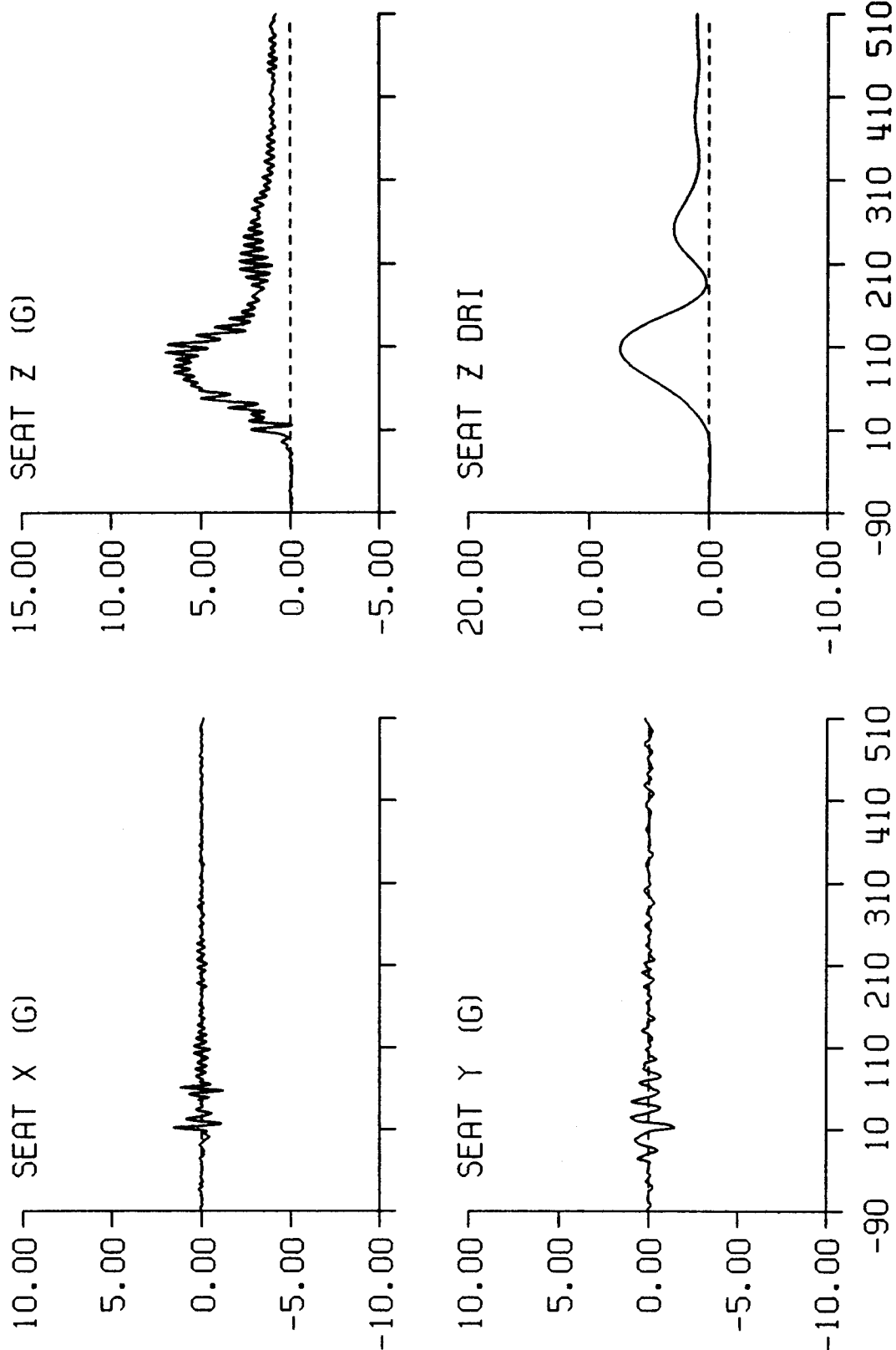


DP2 STUDY TEST: 2683 SUBJ: C-9 CELL: A



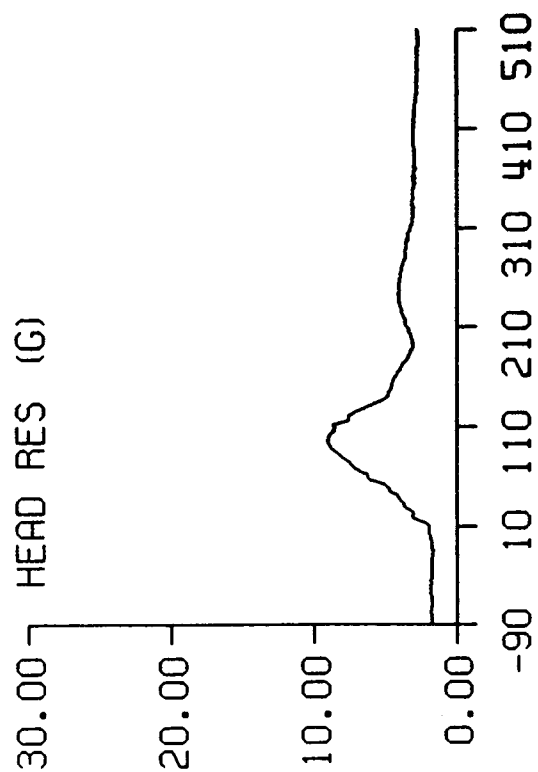
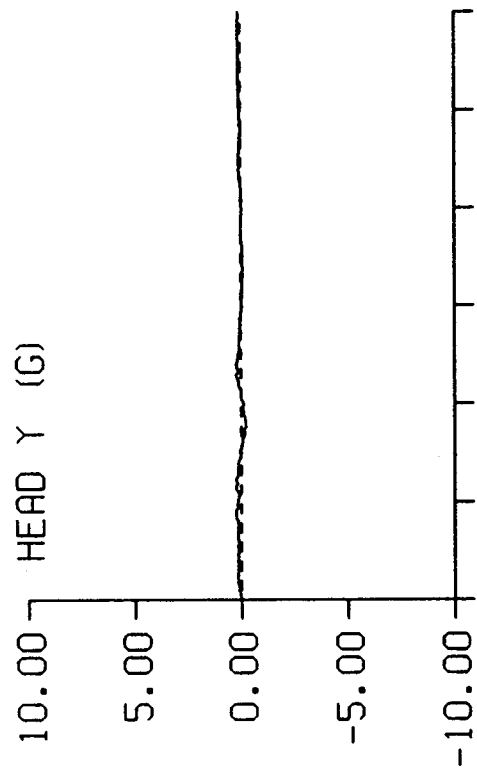
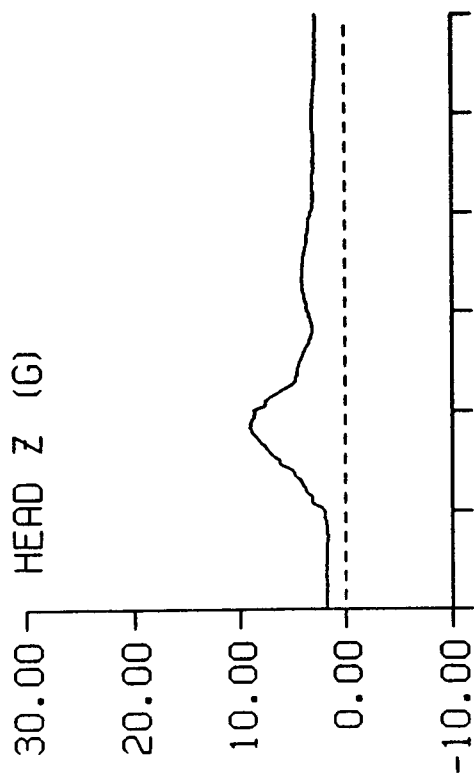
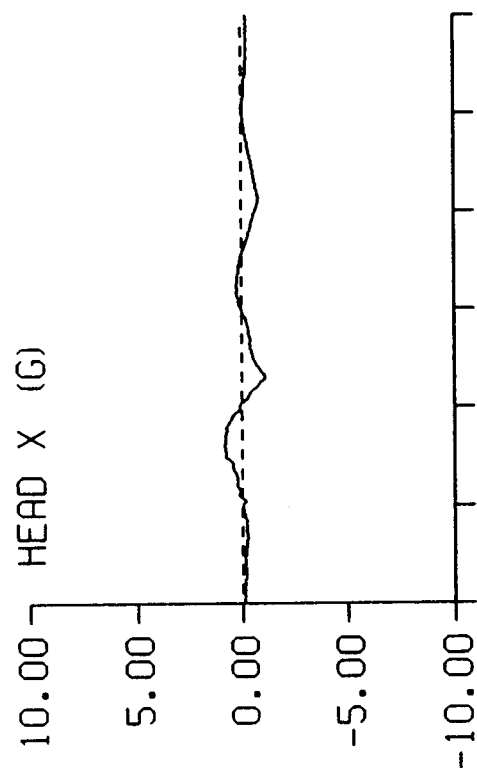
TIME IN MILLISECONDS

DP2 STUDY TEST: 2683 SUBJ: C-9 CELL: A



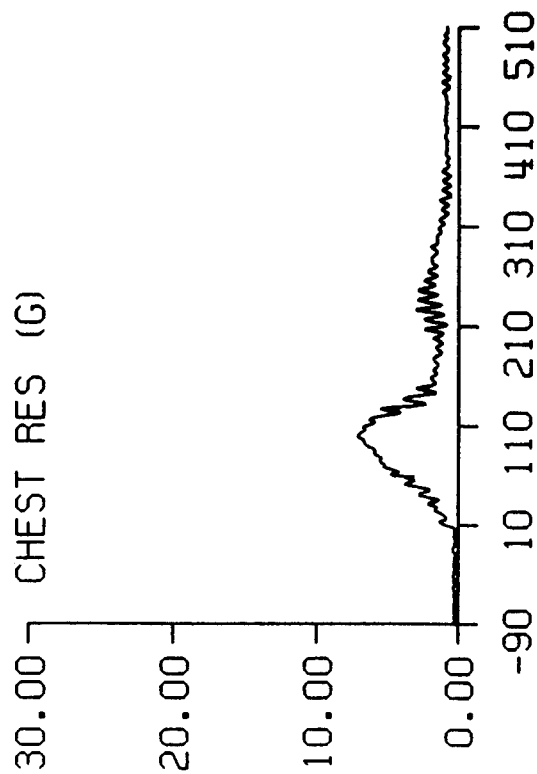
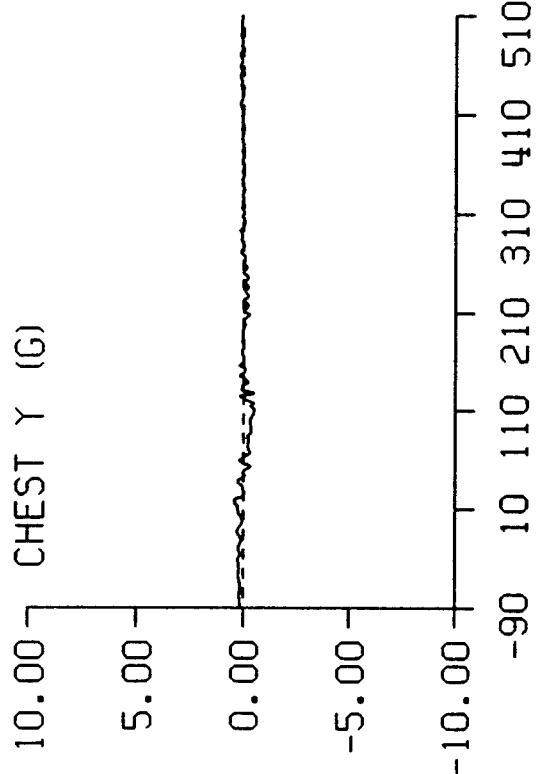
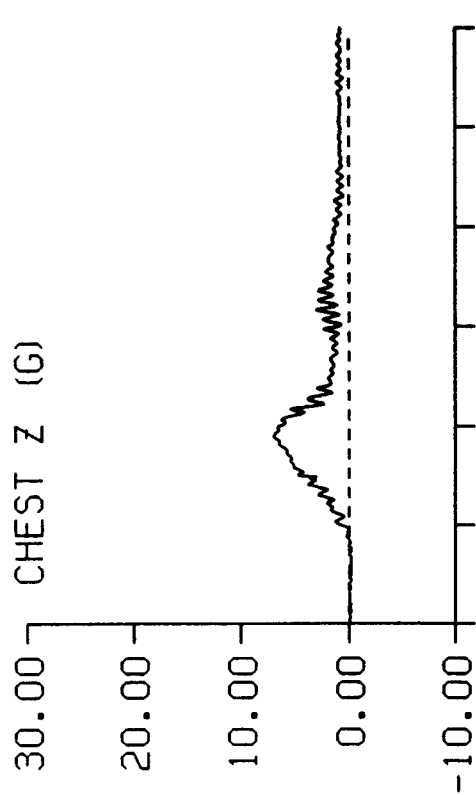
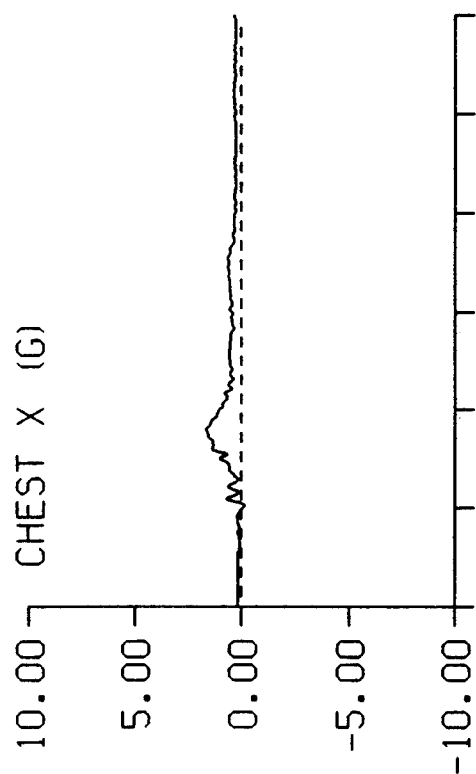
TIME IN MILLISECONDS

DP2 STUDY TEST: 2683 SUBJ: C-9 CELL: A



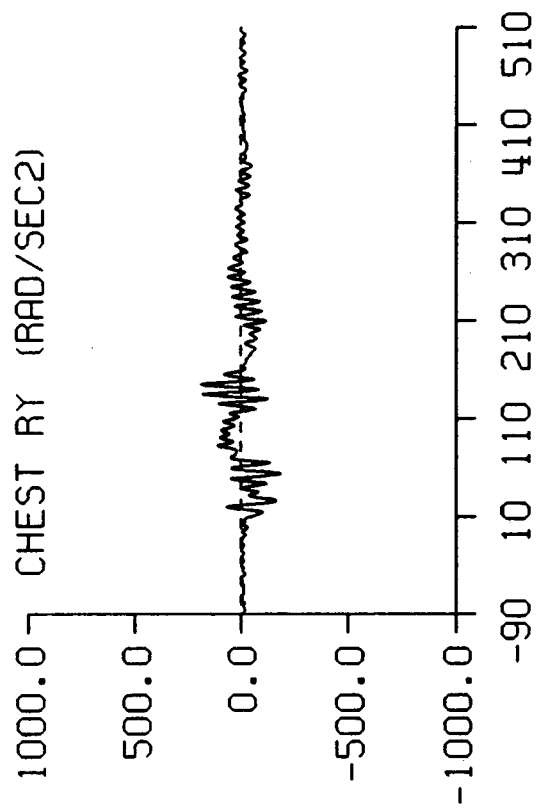
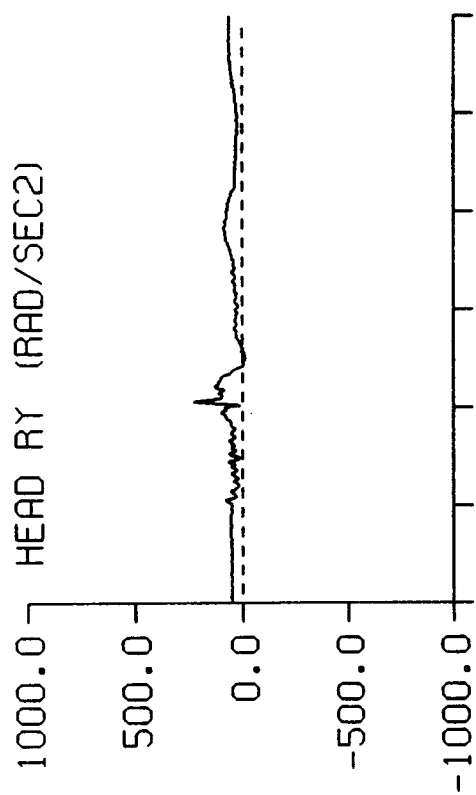
TIME IN MILLISECONDS

DP2 STUDY TEST: 2683 SUBJ: C-9 CELL: A



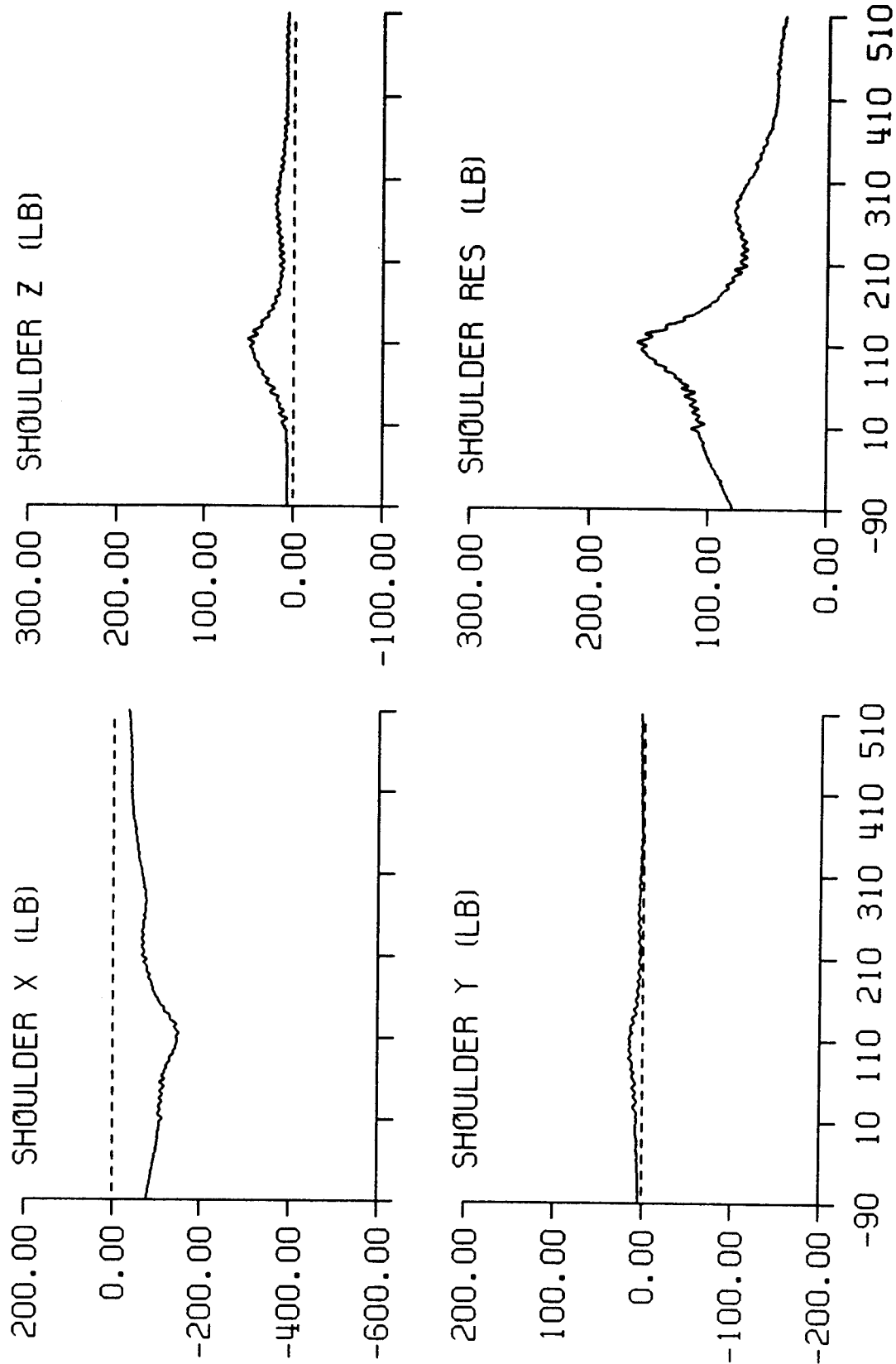
TIME IN MILLISECONDS

DP2 STUDY TEST: 2683 SUBJ: C-9 CELL: A



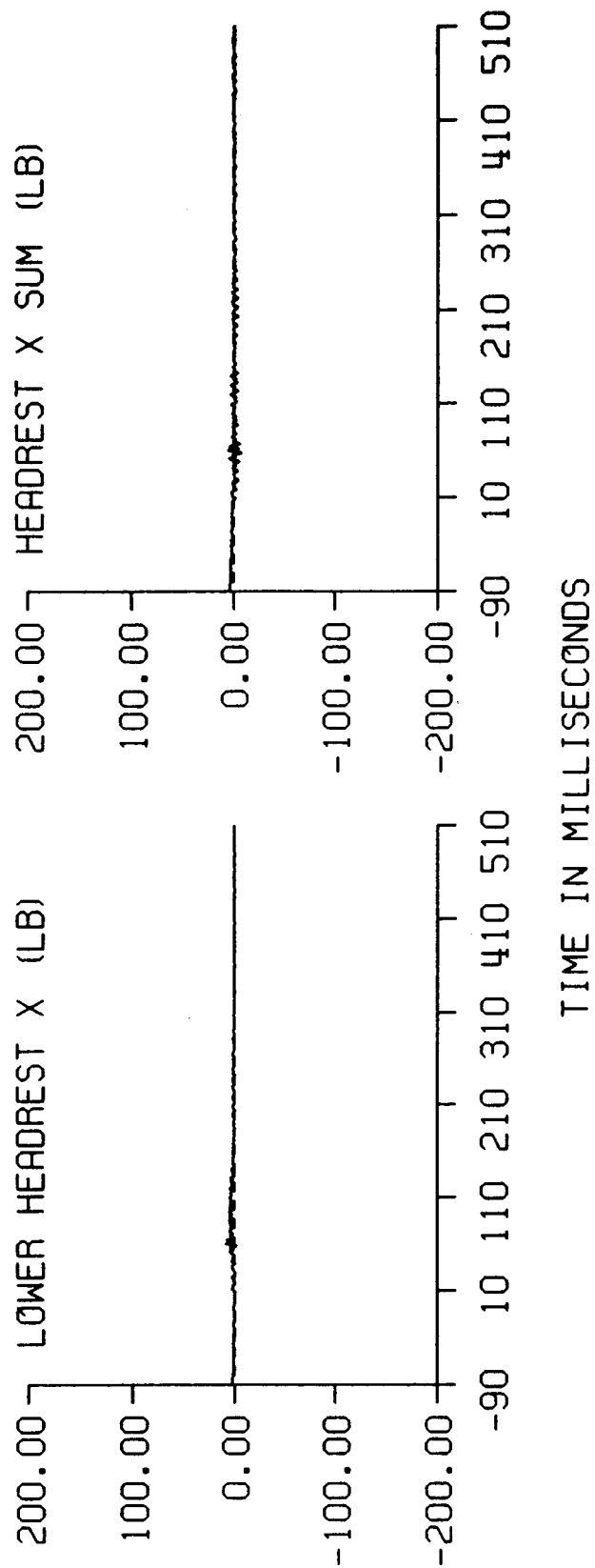
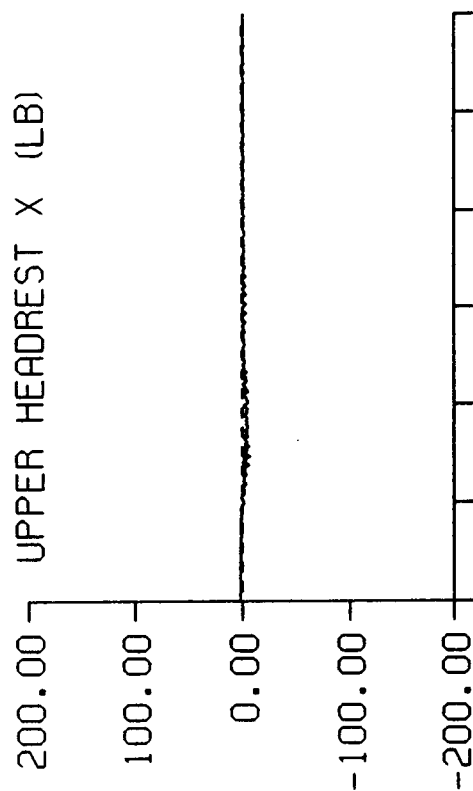
TIME IN MILLISECONDS

DP2 STUDY TEST: 2683 SUBJ: C-9 CELL: A

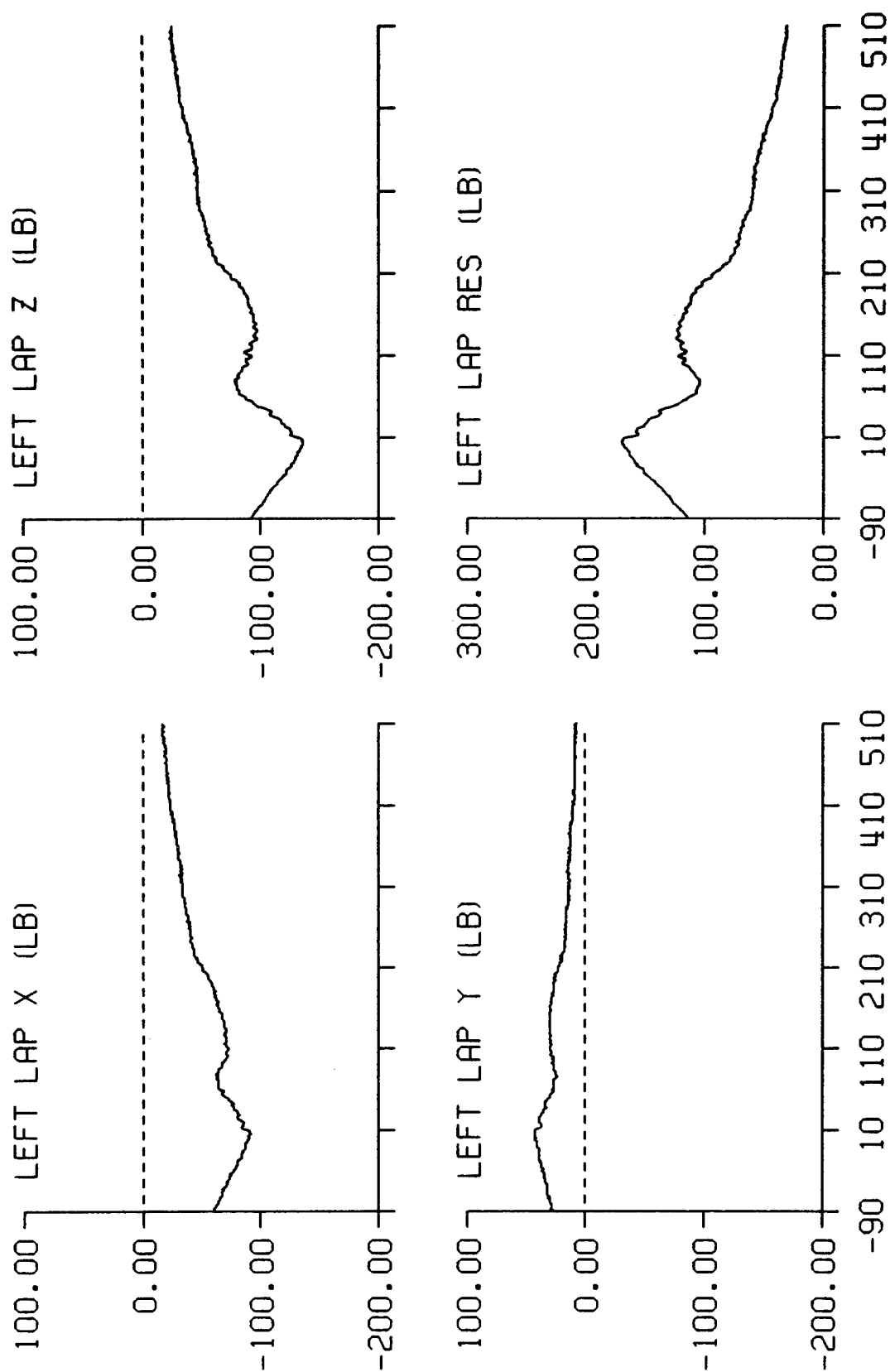


TIME IN MILLISECONDS

DP2 STUDY TEST: 2683 SUBJ: C-9 CELL: A



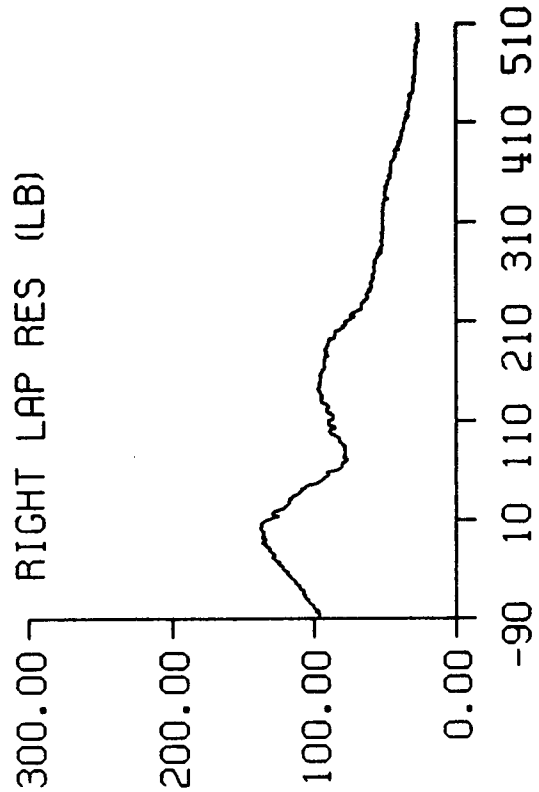
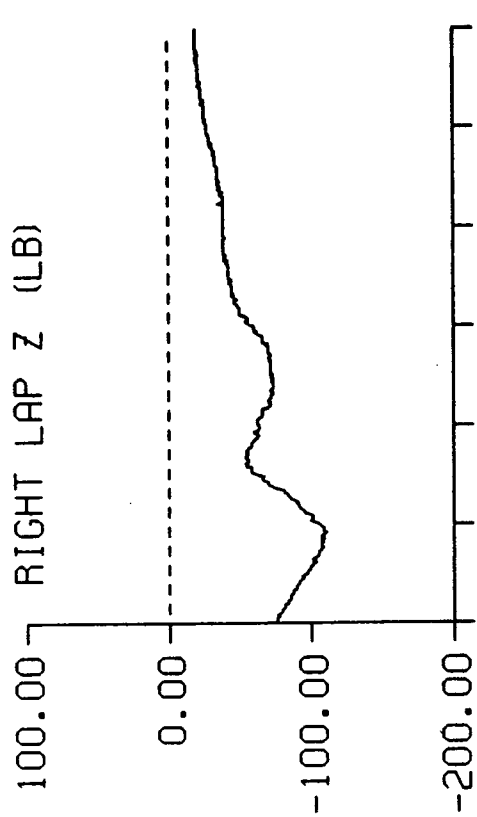
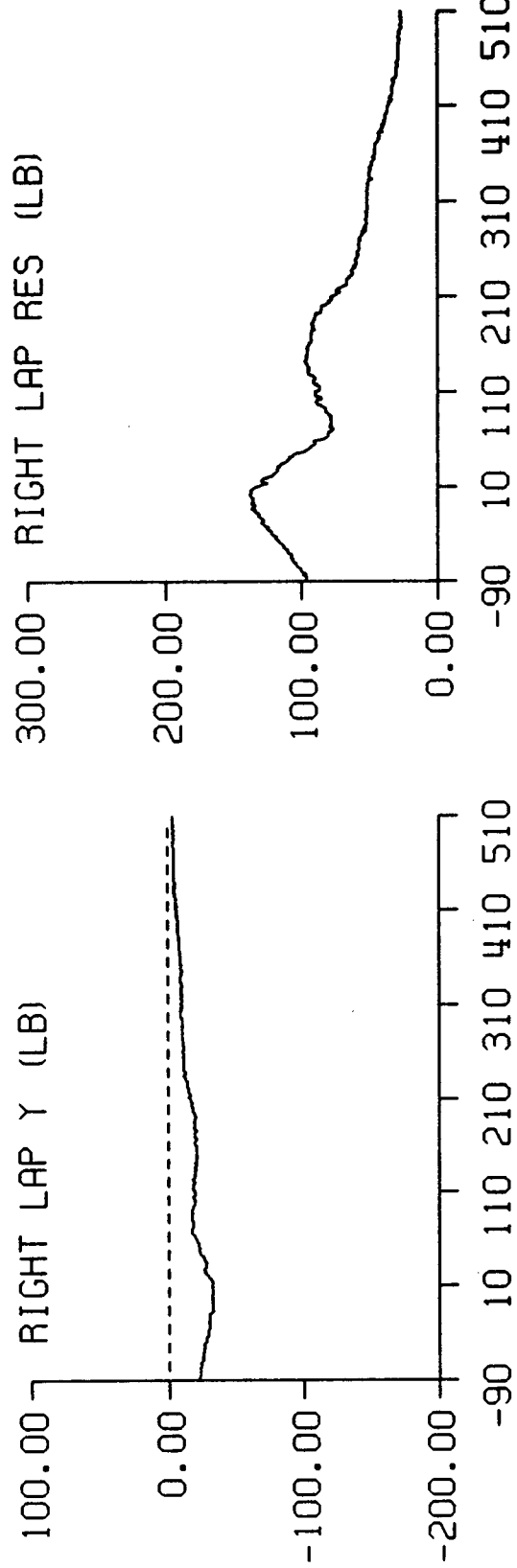
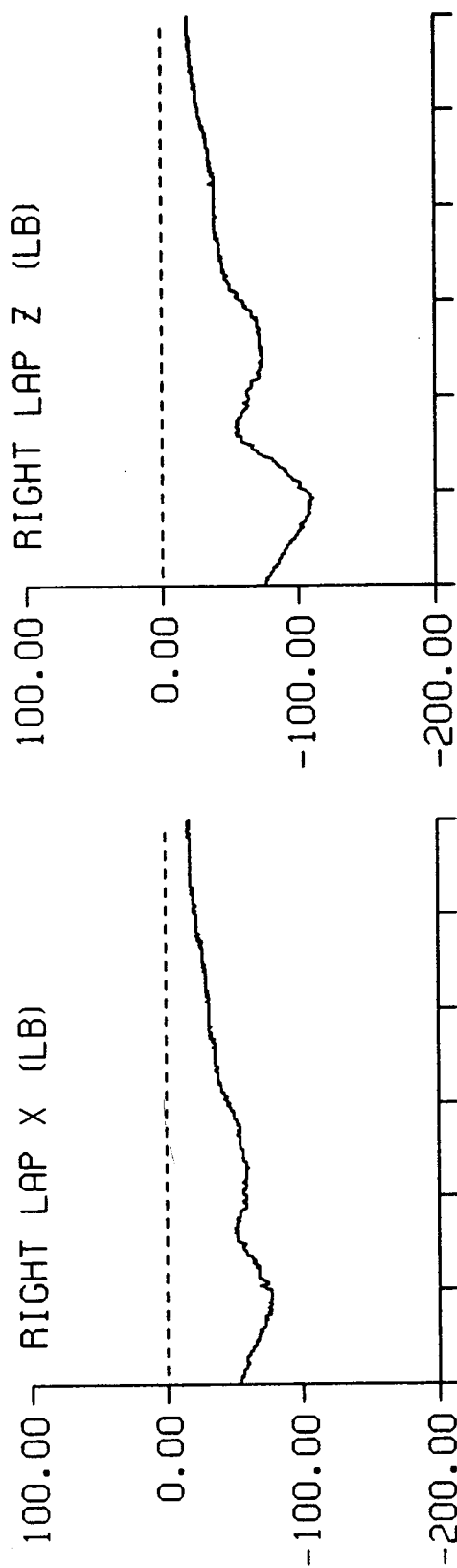
DP2 STUDY TEST: 2683 SUBJ: C-9 CELL: A



TIME IN MILLISECONDS

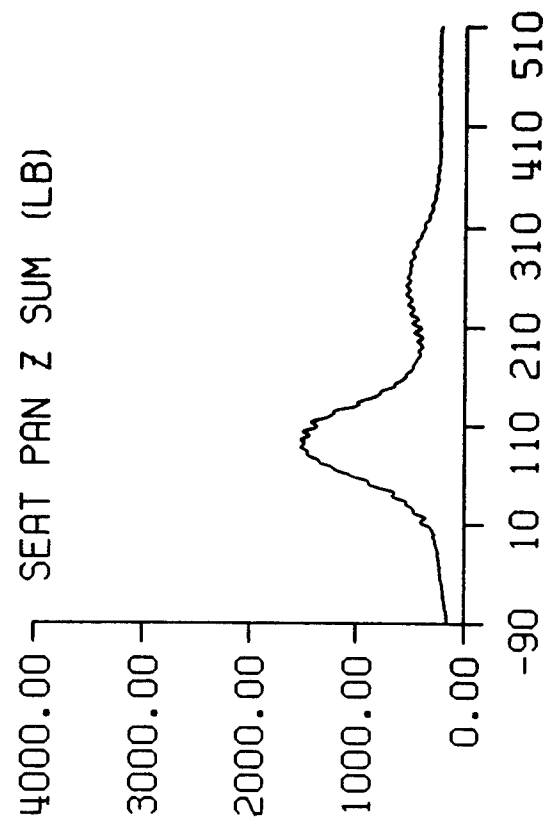
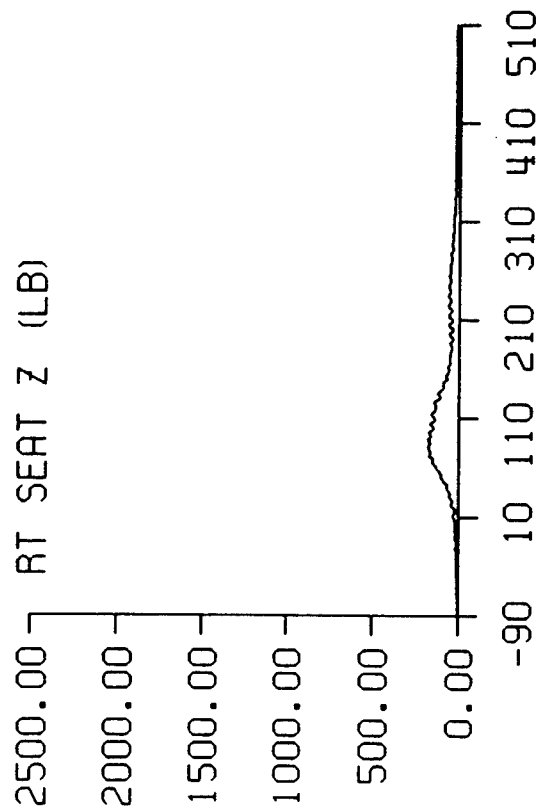
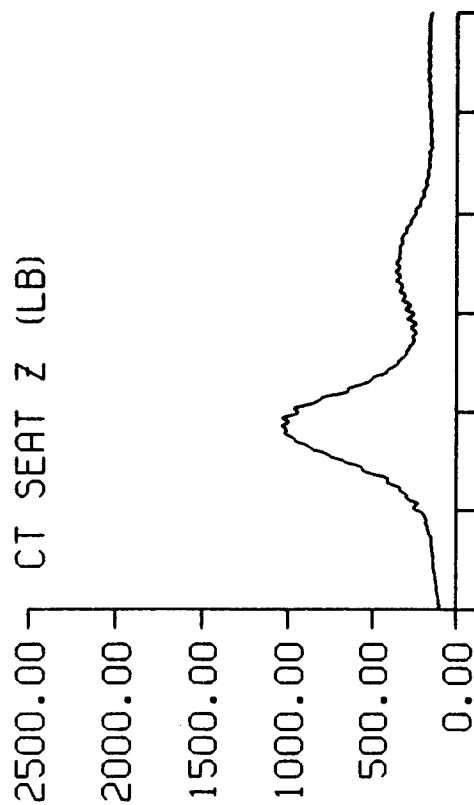
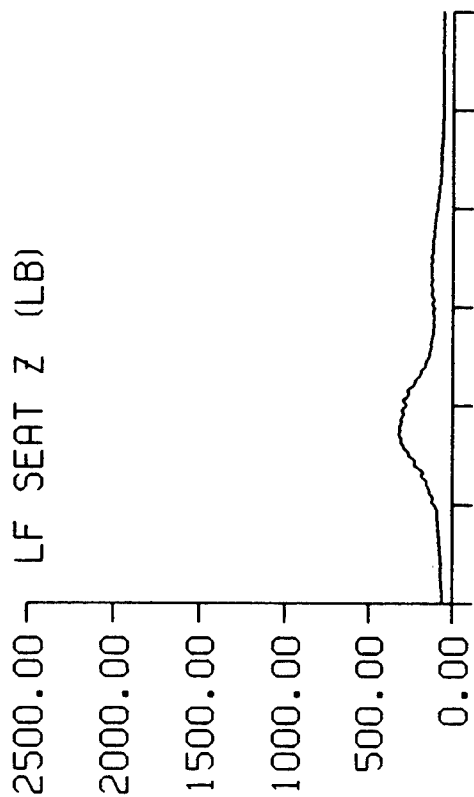


DP2 STUDY TEST: 2683 SUBJ: C-9 CELL: A



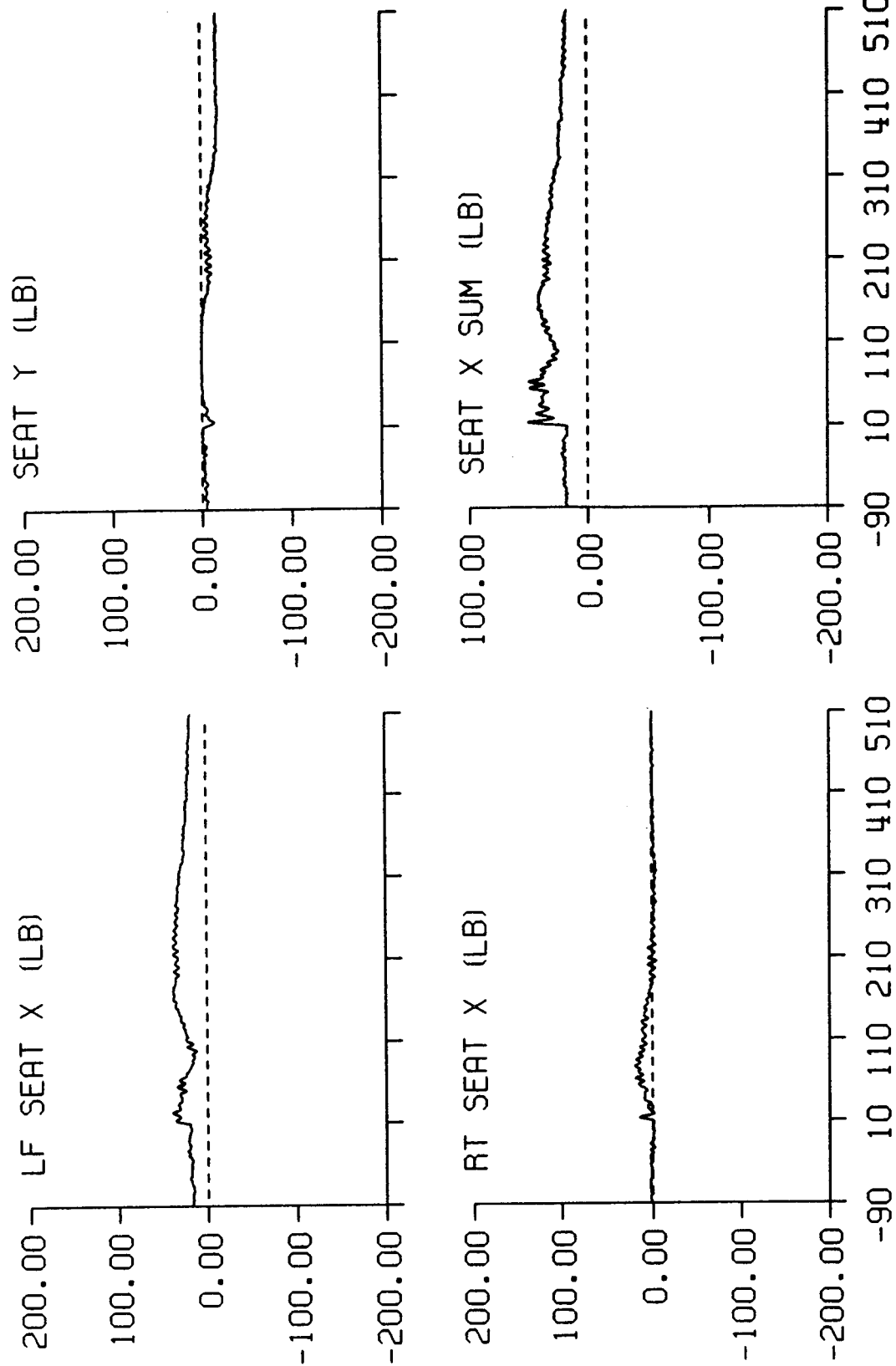
TIME IN MILLISECONDS

DP2 STUDY TEST: 2683 SUBJ: C-9 CELL: A



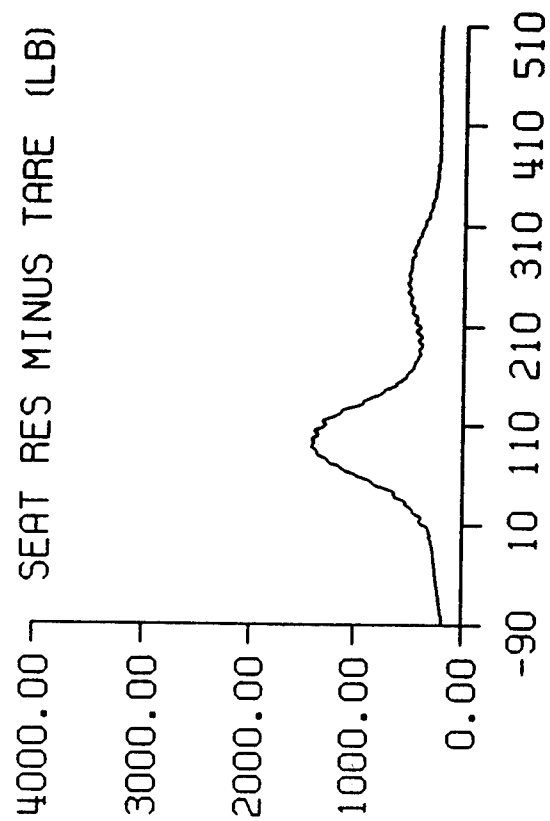
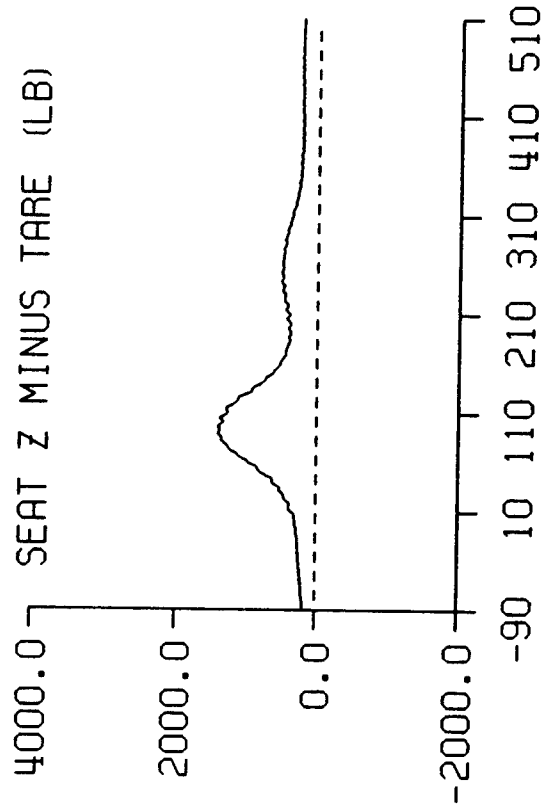
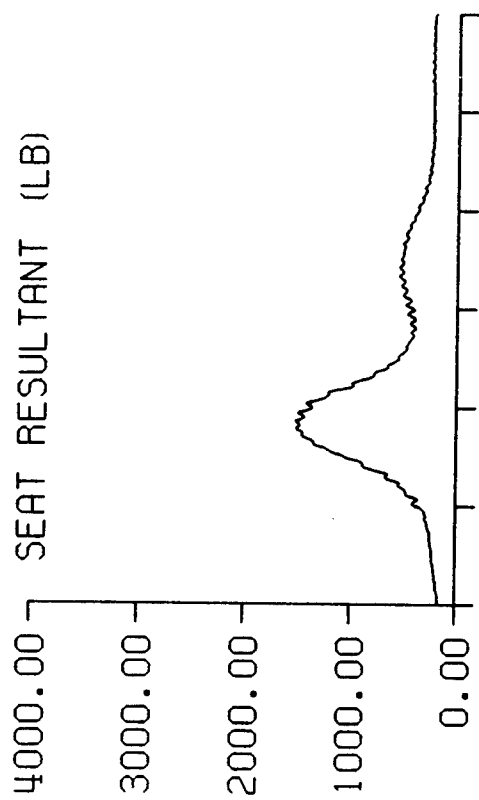
TIME IN MILLISECONDS

DP2 STUDY TEST: 2683 SUBJ: C-9 CELL: A



TIME IN MILLISECONDS

DP2 STUDY TEST: 2683 SUBJ: C-9 CELL: A



TIME IN MILLISECONDS

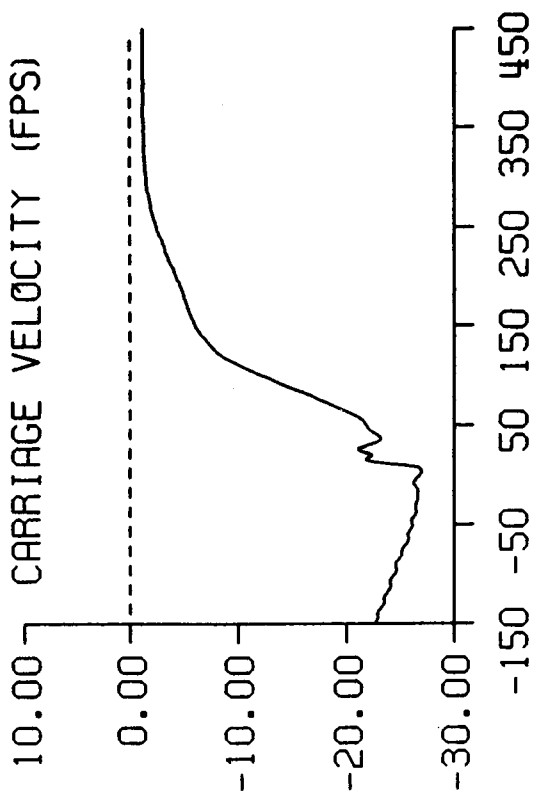
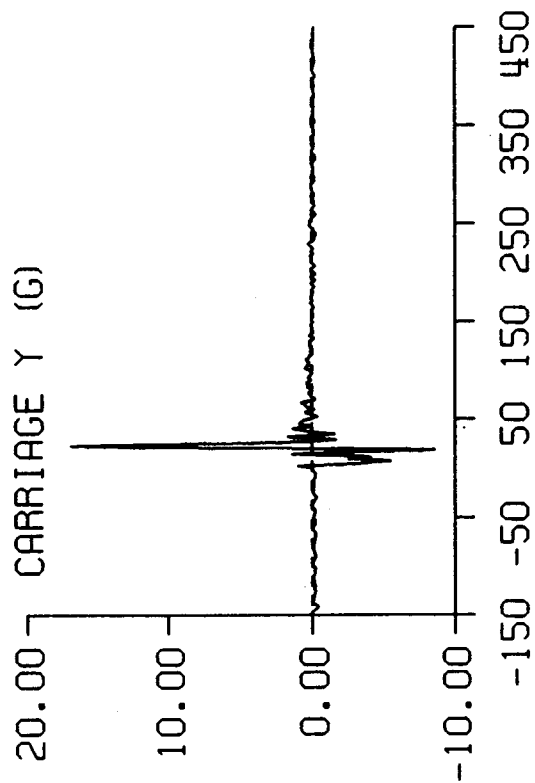
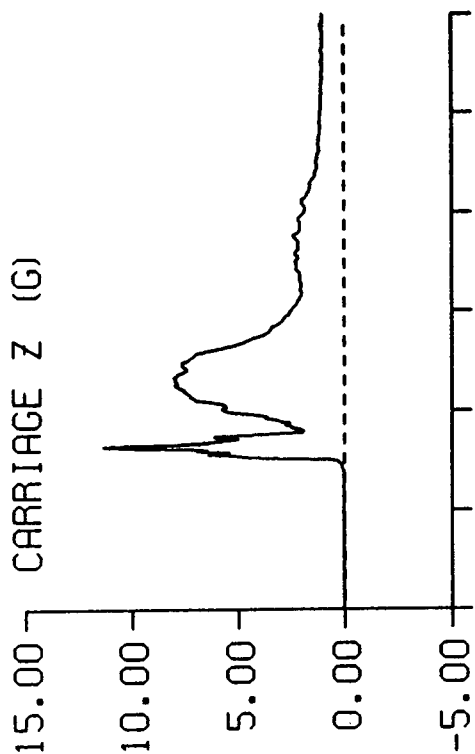
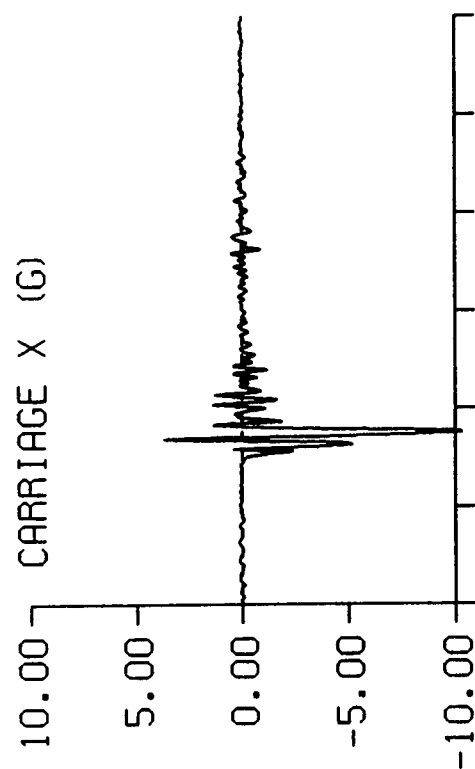
DP2 STUDY TEST: 2735 SUBJ: S-13 WT: 186.0 NOM G: 10.0 CELL: B

DATA ID	IMMEDIATE PREIMPACT	MAXIMUM VALUE	MINIMUM VALUE	TIME OF MAXIMUM	TIME OF MINIMUM
REFERENCE MARK TIME (MS)				-154.	
2.5V EXT PWR (VOLTS)	2.50	2.50	2.49	10.	23.
10V EXT PWR (VOLTS)	10.00	10.00	10.00	0.	4.
CARRIAGE ACCELERATION (G)					
X AXIS	0.03	3.67	-10.32	18.	25.
Y AXIS	-0.16	16.87	-8.62	22.	18.
Z AXIS	0.03	11.34	0.32	15.	0.
CARRIAGE VELOCITY (FPS)	-26.48	-1.19	-26.95	363.	3.
SEAT ACCELERATION (G)					
X AXIS	-0.01	5.24	-2.33	17.	21.
Y AXIS	0.06	2.59	-1.26	31.	61.
Z AXIS	-0.08	17.87	-2.76	18.	24.
Z AXIS DRI	-0.12	7.85	-0.13	48.	0.
HEAD ACCELERATION (G)					
X AXIS	-0.05	2.56	-2.05	29.	128.
Y AXIS	-0.01	0.89	-0.10	101.	164.
Z AXIS	0.32	9.51	0.02	25.	0.
RESULTANT	0.38	9.72	0.26	25.	2.
RY (RAD/SEC2)	30.71	331.71	-227.28	54.	30.
CHEST ACCELERATION (G)					
X AXIS	-0.06	2.46	-1.21	85.	51.
Y AXIS	0.06	1.03	-1.04	67.	43.
Z AXIS	-0.20	9.46	-0.26	93.	0.
RESULTANT	0.24	9.56	0.08	93.	4.
RY (RAD/SEC2)	-10.40	999.31	-1083.80	41.	18.
SHOULDER STRAP FORCES (LB)					
X AXIS	-117.19	-33.06	-183.58	449.	50.
Y AXIS	5.76	16.99	-2.32	23.	26.
Z AXIS	26.07	92.12	12.68	102.	409.
RESULTANT	120.19	199.31	35.53	50.	449.
HEADREST FORCES (LB)					
UPPER X AXIS	1.91	9.19	-27.93	33.	20.
LOWER X AXIS	7.90	26.02	-9.84	15.	30.
X AXIS SUM	9.81	24.74	-24.36	13.	41.

DP2 STUDY TEST: 2735 SUBJ: S-13 WT: 186.0 NOM G: 10.0 CELL: B

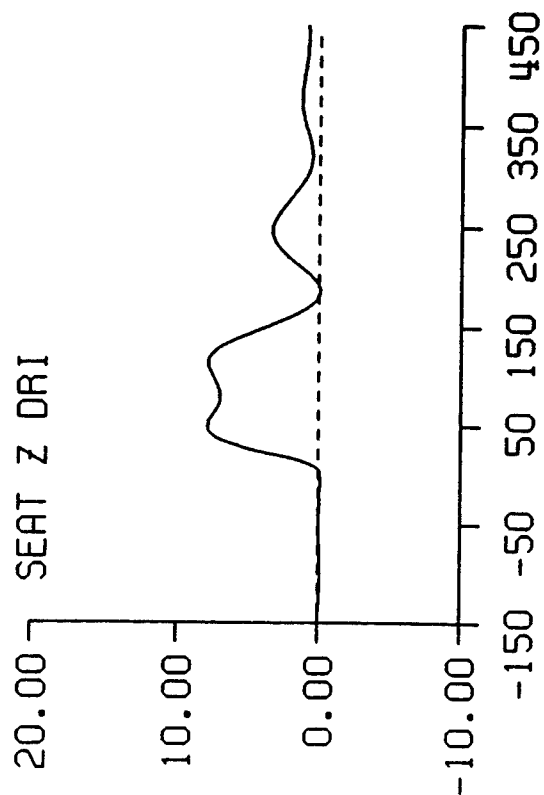
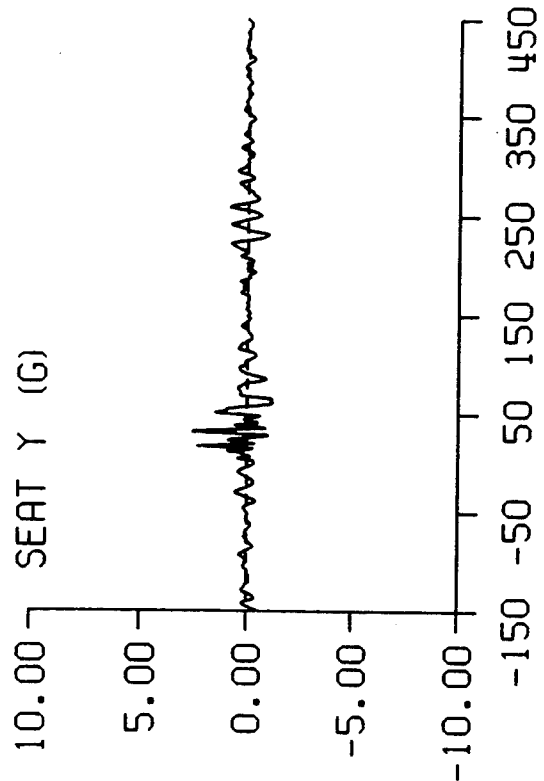
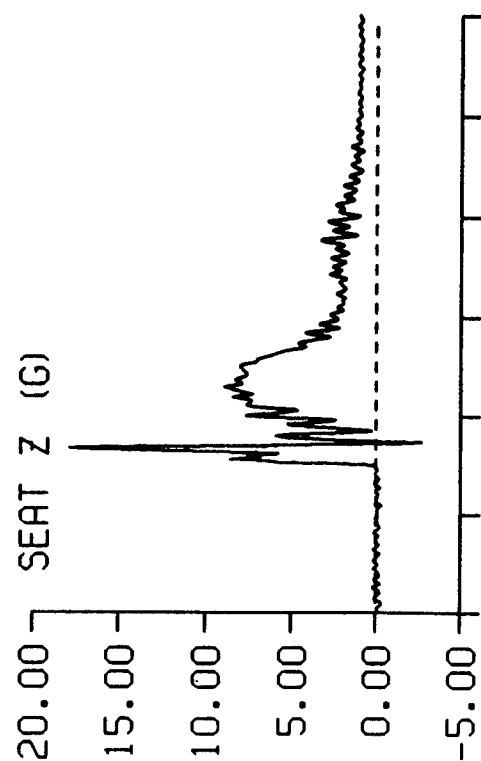
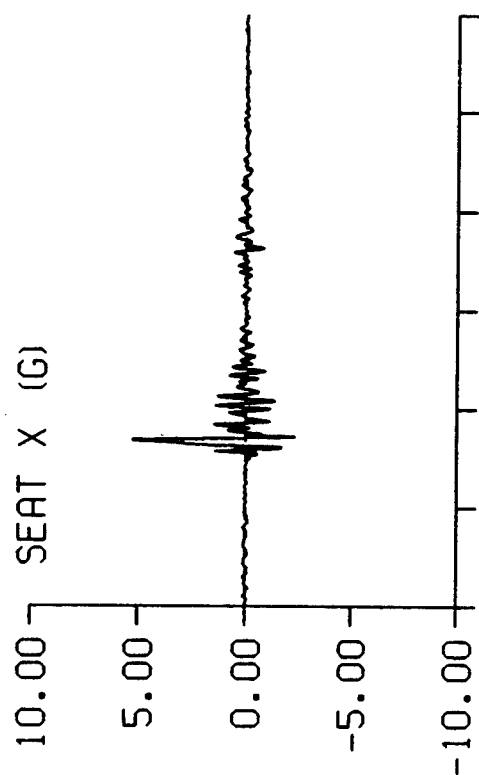
DATA ID	IMMEDIATE PREIMPACT	MAXIMUM VALUE	MINIMUM VALUE	TIME OF MAXIMUM	TIME OF MINIMUM
LAP FORCES (LB)					
LEFT X AXIS	-76.62	-22.08	-89.28	442.	51.
LEFT Y AXIS	44.54	47.31	12.19	47.	21.
LEFT Z AXIS	-136.29	-33.01	-136.35	20.	0.
LEFT RESULTANT	162.58	162.85	41.54	0.	447.
RIGHT X AXIS	-87.90	-29.00	-101.60	449.	48.
RIGHT Y AXIS	-43.41	-9.27	-44.82	434.	0.
RIGHT Z AXIS	-134.65	-35.19	-136.53	18.	0.
RIGHT RESULTANT	166.56	169.69	46.53	1.	449.
SEAT FORCES (LB)					
LEFT X AXIS	44.65	187.46	-11.15	20.	39.
RIGHT X AXIS	16.57	101.35	-24.24	14.	66.
X AXIS SUM	61.22	242.72	-20.54	20.	117.
Y AXIS	-9.21	42.32	-103.53	39.	19.
LEFT Z AXIS	-4.21	222.99	-30.62	103.	25.
RIGHT Z AXIS	-5.75	227.50	-9.15	86.	14.
CENTER Z AXIS	312.61	1398.57	198.80	81.	333.
Z AXIS SUM	302.65	1811.76	246.38	81.	445.
RESULTANT	308.98	1811.76	246.38	81.	446.
Z SUM MINUS TARE	322.71	1671.01	248.49	81.	446.
RESULTANT MINUS TARE	328.47	1671.04	248.49	81.	446.

DP2 STUDY TEST: 2735 SUBJ: S-13 CELL: B



TIME IN MILLISECONDS

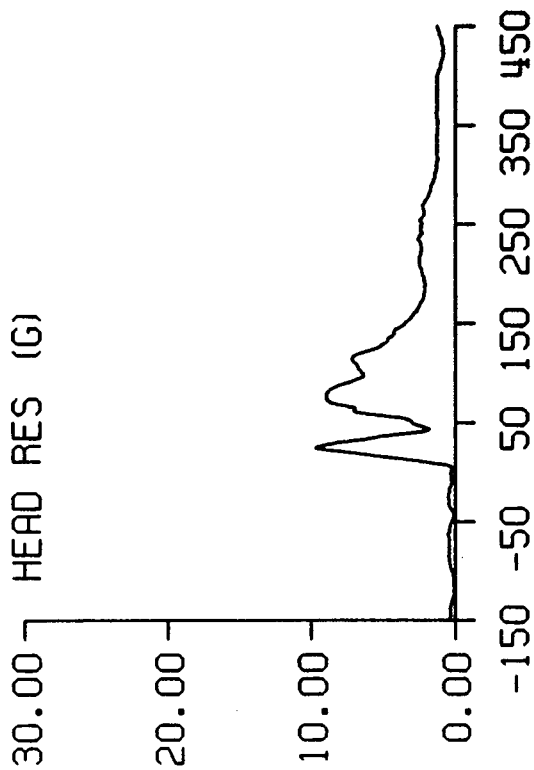
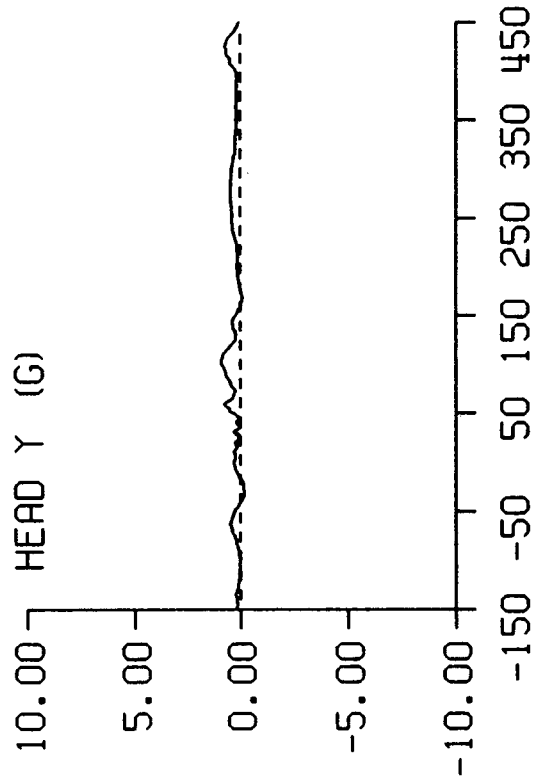
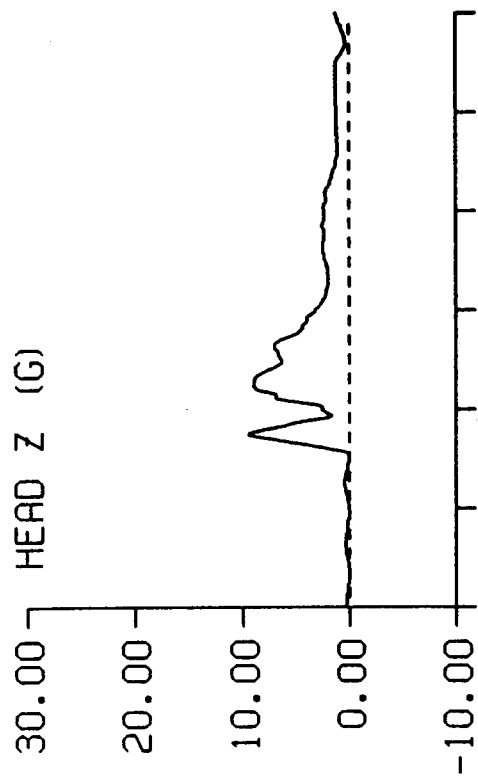
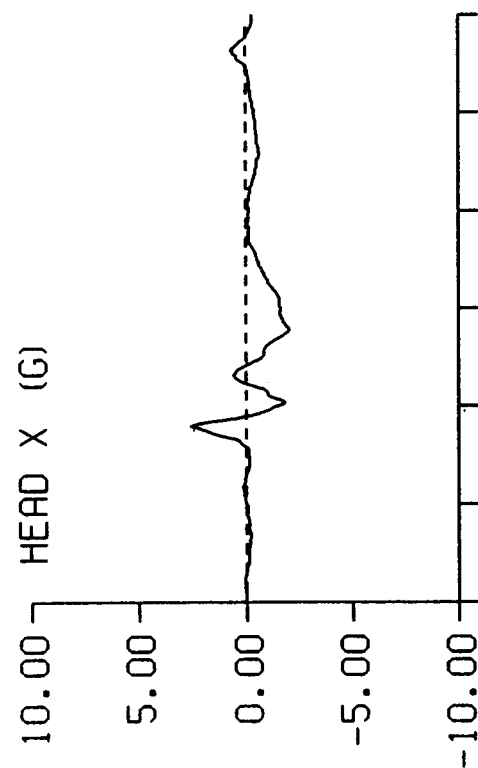
DP2 STUDY TEST: 2735 SUBJ: S-13 CELL: B



TIME IN MILLISECONDS

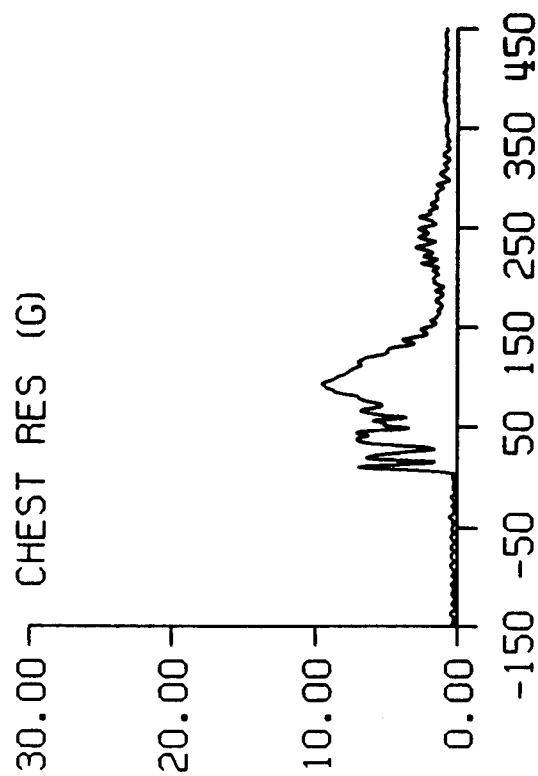
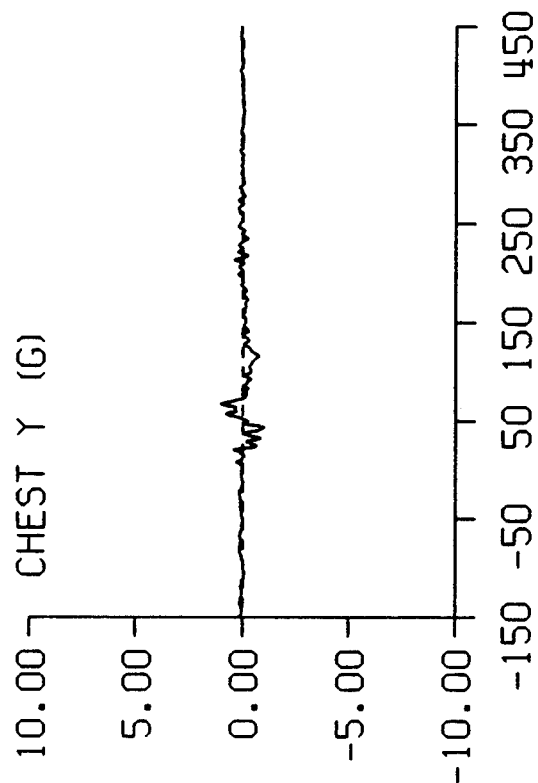
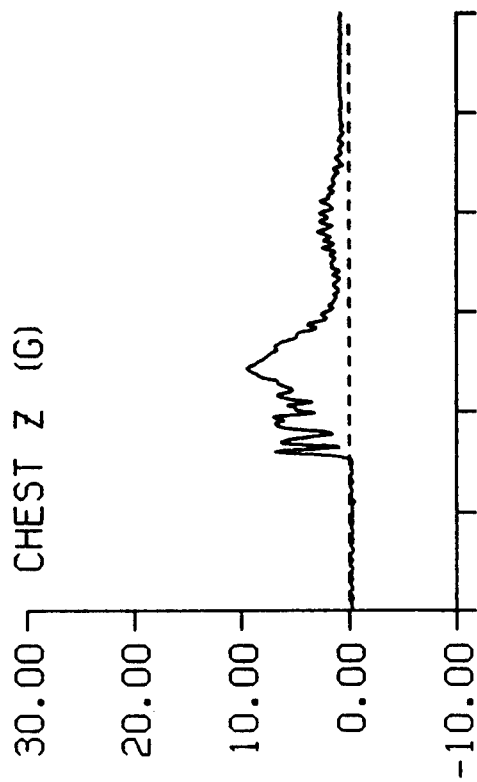
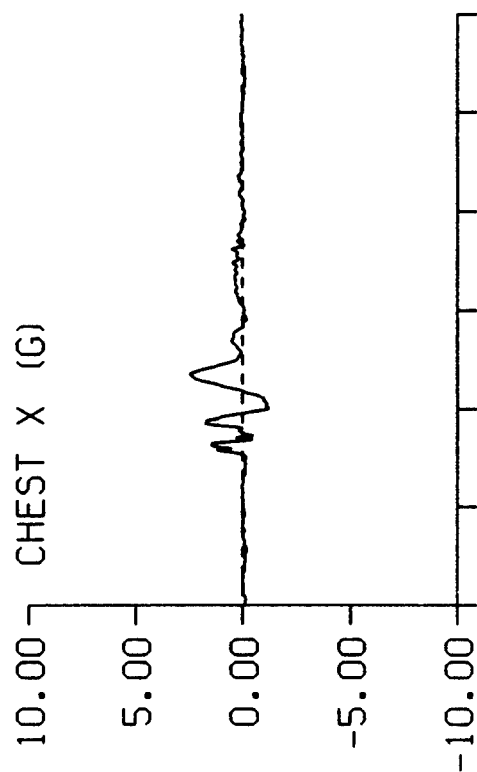


DP2 STUDY TEST: 2735 SUBJ: S-13 CELL: B



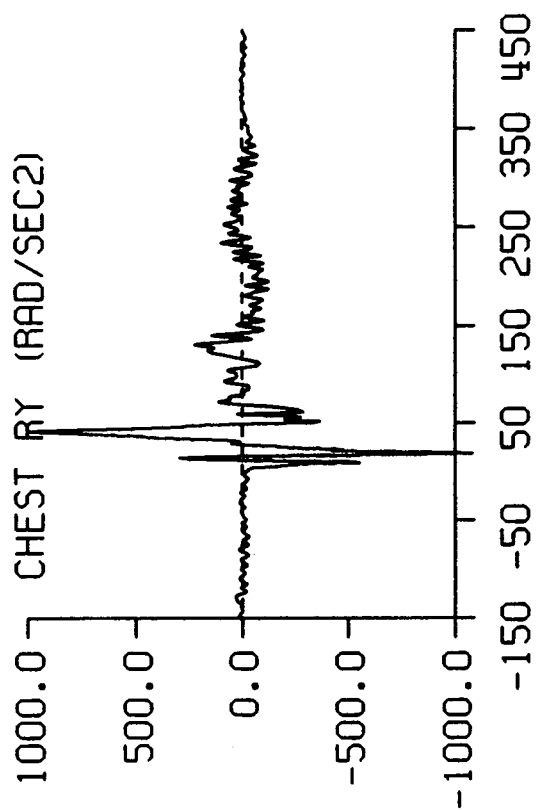
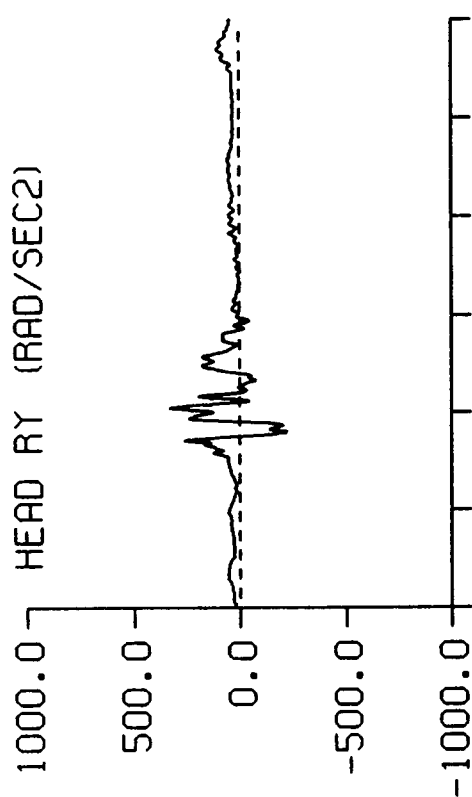
TIME IN MILLISECONDS

DP2 STUDY TEST: 2735 SUBJ: S-13 CELL: B



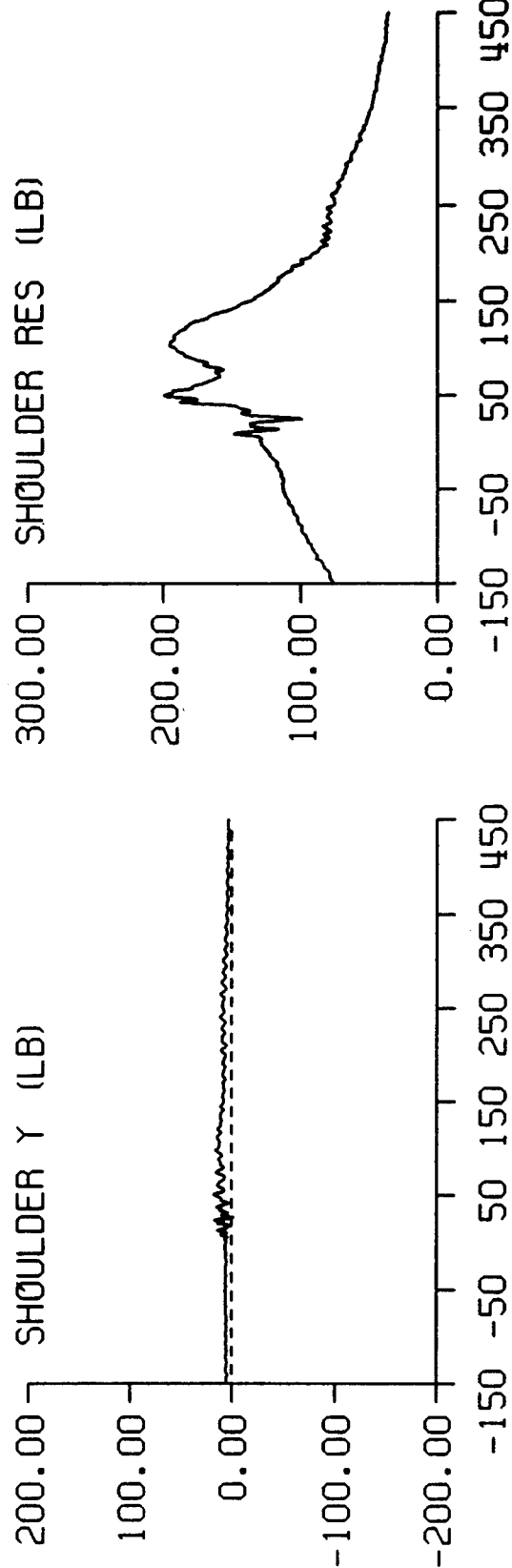
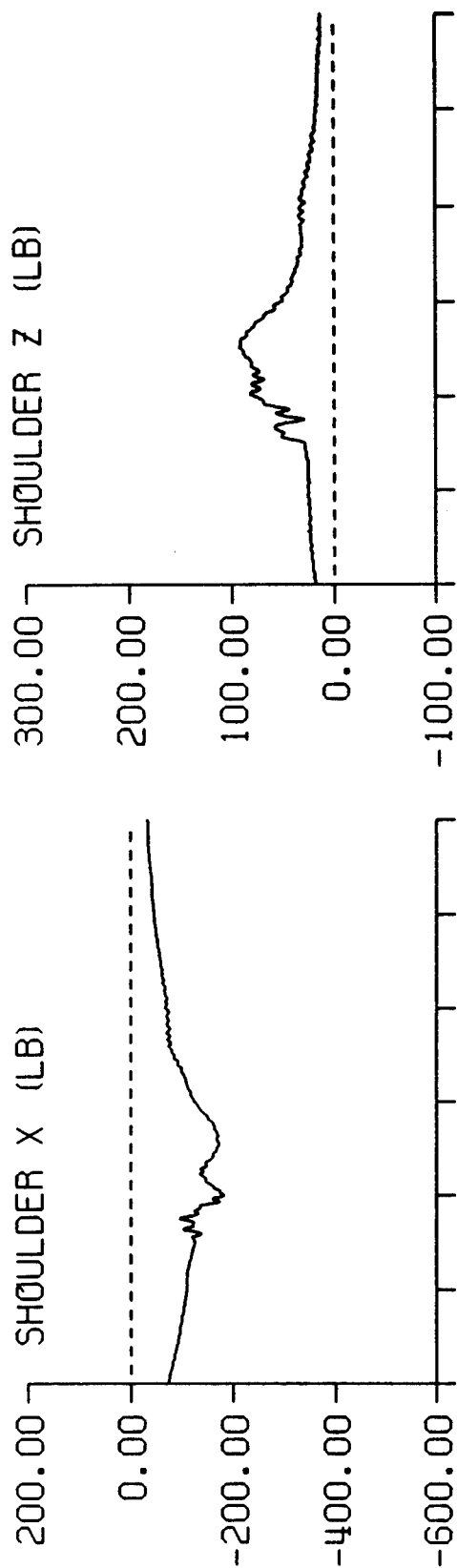
TIME IN MILLISECONDS

DP2 STUDY TEST: 2735 SUBJ: S-13 CELL: B



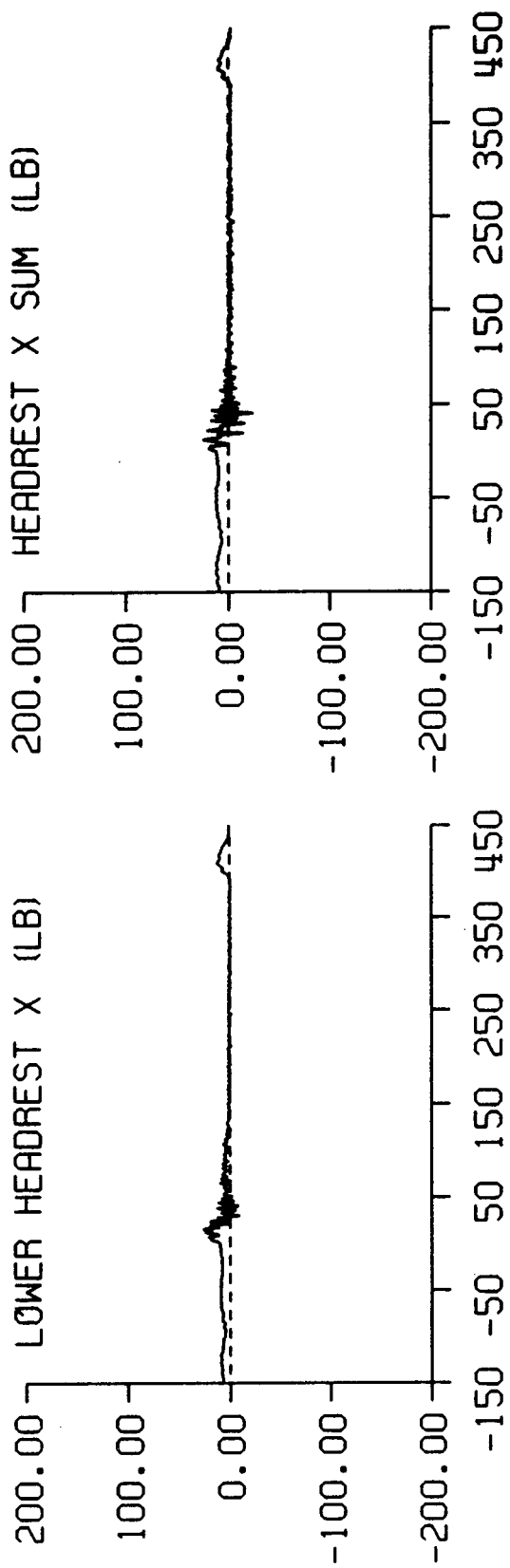
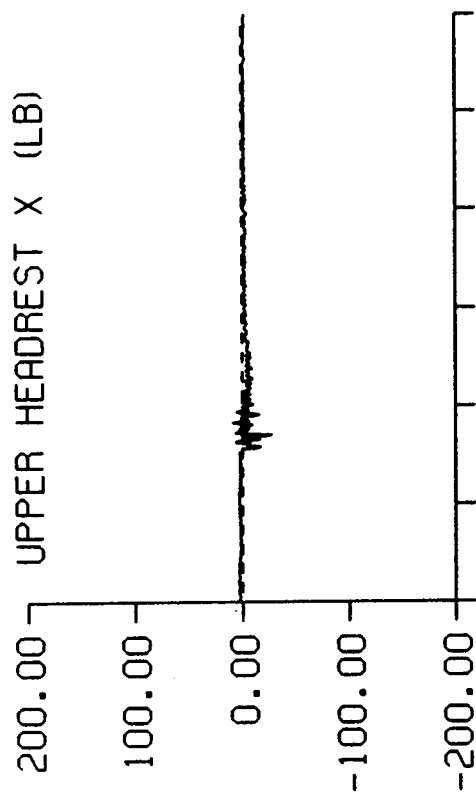
TIME IN MILLISECONDS

DP2 STUDY TEST: 2735 SUBJ: S-13 CELL: B



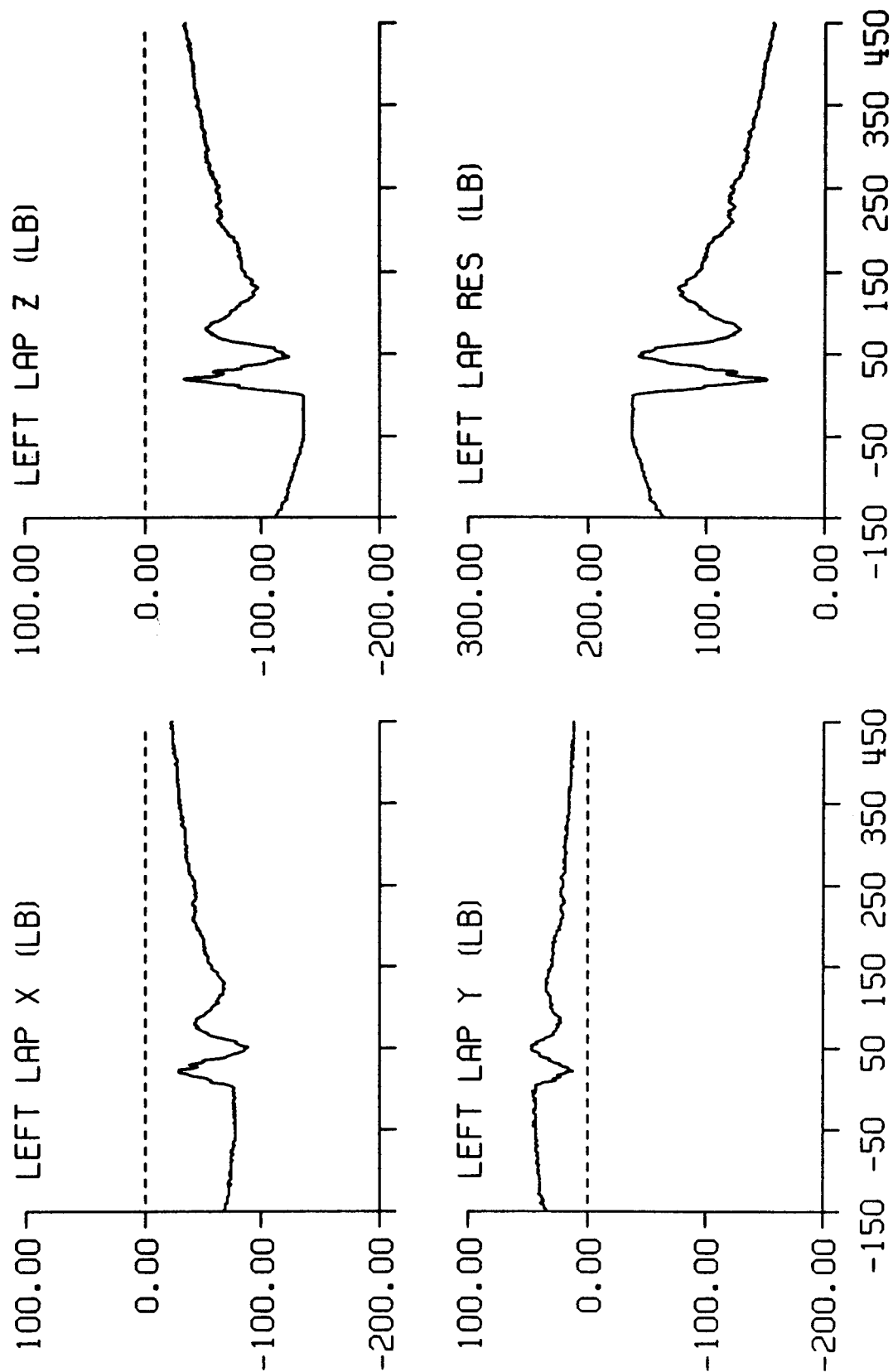
TIME IN MILLISECONDS

DP2 STUDY TEST: 2735 SUBJ: S-13 CELL: B

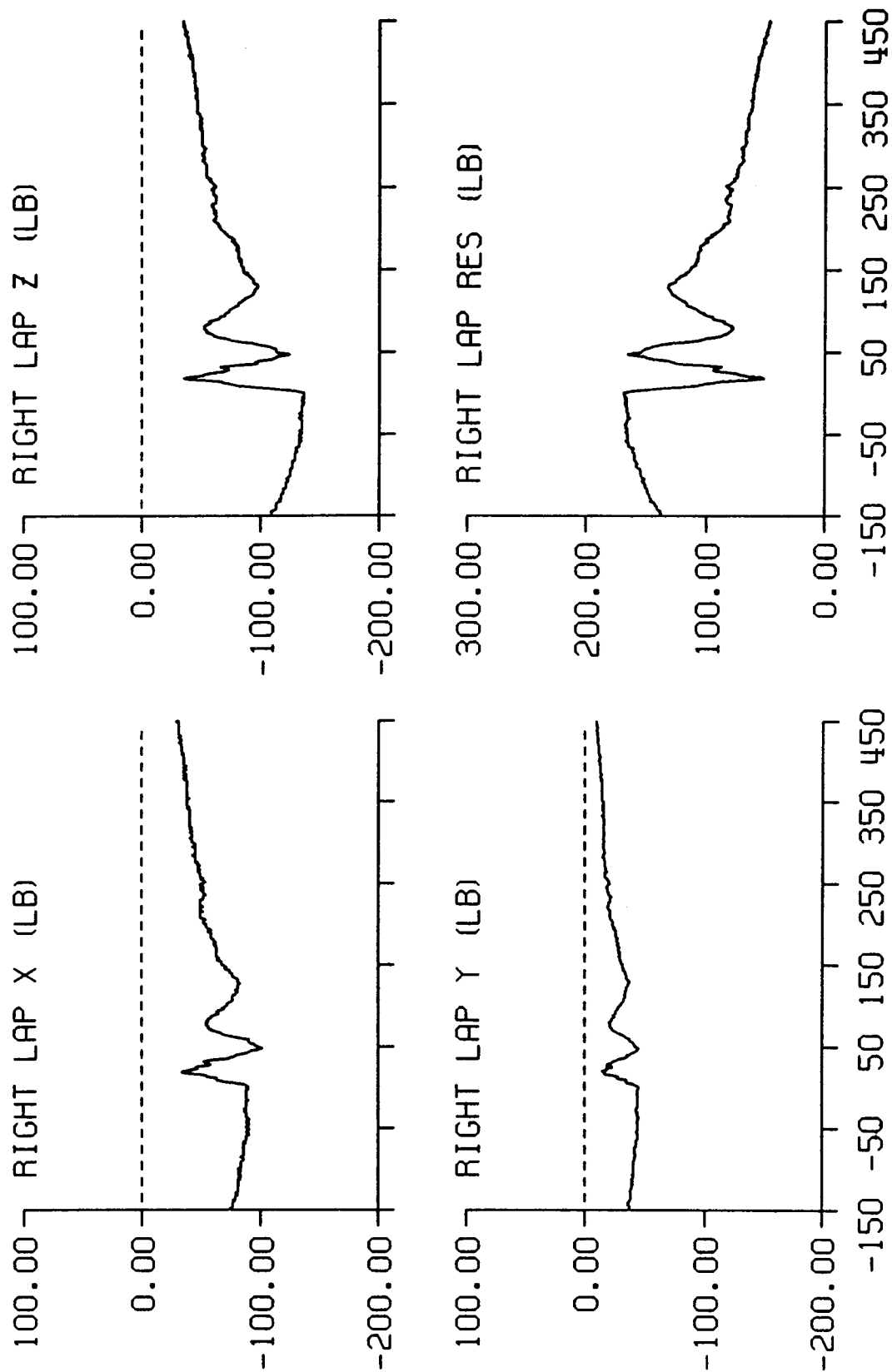


TIME IN MILLISECONDS

DP2 STUDY TEST: 2735 SUBJ: S-13 CELL: B

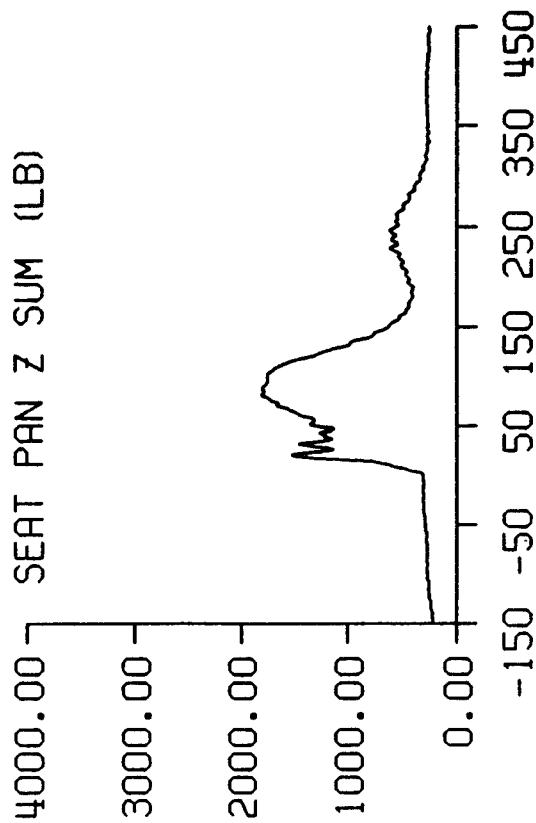
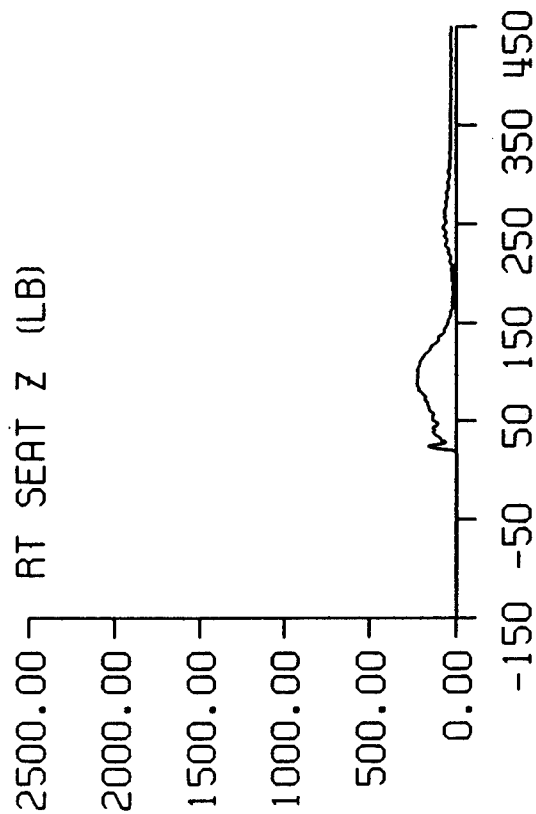
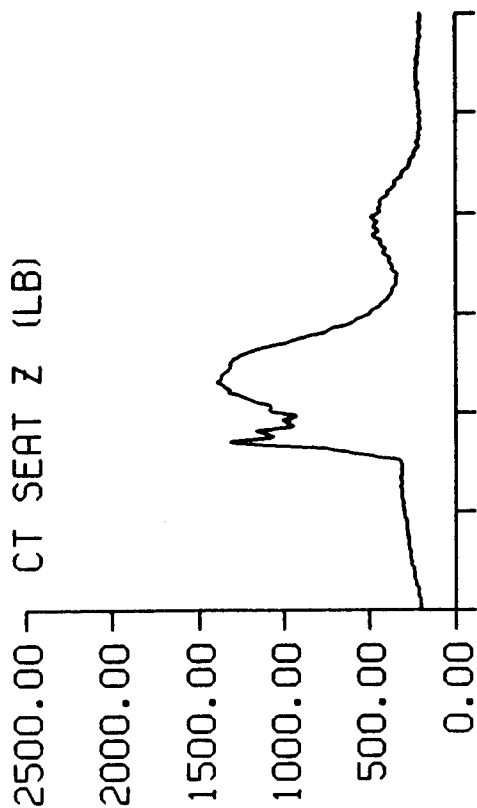
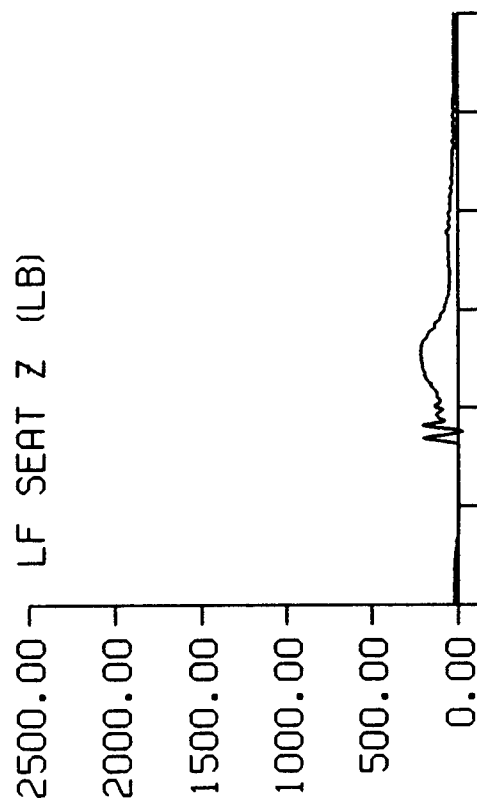


DP2 STUDY TEST: 2735 SUBJ: S-13 CELL: B



TIME IN MILLISECONDS

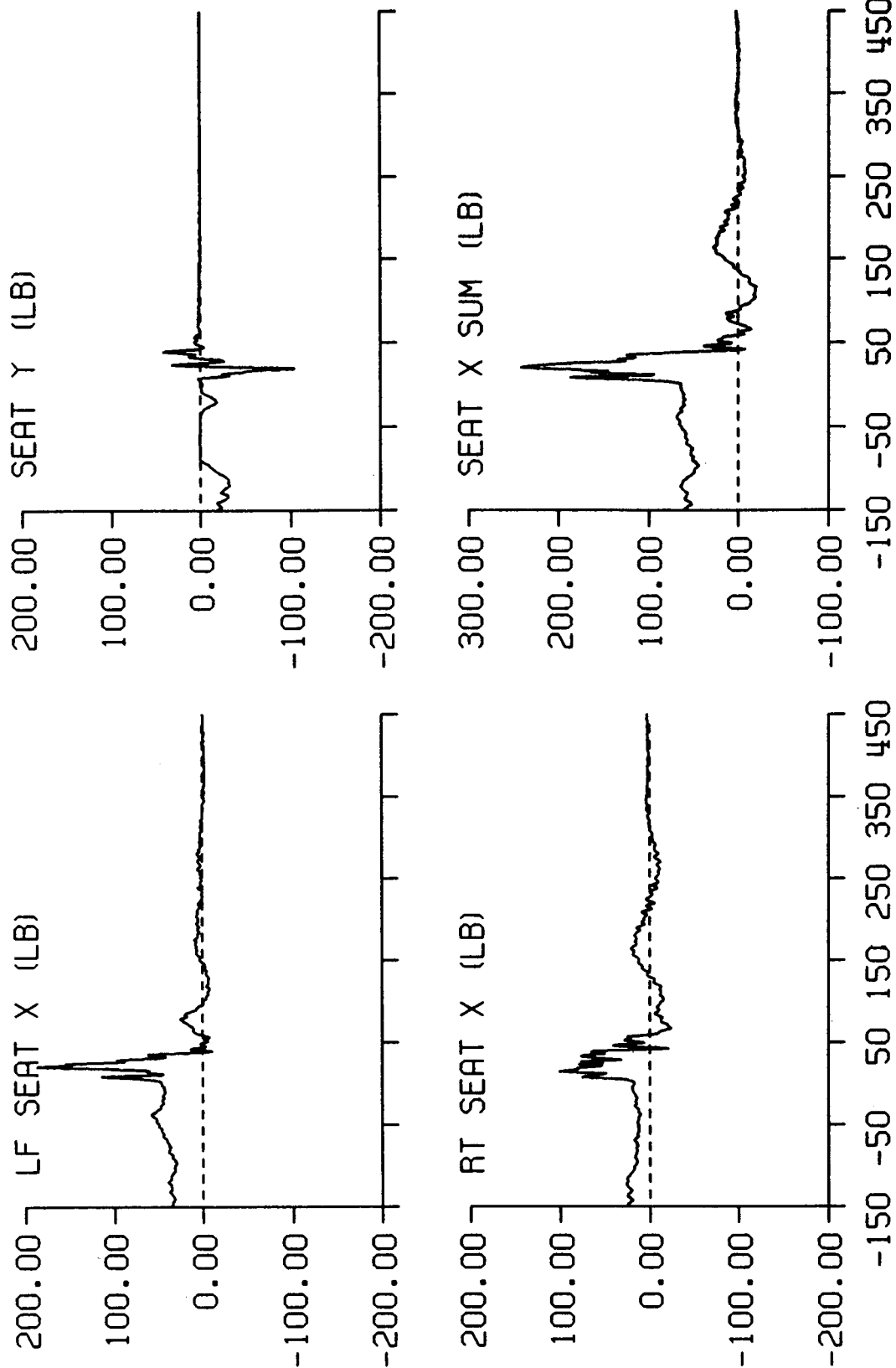
DP2 STUDY TEST: 2735 SUBJ: S-13 CELL: B



TIME IN MILLISECONDS

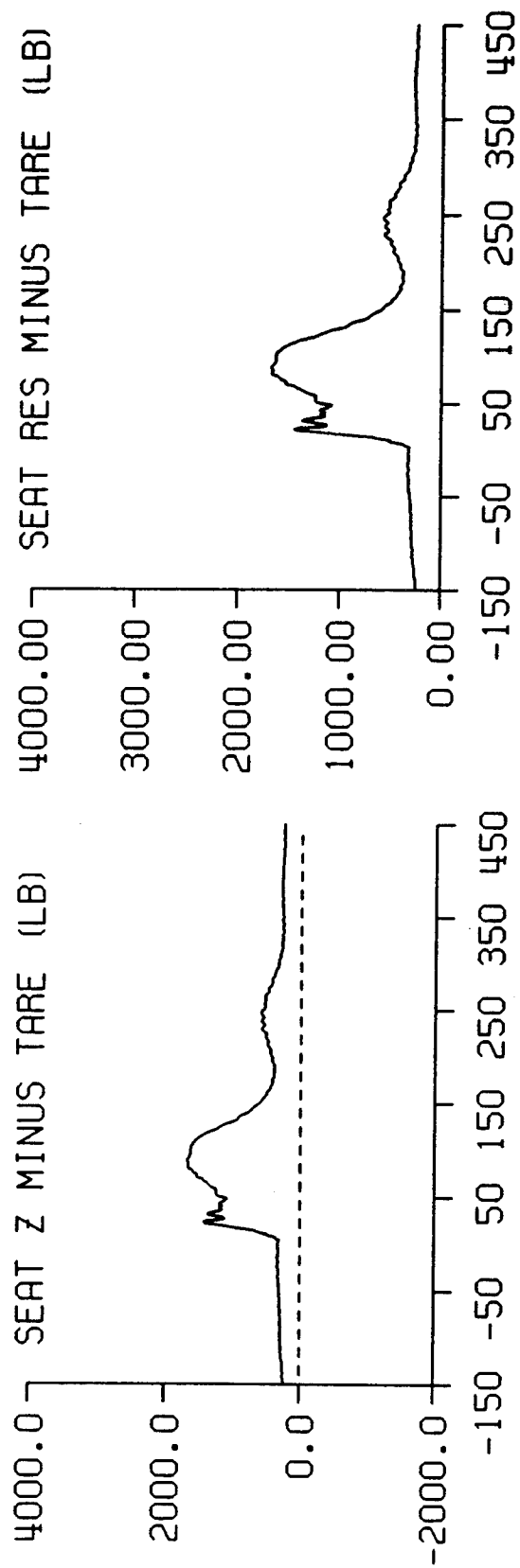
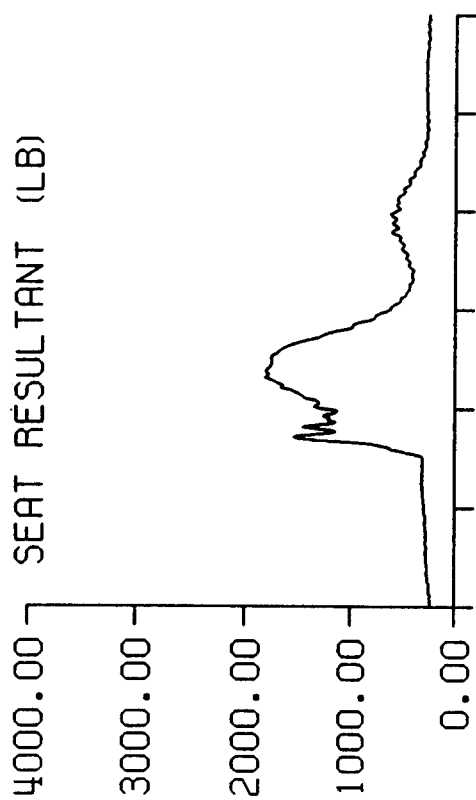


DP2 STUDY TEST: 2735 SUBJ: S-13 CELL: B



TIME IN MILLISECONDS

DP2 STUDY TEST: 2735 SUBJ: S-13 CELL: B



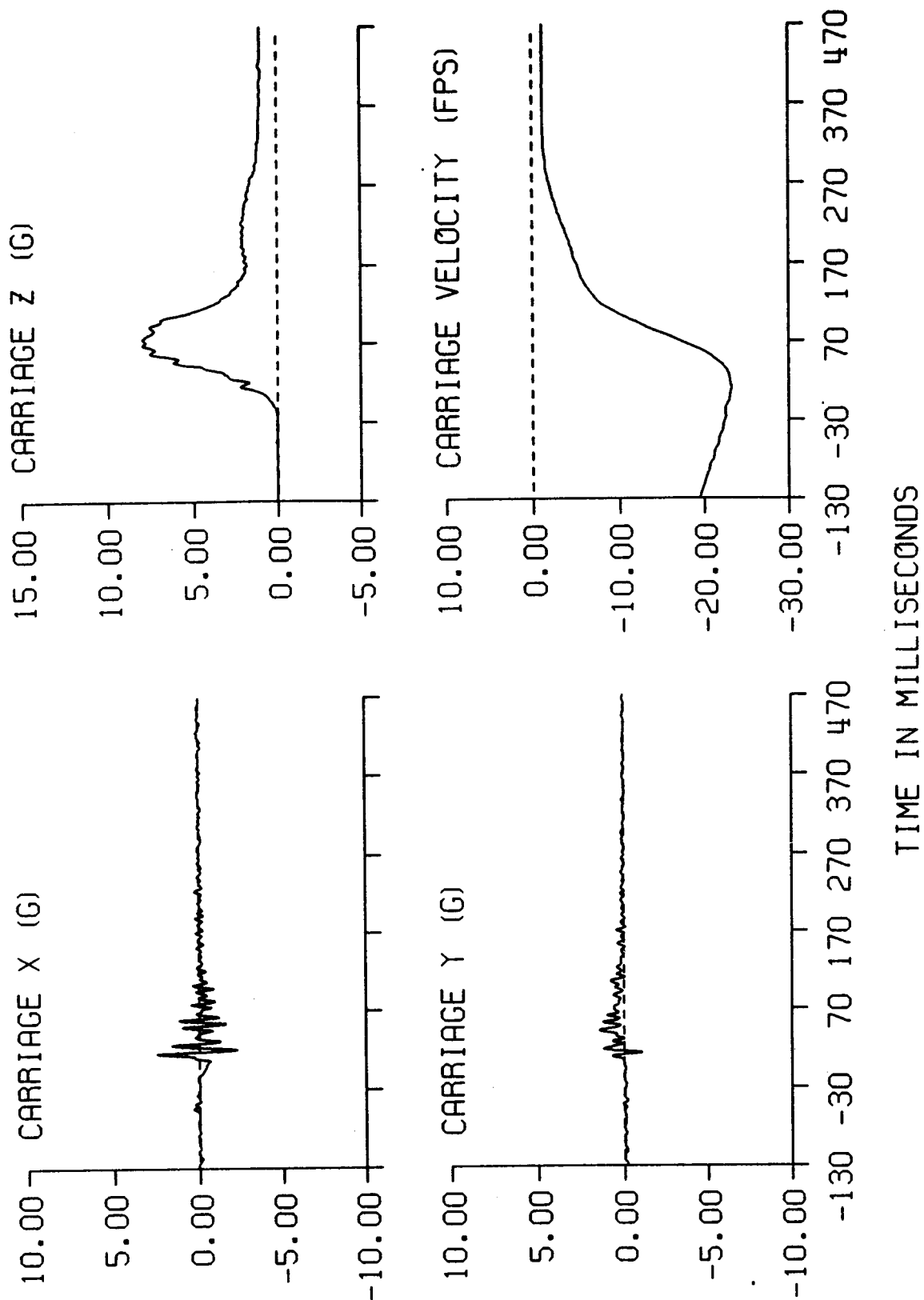
DP2 STUDY TEST: 2699 SUBJ: L-9 WT: 155.0 NOM G: 8.0 CELL: C

DATA ID	IMMEDIATE PREIMPACT	MAXIMUM VALUE	MINIMUM VALUE	TIME OF MAXIMUM	TIME OF MINIMUM
REFERENCE MARK TIME (MS)				-130.	
2.5V EXT PWR (VOLTS)	2.50	2.50	2.50	398.	12.
10V EXT PWR (VOLTS)	10.00	10.00	10.00	17.	65.
CARRIAGE ACCELERATION (G)					
X AXIS	-0.06	2.52	-2.29	16.	21.
Y AXIS	-0.08	1.47	-1.07	41.	13.
Z AXIS	0.10	7.97	0.51	69.	0.
CARRIAGE VELOCITY (FPS)	-22.64	-1.13	-23.24	388.	8.
SEAT ACCELERATION (G)					
X AXIS	-0.09	2.17	-1.95	15.	20.
Y AXIS	0.00	1.97	-2.82	12.	20.
Z AXIS	-0.03	9.11	0.04	94.	20.
Z AXIS DRI	-0.02	10.35	-0.75	98.	173.
HEAD ACCELERATION (G)					
X AXIS	-0.16	2.10	-3.41	139.	115.
Y AXIS	0.11	1.80	-1.27	142.	190.
Z AXIS	-0.23	11.91	-0.28	84.	0.
RESULTANT	0.31	11.98	0.27	84.	5.
RY (RAD/SEC2)	45.48	330.79	-149.28	22.	85.
CHEST ACCELERATION (G)					
X AXIS	-0.07	3.08	-0.56	78.	17.
Y AXIS	0.10	0.74	-1.15	22.	96.
Z AXIS	-0.14	11.05	-0.86	82.	25.
RESULTANT	0.19	11.46	0.14	83.	0.
RY (RAD/SEC2)	-17.33	127.76	-229.77	105.	18.
SHOULDER STRAP FORCES (LB)					
X AXIS	-50.86	-31.28	-104.58	389.	84.
Y AXIS	3.06	17.06	0.68	78.	15.
Z AXIS	14.11	83.17	12.56	87.	351.
RESULTANT	52.88	132.92	33.75	87.	458.
HEADREST FORCES (LB)					
UPPER X AXIS	16.71	18.49	-9.51	1.	73.
LOWER X AXIS	11.36	43.85	0.57	56.	110.
X AXIS SUM	28.07	49.51	-4.68	140.	110.

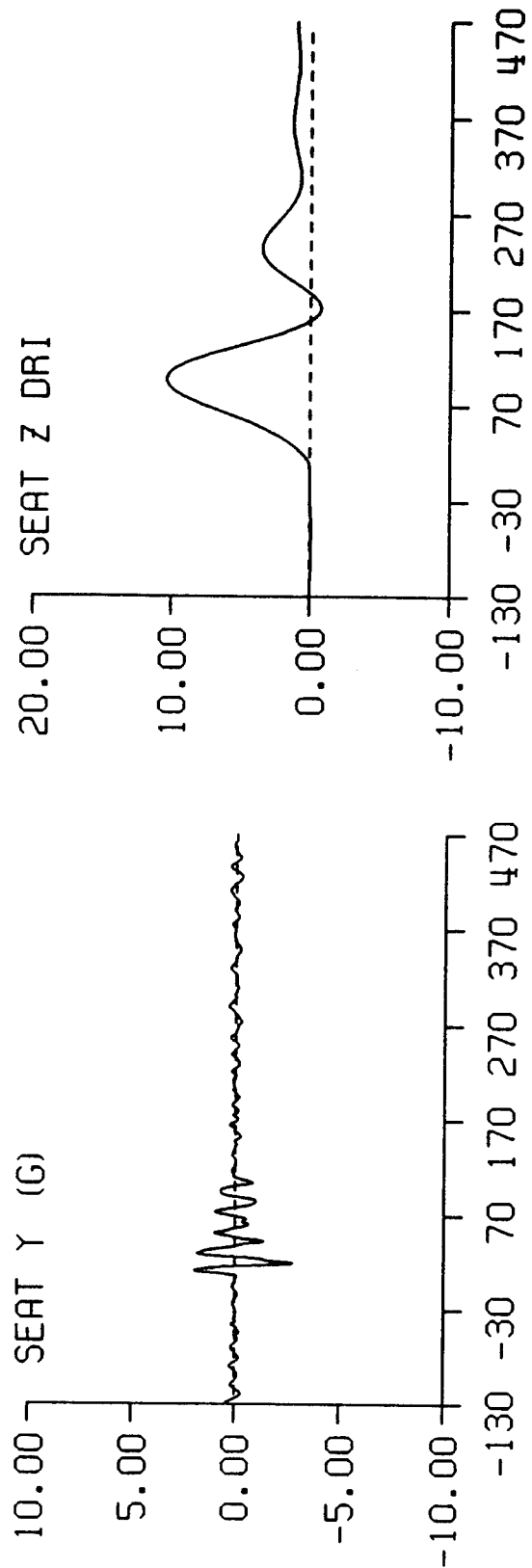
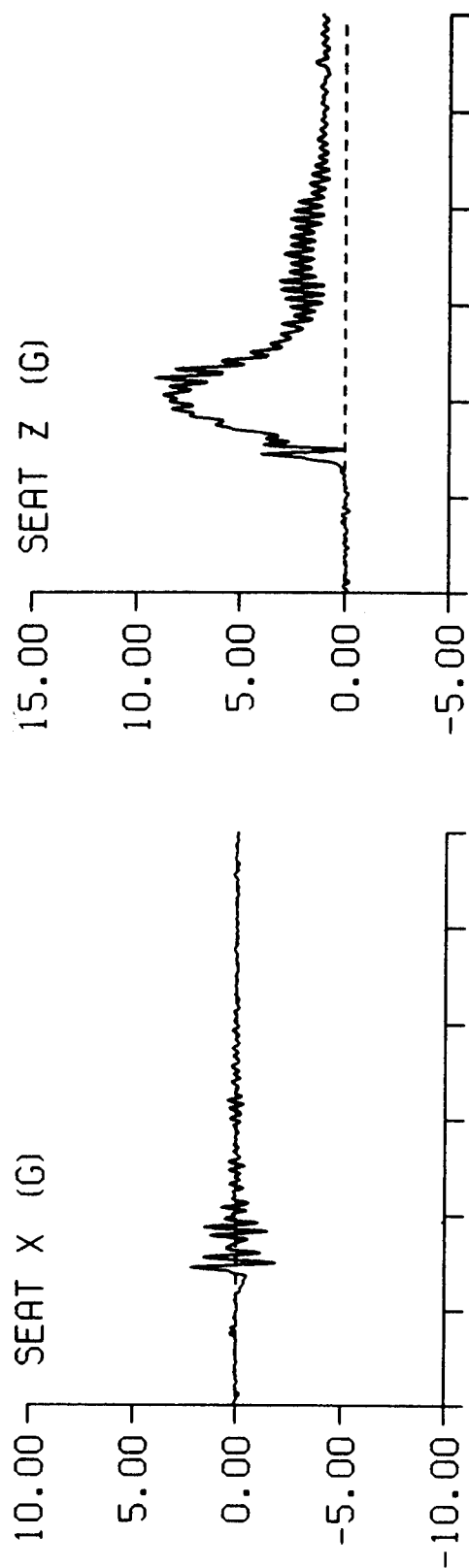
DP2 STUDY TEST: 2699 SUBJ: L-9 WT: 155.0 NOM G: 8.0 CELL: C

DATA ID	IMMEDIATE PREIMPACT	MAXIMUM VALUE	MINIMUM VALUE	TIME OF MAXIMUM	TIME OF MINIMUM
LAP FORCES (LB)					
LEFT X AXIS	-34.44	-16.80	-63.85	465.	90.
LEFT Y AXIS	20.18	29.57	8.50	13.	350.
LEFT Z AXIS	-56.92	-25.18	-67.46	449.	89.
LEFT RESULTANT	69.53	96.47	31.44	90.	465.
RIGHT X AXIS	-38.88	-19.42	-69.33	339.	89.
RIGHT Y AXIS	-28.07	-12.46	-41.13	440.	86.
RIGHT Z AXIS	-63.05	-26.78	-69.65	455.	0.
RIGHT RESULTANT	79.22	106.53	35.34	89.	462.
SEAT FORCES (LB)					
LEFT X AXIS	20.56	61.13	-3.95	48.	98.
RIGHT X AXIS	6.65	43.74	-28.85	16.	21.
X AXIS SUM	27.21	94.77	-29.44	16.	104.
Y AXIS	0.25	103.53	-61.14	96.	22.
LEFT Z AXIS	-5.25	233.14	-8.10	78.	1.
RIGHT Z AXIS	-3.22	239.86	-6.25	67.	0.
CENTER Z AXIS	108.37	1350.45	125.82	85.	0.
Z AXIS SUM	99.90	1782.78	114.56	77.	0.
RESULTANT	103.56	1785.42	117.39	77.	1.
Z SUM MINUS TARE	119.04	1650.42	130.16	79.	1.
RESULTANT MINUS TARE	122.13	1650.50	132.59	79.	1.

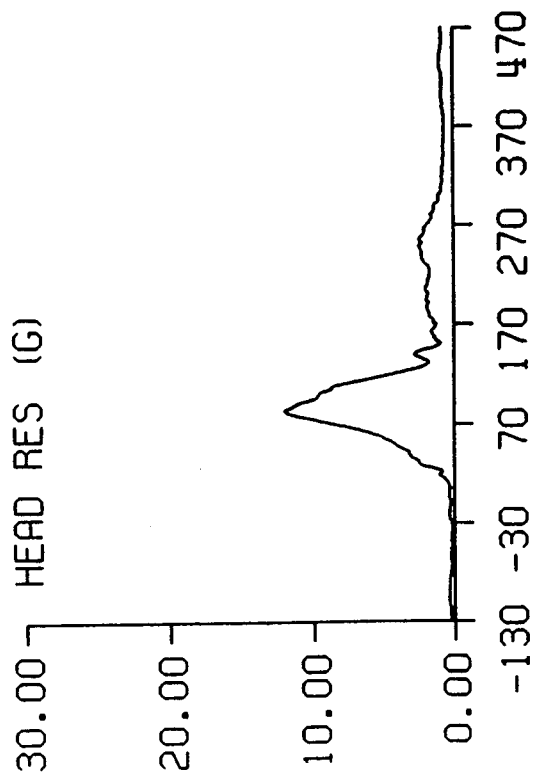
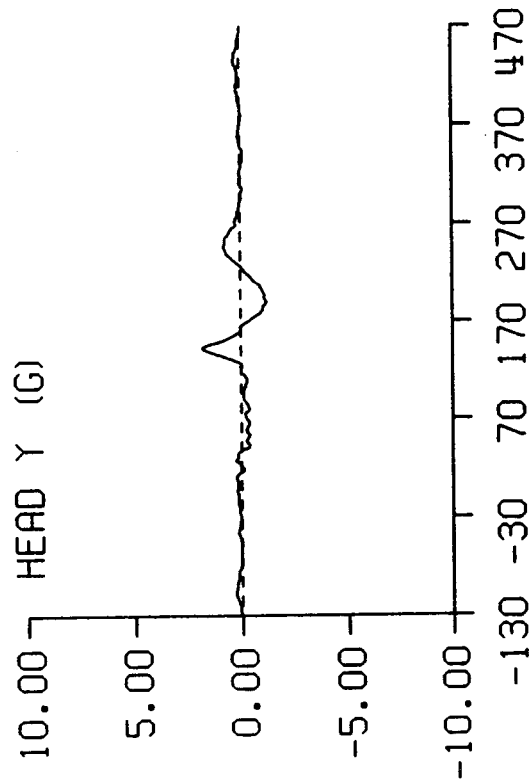
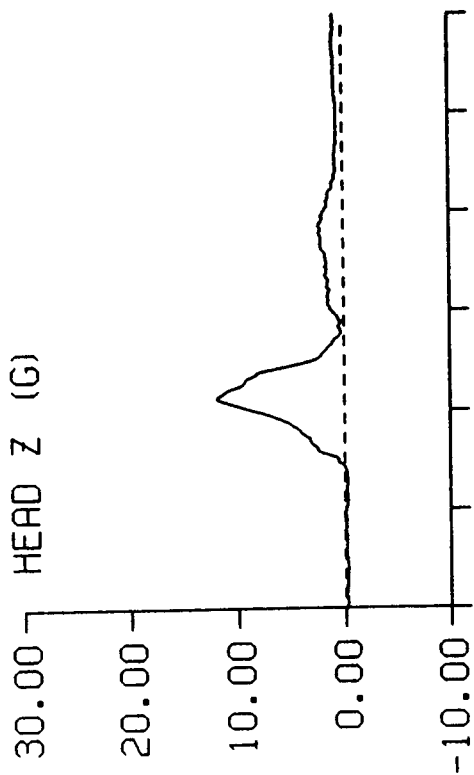
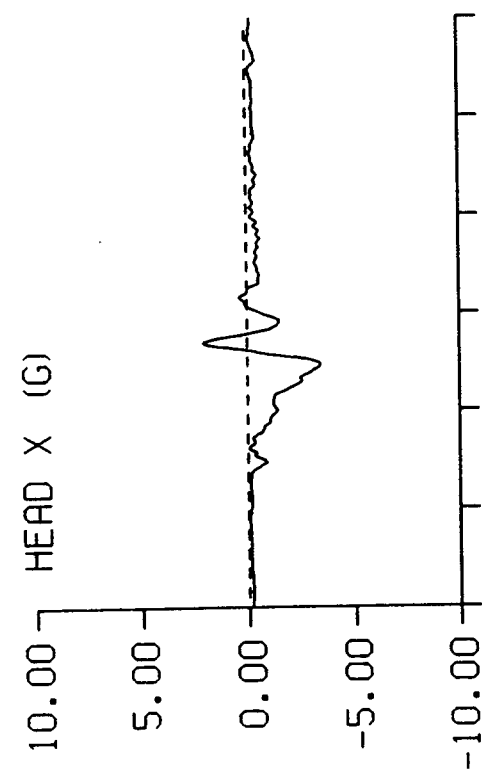
DP2 STUDY TEST: 2699 SUBJ: L-9 CELL: C



DP2 STUDY TEST: 2699 SUBJ: L-9 CELL: C

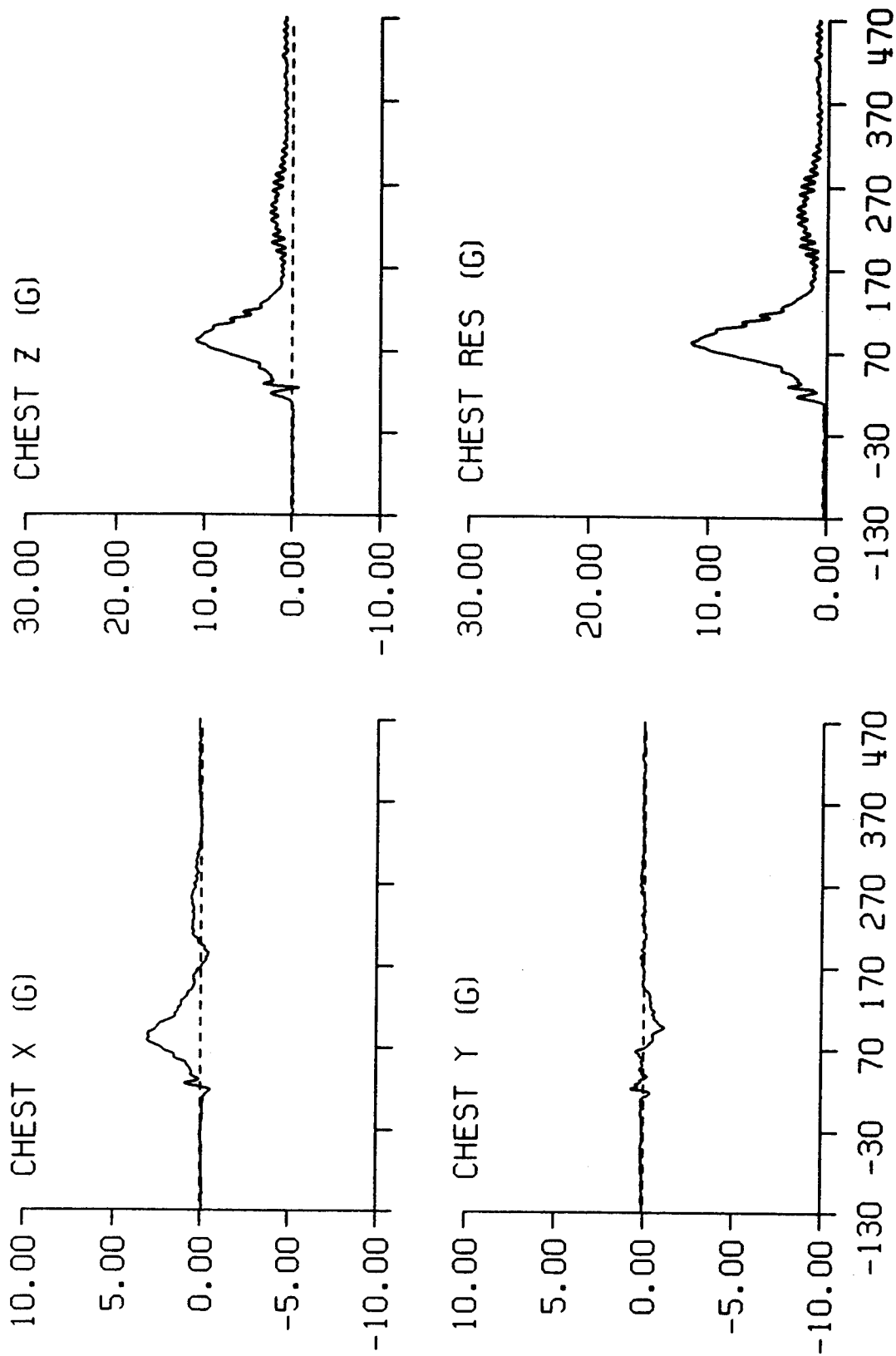


DP2 STUDY TEST: 2699 SUBJ: L-9 CELL: C



TIME IN MILLISECONDS

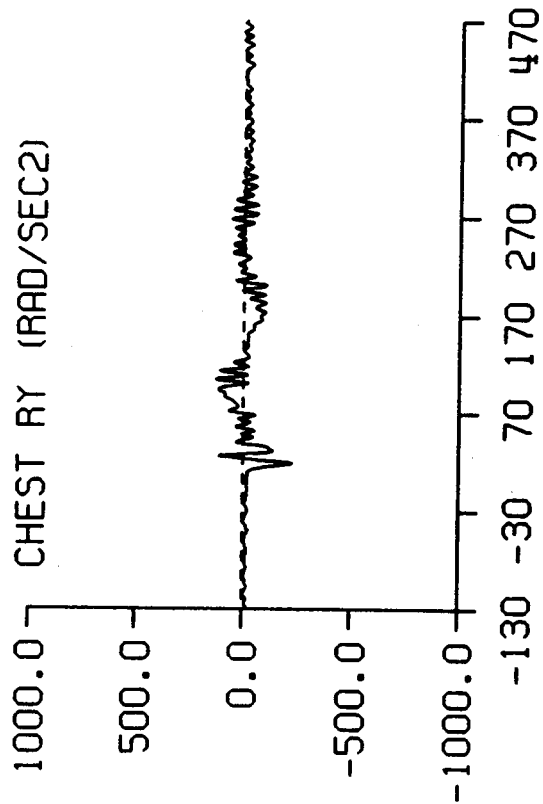
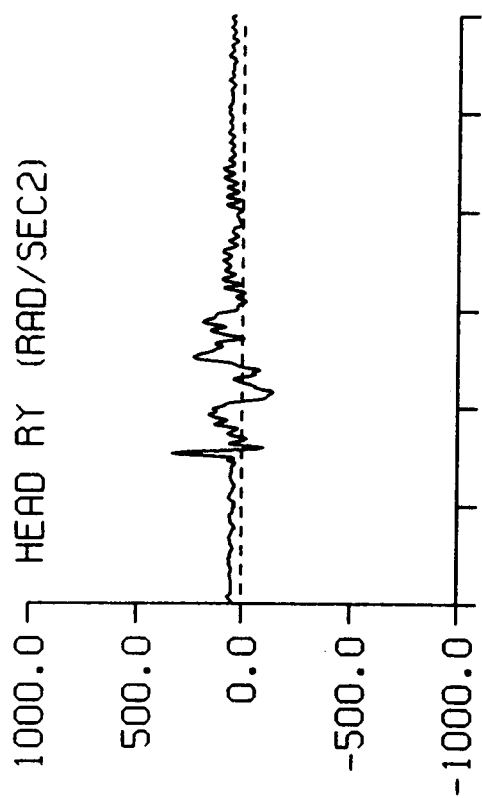
DP2 STUDY TEST: 2699 SUBJ: L-9 CELL: C



TIME IN MILLISECONDS

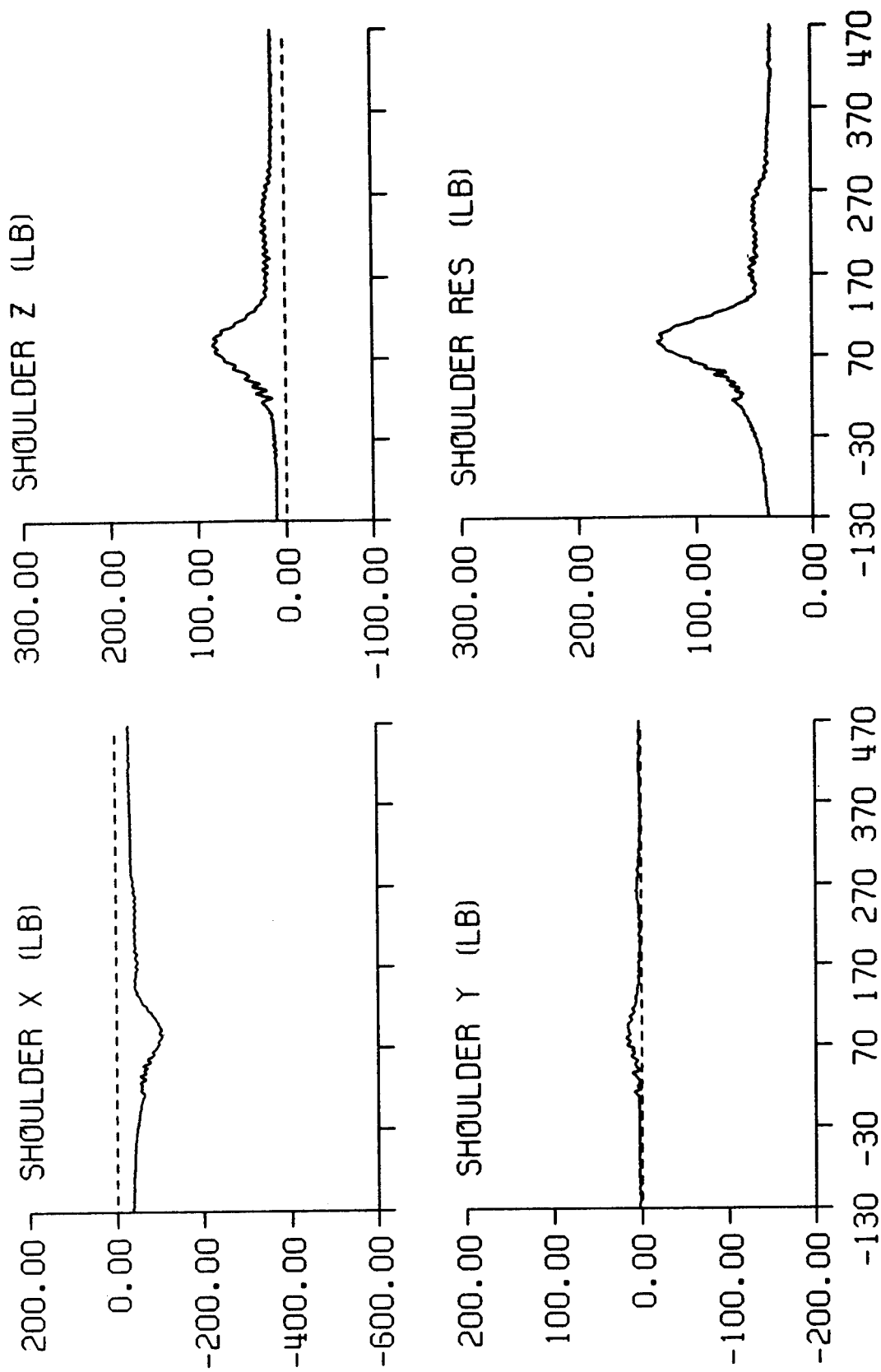


DP2 STUDY TEST: 2699 SUBJ: L-9 CELL: C



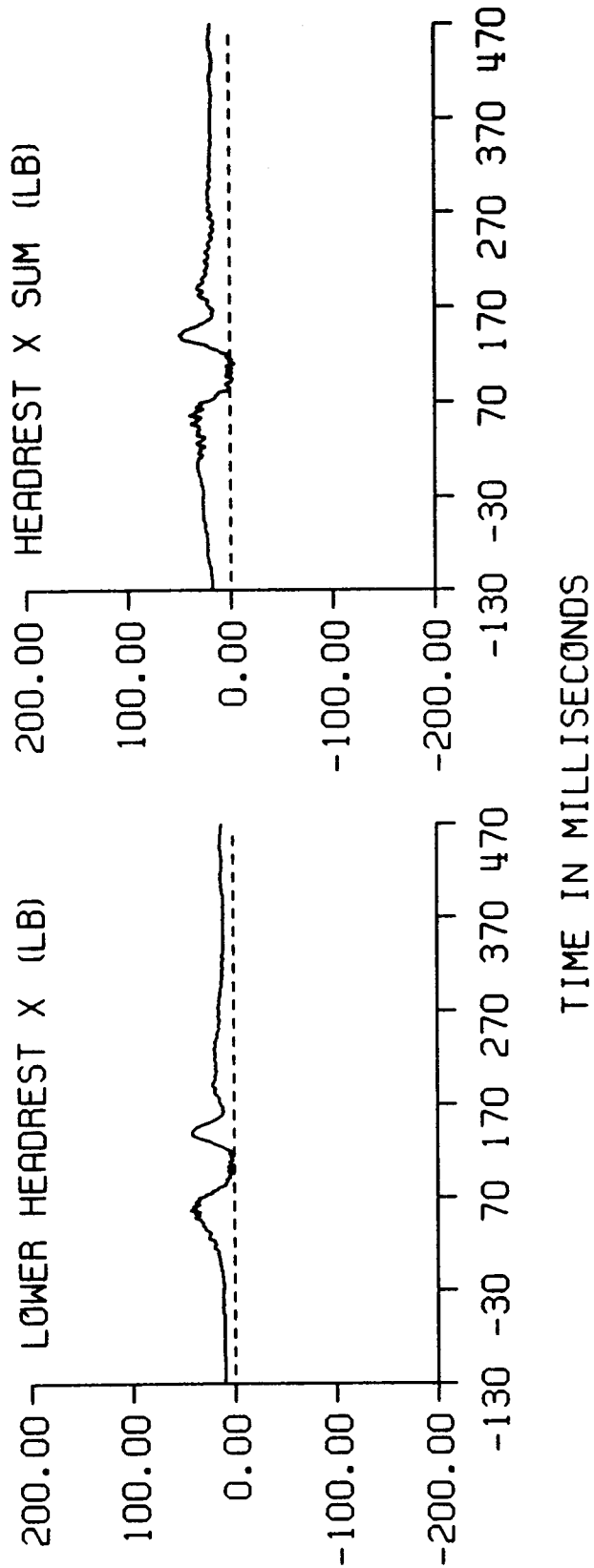
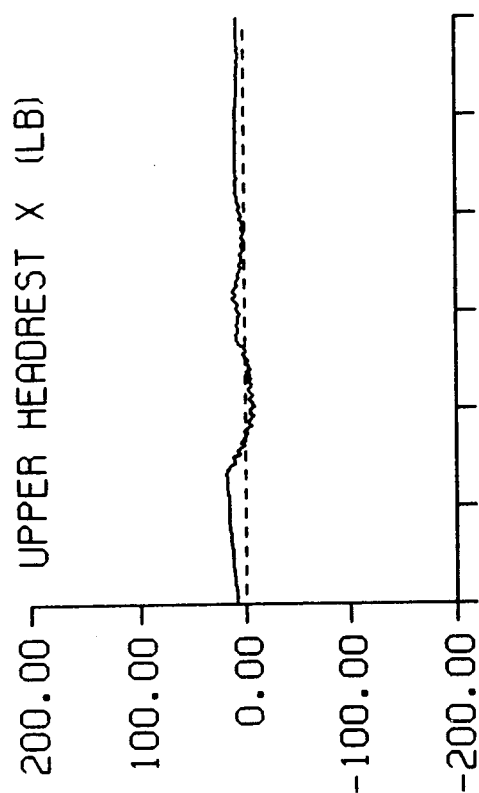
TIME IN MILLISECONDS

DP2 STUDY TEST: 2699 SUBJ: L-9 CELL: C

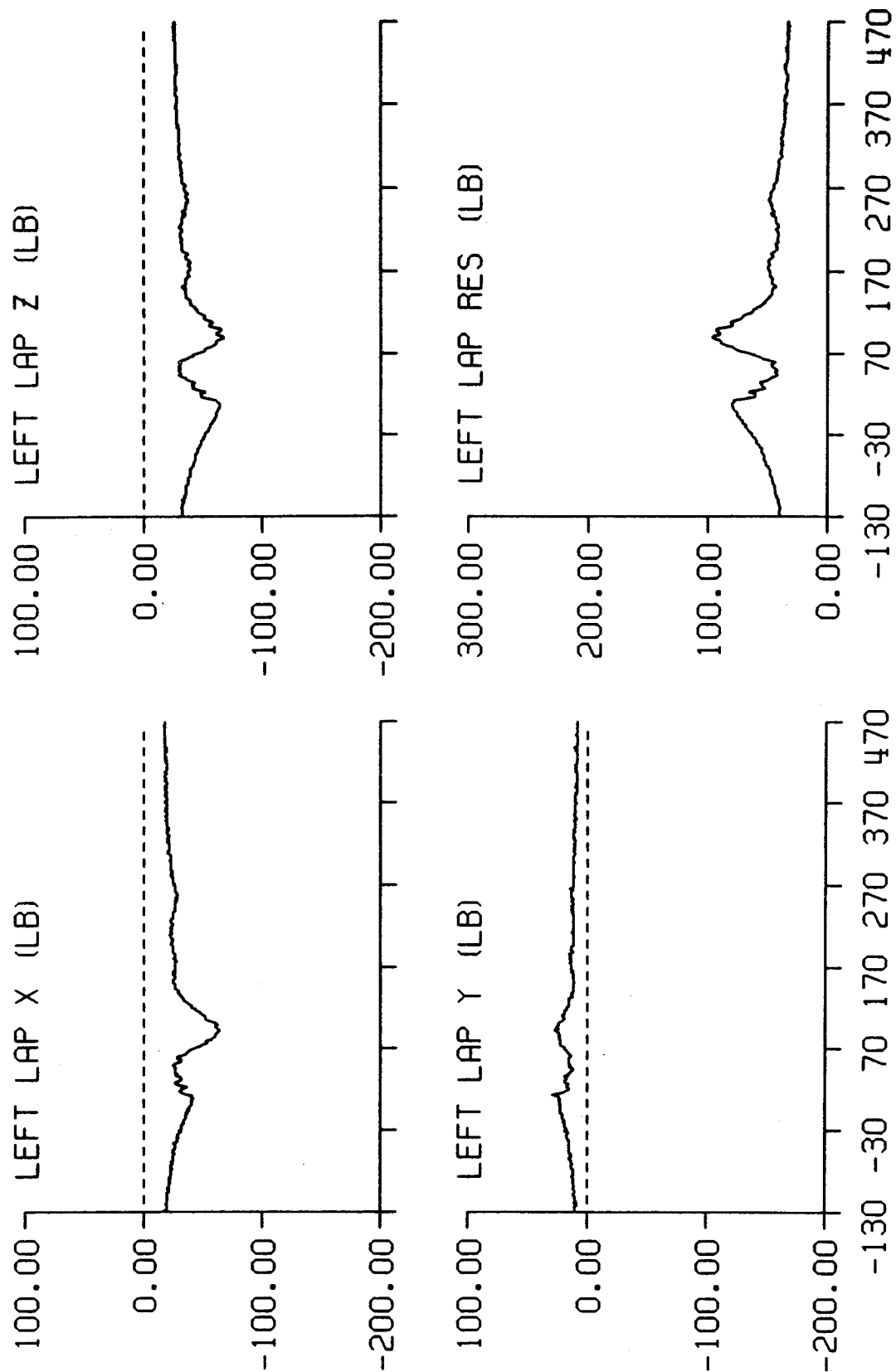


TIME IN MILLISECONDS

DP2 STUDY TEST: 2699 SUBJ: L-9 CELL: C

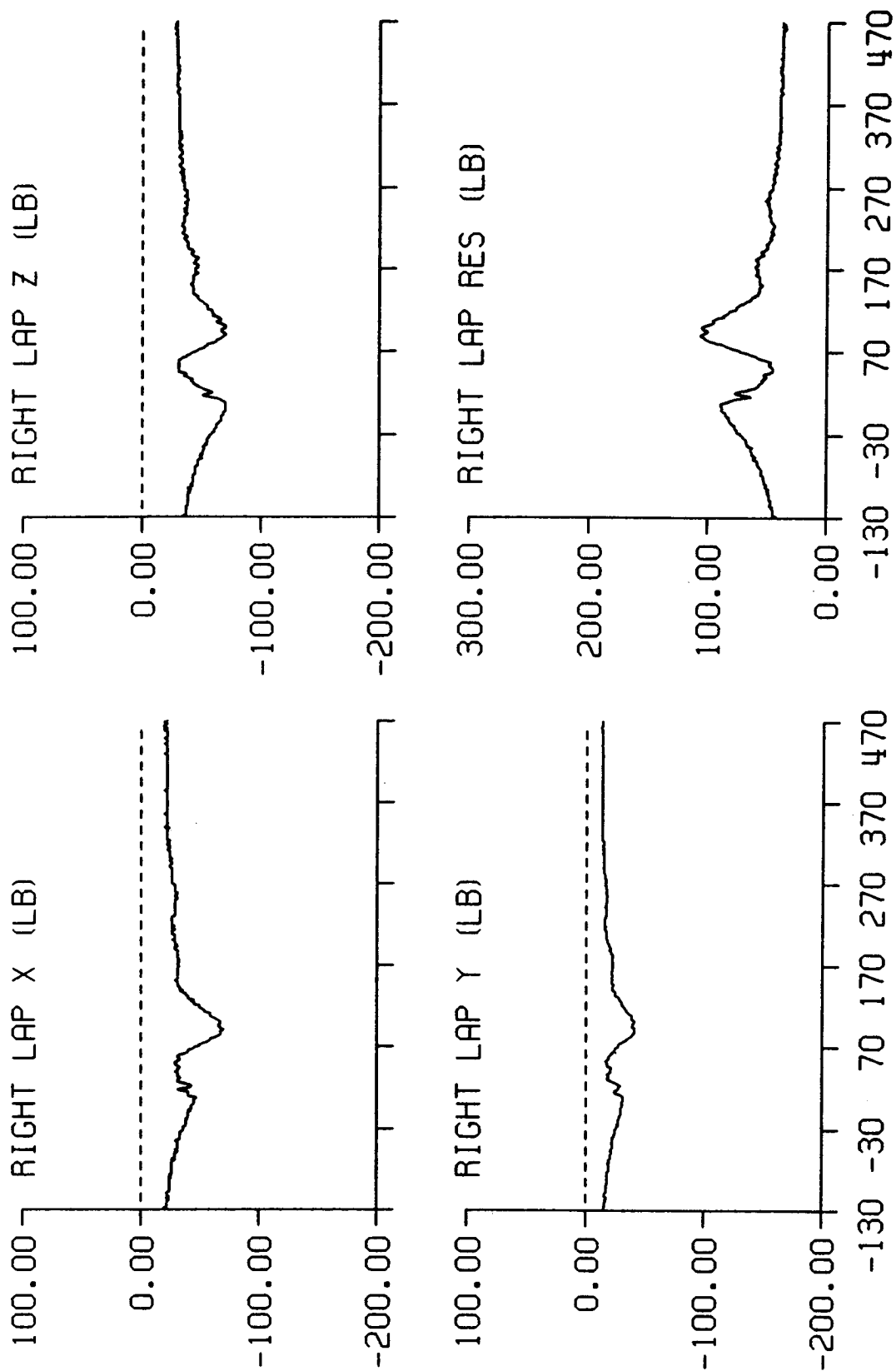


DP2 STUDY TEST: 2699 SUBJ: L-9 CELL: C

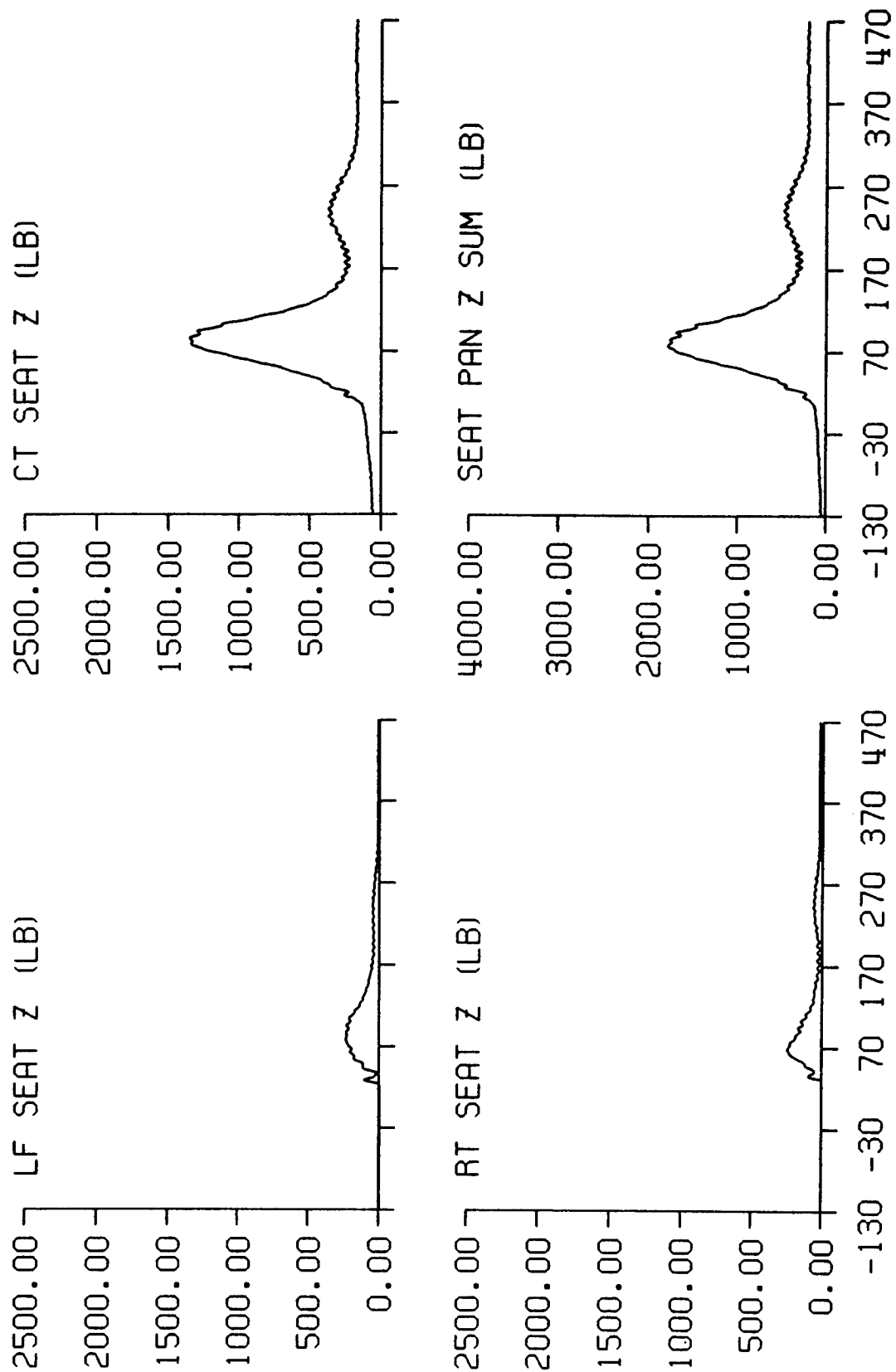


TIME IN MILLISECONDS

DP2 STUDY TEST: 2699 SUBJ: L-9 CELL: C

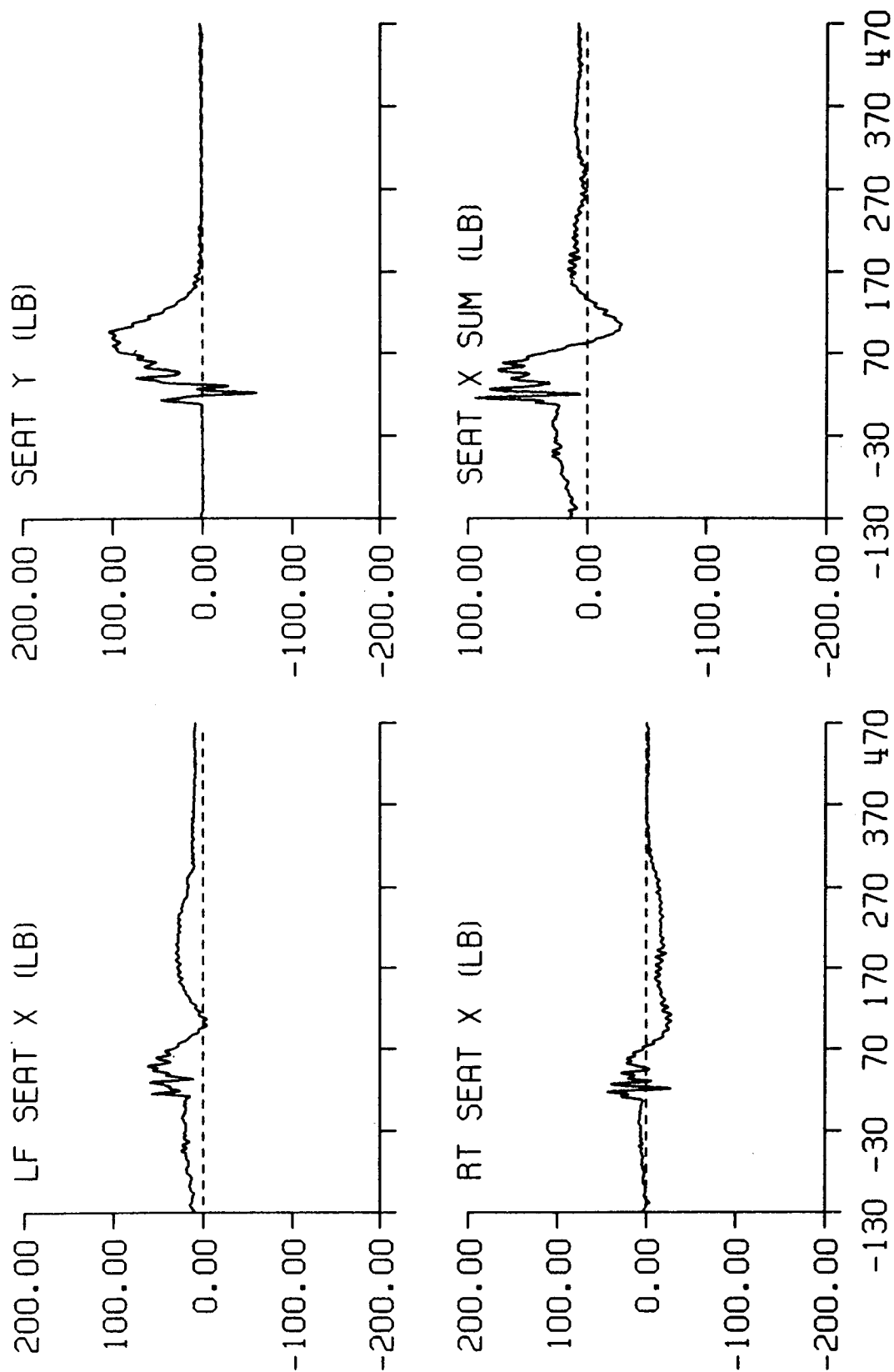


DP2 STUDY TEST: 2699 SUBJ: L-9 CELL: C



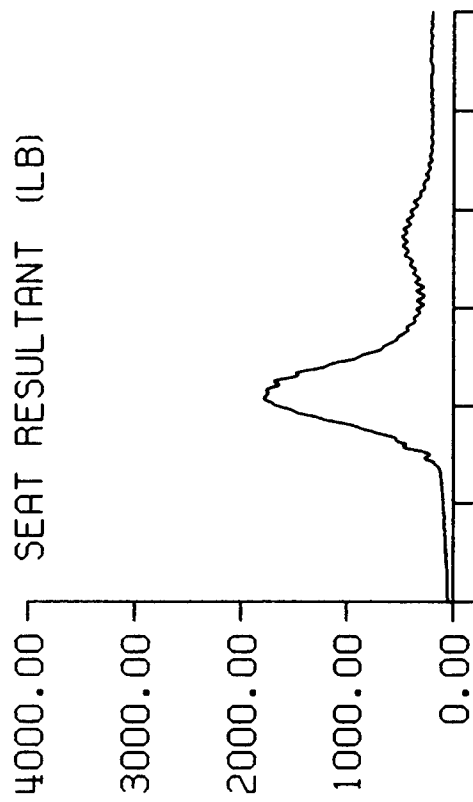
TIME IN MILLISECONDS

DP2 STUDY TEST: 2699 SUBJ: L-9 CELL: C

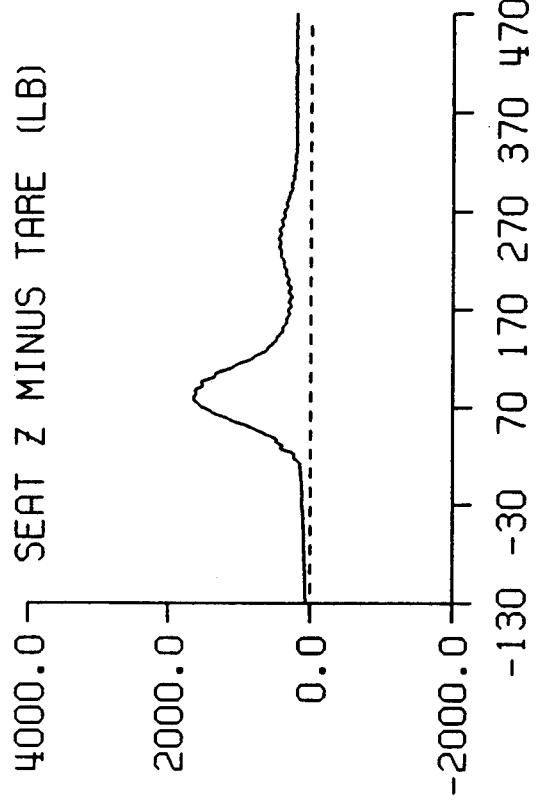


DP2 STUDY TEST: 2699 SUBJ: L-9 CELL: C

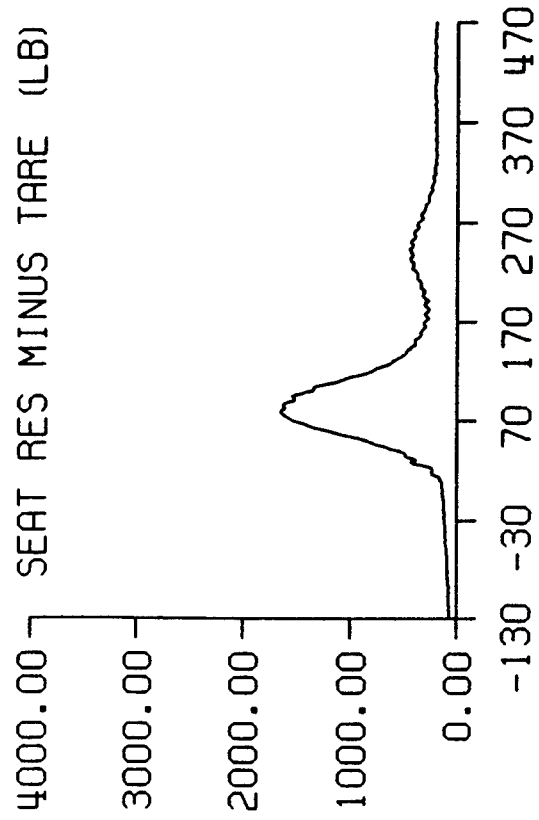
SEAT RESULTANT (LB)



SEAT Z MINUS TARE (LB)



SEAT RES MINUS TARE (LB)



TIME IN MILLISECONDS